Synthesis of Furfural from Xylose Using Carbon Based Bi-Functional Solid Acid Catalyst in Biphasic System

Megersa Taddesse Adugna

A thesis paper submitted to
the Department of Chemical Engineering
School of Mechanical, Chemical, and Material Engineering

Presented in Partial Fulfillment of the Requirement for the Degree of Master's in Chemical Engineering (Specialization in Process Engineering)

Office of Graduate Studies
Adama Science and Technology University

September, 2022

Adama, Ethiopia

Synthesis of Furfural from Xylose Using Carbon Based Bi-Functional Solid Acid Catalyst in Biphasic System

Megersa Taddesse Adugna

Advisor: Dr. Zelalem Tumsa

Co-Advisor: Dr. Mulugeta Yilma

A thesis Paper Submitted to

the Department of Chemical Engineering

School of Mechanical, Chemical, and Material Engineering

Presented in Partial Fulfillment of the Requirement for the Degree of Master's in Chemical Engineering (Specialization in Process Engineering)

Office of Graduate Studies

Adama Science and Technology University

September, 2022

Adama, Ethiopia

DECLARATION

I hereby declare that this Master Thesis entitled "Synthesis of Furfural from Xylose Using Carbon Based Bi-Functional Solid Acid Catalyst in Biphasic System" is my original work. That is, it has not been submitted for the award of any academic degree, diploma, or certificate in any other university. All sources of materials that are used for this thesis have been duly acknowledged through citation.

.

Megersa Taddesse Adugna _____ _____

Name of student Signature Date

RECOMMENDATION

We, the advisor(s) of this thesis, hereby certify that we have read the revised version of the thesis entitled "Synthesis of Furfural from Xylose Using Carbon Based Bi-Functional Solid Acid Catalyst in Biphasic System "prepared under our guidance by Megersa Taddesse Adugna submitted in partial fulfillment of the requirements for the degree of Mater's of Science in Process Engineering. Therefore, we recommend the submission of revised version of the thesis to the department following the applicable procedures.

Dr.Zalalem Tumsa _____ _____

Major Advisor Signature Date

Dr.Mulugeta Yilma _____ _____

Co-advisor Signature Date

APPROVAL SHEET

We, the advisors of the thesis entitled "Synthesis of furfural from xylose using carbon based bi-functional solid acid catalyst in biphasic system" and developed by Megersa Taddesse Adugna, hereby certify that the recommendation and suggestions made by the board of examiners are appropriately incorporated into the final version of the thesis.

Dr.Zalalem Tumsa		
Major Advisor	Signature	Date
Dr.Mulugeta Yilma		
Co-Advisor	Signature	Date

We, the undersigned, members of the Board of Examiners of the thesis by Megersa Taddesse Adugna have read and evaluated the thesis entitled "Synthesis of furfural from xylose using carbon based bi-functional solid acid catalyst in biphasic system" and examined the candidate during open defense. This is, therefore, to certify that the thesis is accepted for partial fulfillment of the requirement of the degree of Master of Science in Process Engineering.

Fikadu Lemessa (PhD)		
Chairperson	Signature	Date
Melaku Tesfaye (PhD)		
Internal examiner	Signature	Date
Ali Shemsedin (PhD)		
External examiner	Signature	Date

Finally, approval and acceptance of the thesis is contingent upon submission of its final copy to the Office of Postgraduate Studies (OPGS) through the Department Graduate Council (DGC) and School Graduate Committee (SGC).

Department Head	Signature	Date
School Dean	Signature	Date
Office of Postgraduate Studies	Signature	Date

ACKNOWLEDGEMENTS

First, I would like to thank the almighty of **GOD** for giving me healthy, strength, and patience throughout the entire situations and challenges that I faced for successful completion of this thesis.

Secondly, I would like to express my utmost gratitude to my advisor Dr. Zelalem Tumsa and Co-advisor Dr. Mulugeta Yilma for their guidance, and support in checking, commenting and giving constructive advices all along my activities starting from proposal development and throughout my study.

Next, my deepest thanks to all my teachers in School of Mechanical, Chemical and Materials Engineering at department of Chemical Engineering who had laid a critical foundation of knowledge that inspired me in many ways. I would also like to express my appreciation towards to AASTU laboratory technician under the college of Biological and Chemical Engineering for their essential and valuable help during my experimental work.

Last but not least, I want to express my sincere gratitude to my loving parents for their constant support and encouragement during my endeavor. Not to forget all the postgraduate students and classmates who freely provided crucial advice and support.

TABLE OF CONTENTS

Table of Contents Pages

LIST OF TABLES

Tables **Pages**

LIST OF FIGURES

Figures **Pages**

LIST OF ABBREVIATIONS AND ACRONYMS

BET	Brunauer-Emmett-Teller
CBSC	Carbon Based Sulfonated Catalyst
CPME	Cyclo-Pentyl Methyl Ether
2-MeTHF	2-Methyl Tetra Hydo Furan
DMSO	Dimethyl Sulfoxide
FTIR	Fourier-Transform Infrared Spectroscopy
GVL	Gamma-Valerolactone
HPLC	High Performance Liquid Chromatography
MIBK	Methyl Isobutyl Ketone
IMP	Impregnation
SO_3H@Fe/MC	Mesoporous Carbon Bearing SO_3H Group
PAL-SO_3H	Polygorskite solid acid catalyst
SAC-WP-C1SO_3H	Sulfonated Amorphous Carboneous wood powder catalyst
SABBC	Sulfonated Al-biochar Based Catalyst
SC-CCA	Sulfonated Carbon-Carbon coated Alumina
SEM	Scanning Electron Microscopy
SGO	Sulfonated Graphene Oxide
S-RFC	Sulfonated Resorcinol-Formaldyde resin Carbon
TGA	Thermogravimetric Analysis
UV-Vis	Ultraviolet–Visible spectroscopy
XRD	X-Ray Diffraction

ABSTRACT

Furfural as versatile organic compounds is considered as xylose derived product via dehydration reaction. The purpose of this study was to synthesize furfural from xylose using carbon-based bi-functional solid acid catalyst from flax straw and in biphasic or a mixed solvent consisting of Water and 2-Methyl Tetra Hydro Furan. The carbon based bi-functional catalyst was prepared by impregnation-carbonization followed by sulfonation methods. The characterization of biochar, Al-biochar, and sulfonated Al-biochar catalyst were carried out by using Brunauer Emmet Teller (BET), Fourier transform infrared spectroscopy (FT-IR), X-ray diffraction (XRD), Thermogravimetric analysis (TGA), and SEM (Scanning electron microscopy). The surface area, total acid density and SO_3H density of the sulfonated Al-biochar catalyst were 516.03 m^2/g, 4.767 $\pm$ 0.23 mmol/g and 1.033 $\pm$ 0.1 mmol/g, respectively. The result of FTIR indicated that the presence of the different functional groups such as phenolic group (-OH), carboxylic group (-COOH), sulfoxide group (-SO_3H) and Al-O-Al on the surface of prepared catalyst. The effects of dehydration reaction parameters (reaction temperature, reaction time, and catalyst loading) on the formation of furfural were studied. The maximum furfural formation was obtained at 180 ^oC, 2 hr and 0.2 gm of catalyst loading. The result of HPLC revealed that the furfural yield and selectivity were 64.7%, and 88.0% respectively. The FTIR result also showed that the presence of conjugated carbonyl groups at a band intensity of 1710 cm^{-1} and aldehyde functional groups at wavelength of 2884 cm^{-1} and 2947 cm^{-1} that confirmed the formation of furfural. In general, the conversion of xylose into furfural has been successfully achieved.

Key words*:* Bi-functional solid acid catalyst, Dehydration, Furfural, and Xylose

CHAPTER ONE

1. INTRODUCTION

1.1. Background

Renewable resources are gaining more and more attention due to the growing energy problem and the gradual depletion of non-renewable resources (Lin et al., 2019). In particular, the use of sustainable biomass as a source of raw materials to produce significant chemical platform molecules instead of petroleum has a very significant strategic relevance (S. Hu et al., 2018). Renewable resources, lignocellulosic biomass mostly constituted of hemicellulose, cellulose, and lignin used for the synthesis of second-generation biofuels and biochemical. Among, furfural (FUR) and hydroxymethylfurfural (HMF), which are produced from C_5 and C_6 carbohydrates, respectively, show promise as building blocks for high-value-added products (Agirrezabal-Telleria et al., 2014). Furfural is a major important platform chemical that could be a product of lignocellulosic materials by hydrolysis in acidic media. Furfural has been considered one of the top value-added chemicals from xylose-rich biomass and could be the raw material to synthesize more than 1600 products (L. Gong et al., 2019). According to the US Department of Energy, furfural is one of the bio-based chemicals that should utilize to generate C_4 and C_5 chemicals in a sustainable manner. Through regulation of dehydration conditions, D-xylose and pentosan are promising non-toxic renewable feedstocks for furfural synthesis (X. Guo et al., 2018).

Furfural is a biomass-derived chemical that should be employed in a variety of industrial applications. The chemical industry, oil-refining industry, food industry, pharmaceutical industry, paint industry, and agricultural industry are examples of industries. It is also used to refine lubricating oils and resins, as well as to improve the qualities of diesel fuel. It is primarily employed in large-scale enterprises as a starting material for the production of a group of derived solvents such as furfuryl alcohol and tetrahydrofuran and also in the preparation of resin for metal coating (Dawale et al., 2020). Furfural is also utilized in the production of thermosetting copolymer resins such as furfural–phenol, furfural–acetone, furfural–urea, and furfural–formol, as well as other high-molecular-weight plastics like polyvinylfurfural (Cortés Ortiz et al., 2013).

Amongst the numerous routes of lignocellulosic biomass valorization, catalytic hydrolysis, and dehydration of D-xylose to produce furfural represents an attractive strategy. This is because of the versatility of using furfural as an important platform molecule to synthesize an

array of intermediate chemicals, from which a diverse range of biofuels as well as commodity and fine chemicals should be generated under different reaction conditions like hydrogenation, oxidation, chlorination, nitrification, and Decarboxylation (Chen et al., 2015). In the beginning, high pressure, high temperature, and high sulphuric acid concentrations were used to make furfural. These conditions resulted in a large cost of furfural production, both in terms of capital expenditures and operating expenses, due to the corrosive effects of the sulphuric acid and the high pressures and temperatures that had to be maintained (Z. Qi et al., 2020). This method is not ideal for making furfural since it had low yields of around 53%, and harmful to the environment (Dulie, Woldeyes, Demsash, et al., 2021).

Because of their great hydrothermal stability and inexpensive cost, carbon-based solid acids have gotten more attention. Based on the carbon sources and preparation processes, the carbon-based solid acids currently employed for biomass conversion can be split into two types. The first group is made up of biomass or biomass leftovers. Carbon was obtained from lignocellulosic biomass such as wood sawdust, corncobs, miscanthus cassava, Flax straw, and water hyacinth. The second group is made from biomass-derived monosaccharides or other small-molecule organic molecules using hydrothermal synthesis or aldol condensation (Xu et al., 2021).

The cellulose, hemicellulose, and lignin found in flax straw make it lignocellulosic biomass that can be utilized as a starting point for the synthesis of biomaterials, chemicals, and fuel. There have been reports of cellulose and lignin being used as carbon sources to synthesize catalysts (Ji et al., 2021; Xu et al., 2021; L. Zhang et al., 2019). These biopolymers are found in lignin-carbohydrate matrices, which give lignocellulosic biomasses a range of physical and chemical characteristics. In the matrix, lignin serves as a connecting component between hemicellulose and cellulose. The lignin demonstrated a tendency to preserve the native macrostructure of the initial biomass during carbonization (Wei et al., 2020). The hydrogen bonds between the chains and glycosidic bonds between the D-glucopyranose units give cellulose its crystalline and amorphous forms (Paksung et al., 2020).

Recently, carbon based solid acid catalyst is developing rapidly and carbon material has become a hot research area because it can be applied as smart materials (Lathiya et al., 2018). Carbon based solid acid can be functionalized with lewis acid, Bronsted acid, or lewis-bronsted acid groups according to the nature of feedstocks (Hazmi et al., 2022). Laohapornchaiphan et al (2017) found that 57 % of furfural yield was obtained from xylose conversion via dehydration reaction catalyzed by carbon based solid acid catalyst synthesized

from water hyacinth leaves. Dulie et al (2021) synthesized the carbon based solid acid catalyst from teff straw and applied for catalyzing the transformation of xylose into furfural. They found that yield of furfural of 62.4 % could be achieved at 170 ^{o}C for 30 minutes in a biphasic water/toluene system. Sádaba et al (2011) prepared the vanadium phosphates as the catalysts for dehydration xylose into furfural and the results show that the yield of furfural was 56% at 170^{o}C for 6 hr reaction conditions in the water/toluene solvent mixtures. Bi-functional carbon based catalyst consists of Lewis acid used for isomerization of xylose into xylulose with bronsted acid used for dehydration of xylulose into furfural simultaneously (Jiang et al., 2021). Moreover, carbon based bi-functional catalysts are very advantageous compared to other heterogeneous catalysts as they can be recyclable, reused, regenerated, and easily separated from the reaction products (Elias et al., 2020).

Typically, the preparation process of a bi-functional solid acid catalyst was separated into three steps: impregnation, carbonization, and sulfonation. Impregnation is the process of some inorganic or metal compounds captured on the surface of biomass to facilitate the Lewis acidity of the prepared catalyst. In the process of carbonization, carbonaceous organic molecules are pyrolyzed while non-carbon components escape as volatiles to create pores and solid pyrolysis products that are high in carbon (Sun et al., 2020). The process aims to produce a carbonized material that is suited for sulfonation, has fundamental pores, and has a high specific surface area. The third and final step of bi-functional solid acid preparation is the sulfonation process, which is the process that identifies an electrophilic chemical reaction where a sulfonic group SO_3H is incorporated into a molecule with the capacity to donate electrons (Torres Ortega, 2012).

In this study, attempts have been made to investigate the possibilities of using flax straw agricultural residue, as a support for bi-functional solid acid catalyst by applying the process of impregnation, carbonization and sulfonation methods. The produced catalysts surface area, physio-chemical, surface functional group and crystalline structure were aslo examined. Finally, the catalyst activity was evaluated on dehydration of xylose into furfural and the effects of reaction conditions were investigated during the dehydration of xylose into furfural in the 2-MeTHF/water-NaCl biphasic system using bi-functional solid acid catalysts. Additionally, to the best of our knowledge, no studies that examine the value of flax straw as a carbon source in the production of bi-functional acid catalysts for use in the production of furfural have been published.

1.2. Statement of the problem

Furfural can be derived from pentosan-rich lignocellulosic biomass, particularly from xylose, which is a key feedstock that can be transformed into important non-petroleum chemicals and bio-fuels. Traditionally, the production of furfural mainly proceeds via dehydration of xylose in the aqueous phase over a homogenous catalyst such as HCl and H_2SO_4. However, the homogenous catalyst has equipment corrosion, impractical catalyst recovery, as well as environmental hazards (Z. Qi et al., 2020). To overcome the shortcoming in homogenous catalysts, a green approach to chemical processes has stimulated the use of recyclable strong solid acids as replacements for such unrecyclable liquid acid catalysts.

Therefore, several solid acid catalysts developed such as zeolites, cation ion exchange resin, and sulfonated metal oxides recently gained much attention because of their ease of separation and lack of corrosion or toxicity problems for furfural production (D. Hua et al., 2021; Kim et al., 2011; Suzuki et al., 2011). However, these catalysts have several disadvantages like high cost, low catalytic activity, complex fabrication technology, and poor stability. In fact, from heterogeneous catalyst biomass, based sulfonated carbon catalyst has lower cost, abundant, reusability, and renewable compared to other solid acid catalysts (Dulie, Woldeyes, & Demsash, 2021; He et al., 2021). Nevertheless, the yield and selectivity of furfural using sulfonated carbon based catalyst are lower due to its less catalytic activity. Rusanen et al (2020) reported 57% of furfural yield from the reaction of xylose in a water-MIBK biphasic medium using iron supported lignin-based activated carbon. Likewise, Toumsri et al (2021) reported 45% of furfural yield from xylose using SO_3H@Fe/MC as the catalyst in γ-Valerolactone at 170 ^oC for 1hr reaction conditions. Therefore, to address these problems, synthesizing bi-functional carbon based catalysts from biomass that combines the Lewis acid site (isomerization of xylose into xylulose) with the Bronsted acid site (dehydration of xylulose into furfural) is very important. Bi-functional carbon based catalysts are a more promising option because it requires less energy and produces higher furfural yield and selectivity.

1.3. Objectives

1.3.1. General objective

The main objective of the study was to synthesize furfural from xylose using carbon based bi-functional solid acid catalyst in a biphasic system.

1.3.2. Specific objectives

The specific objectives of the study were;

- To synthesize carbon based bi-functional solid acid catalyst from flax straw biomass.
- To investigate the effects of catalyst preparation conditions on the sulfonic acid density of carbon based bi-functional solid acid catalyst.
- To characterize physico-chemical, surface functional group and crystalline structure of the bi-functional flax straw based solid acid catalyst.
- To investigate the effects of dehydration reaction conditions (reaction time, catalyst loading, and reaction temperature) on the conversion of xylose into furfural and formation of furfural using carbon based bi-functional solid acid catalyst.

1.4. Research questions

This study aspires to answer the following research questions;

- Can it be possible to improve the yield and selectivity of furfural from xylose using a carbon-based bi-functional solid acid catalyst synthesized from flax straw?
- How the reaction conditions (parameters) affect the conversion of xylose and/or yield of furfural?

1.5. Significance of the study

The study has great significance to dehydrate xylose into furfural as an alternative form of top platform chemical. This has also a versatile application in different industry such as plastics, pharmaceutical, agrochemical and other. Bi-functional solid acid catalyst that can be derived from flax straw is important to develop a protections mechanism of environmental pollutions, sustainable availability and its inexpensiveness. Besides, it is believed that, the study provide the possibilities of:-

- Increasing the utility value of domestic raw material
- Minimizing environmental load emissions due to commercial catalyst

- The study could be a benchmark for using agricultural residues biomass as a raw material for bi-functional solid acid catalyst preparation for the application of furfural production.

1.6. Scope of the study

The scope of the current study was production of furfural from xylose by using bi-functional carbon based catalyst from flax straw and characterization of the product. It is also about the synthesis of carbon based bi-functional solid acid catalyst from flax straw and explores the effects of catalyst preparation conditions on the acid densities of prepared catalyst. In addition, it includes characterization of physio chemical properties, surface functional group, surface morphology, and crystalline structures of the developed catalyst. Moreover, it investigates the effect of reaction conditions parameters (reaction time, reaction temperature, and catalyst loading) on the furfural concentration.

1.7. Organization of the thesis

The thesis is organized into five chapters as shown in Figure 1.1;

Chapter 1: Describes introduction part of the thesis with including the statement of the problem, objective of the study, significance of the study as well as the scope the study.

Chapter 2: Literature Review provides the potential sources of furfural production, chemistry of furfural formation, various types' solid acid catalyst used for furfural synthesis and the challenges encountered by these catalysts compared with bifunctional solid acid catalyst. It also explores the methods of bifunctional catalyst synthesis from biomass as well as solvent systems used to improve the yield furfural that investigated by different scholars.

Chapter 3: Materials and Methods of the works, including the catalyst preparation procedures and conditions, characterization methods and apparatus as well as catalyst performance on the conversion of xylose into furfural are described in the experimental methodologies.

Chapter 4: Results and Discussions describe the suitability of flax straw based catalyst for the use of furfural production is explored. The effects of the preparation conditions, the carbonization and sulfonation time and temperature, on the functionalization of the carbon structure and the catalytic performance of the prepared flax straw-based catalyst were

evaluated. The catalytic activity of a solid acid catalyst with a -SO_3H and Lewis acid functional group as an active site in a biphasic system is investigated.

Chapter 5: Concludes the study and suggests the possible recommendations.

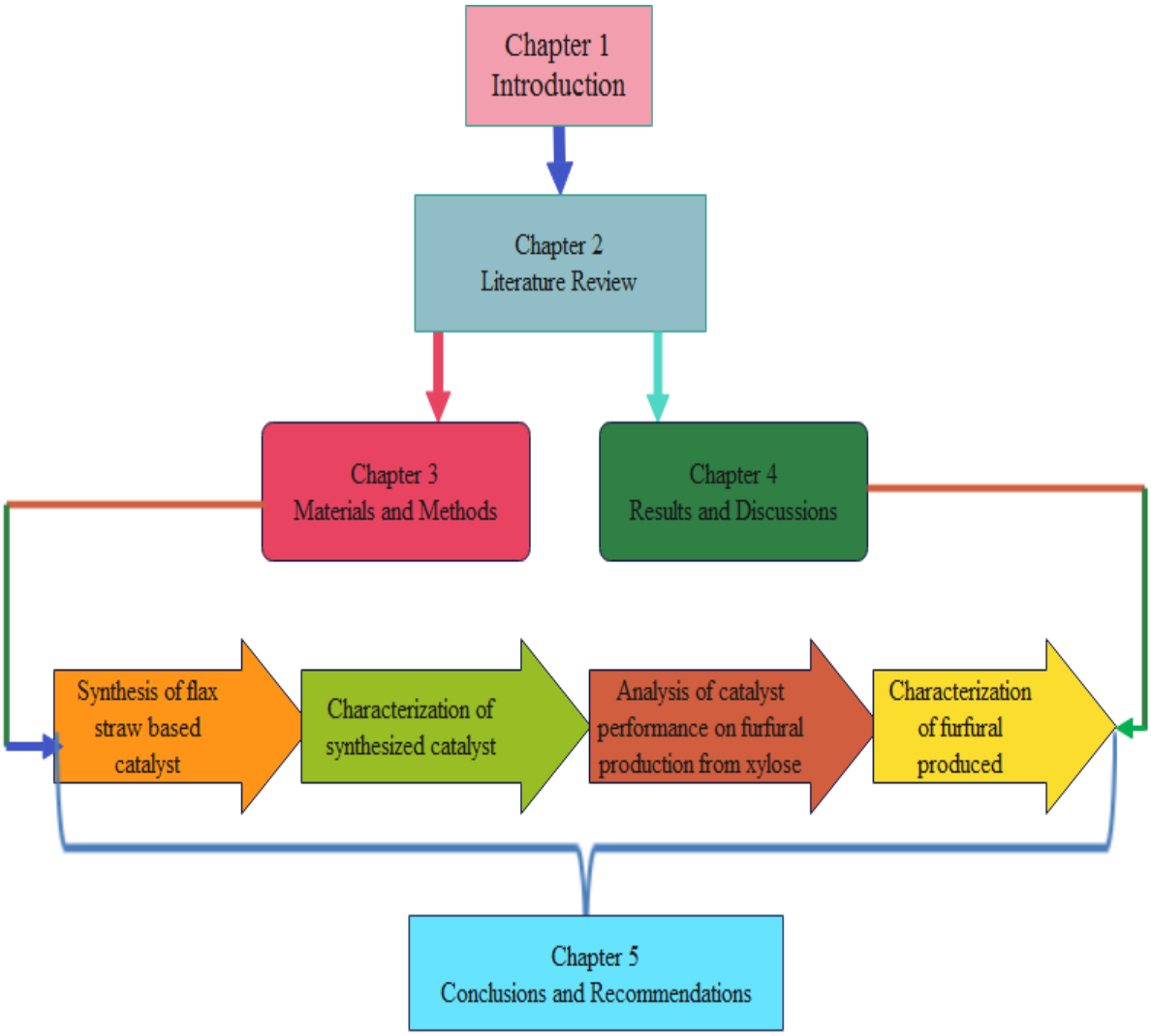

Figure 1. 1. Organizational structure of the thesis

CHAPTER TWO

2. LITERATURE REVIEW

2.1. Background of furfural productions

The manufacturer of furfural ranks one of the largest industries as compared to the others found in the worlds. Globally the production of furfural is led by China, South Africa, and Dominican Republic which accounts 90% of furfural production (Gabriel et al., 2020). China is the major producer as well as major consumer of furfural in the world, which accounts 70% of furfural assembling. It is expected that, the low production cost of furfural in China is to remain as a key driving factor for the domestic market. However, the furfural industry in China has been facing an issue of availability of corn cob (Dalvand et al., 2018; Mishra et al., 2019). However, recently there is an increasing awareness in the United States towards producing furfural and other furanic compounds from biomass because of an increase in oil prices and the potential of these compounds to produce value-added chemicals. Furfural was first isolated in 1821 by German chemist Johann Wolfgang Dobereiner, produced as a byproduct of formic acid synthesis. In 1840, the Scottish chemist John Stenhouse found that furfural is also produced by a more variety of crop material such as corn, oats, bran and saw dust, he also made an empirical formula for furfural as $C_5H_4O_2$ an aldehyde (CHO) and a conjugated system (C=C-C=C) these are two important functional groups of furfural. In 1920, that the first systematic research was conducted to produce furfural from corncobs. Industrial processes for furfural production were developed as early as 1921 when the Quaker Oats batch process was developed to produce furfural from oat hulls (Agirrezabal-Telleria et al., 2014; Dawale et al., 2020).

2.2. Furfural

Furfural frequently called as 2-furaldyde, furan-2-carboxaldyde, fural, and furfural aldehyde, is a chemical compound that can be obtained from the lignocellulosic biomass mainly pentosan group which is called xylose. Its chemical structure shown in Figure 2.1 is dissolves readily in most polar solvents, but it is slightly soluble in either water or alkanes. It is an almond-scented, colorless liquid that turns yellow to dark brown when exposed to air and used as a solvent for refining lubricating oils, and in the production of tetrahydrofuran, an important industrial solvent. Some of furfural physical properties are shown on Table 2.1 Excellent furfural physical properties make it a great selective extractant that can be used in aromatics removal from lubricant oils improving relationship

between viscosity and temperature, aromatics removal from diesel to improve ignition properties, cross-linking in polymers and use as fungicide (Yan et al., 2014).

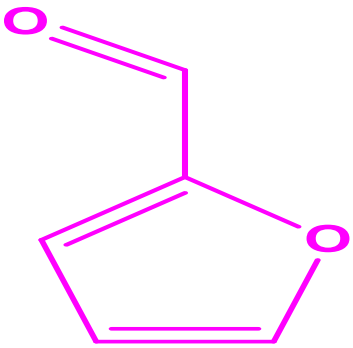

Figure 2. 1: General structure of furfural

Table 2. 1. Physical properties of furfural

Physical properties	Values
Molecular weight (g/mol)	96.08
Freezing point (^{o}C)	-36.5
Boiling point (^{o}C)	161.7
Density at 25^{o}C (g/cm^{3})	1.16
Viscosity at 25^{o}C (mPA)	1.5
Critical pressure (Mpa)	5.502
Critical temperature (^{o}C)	397
Heat combustion at 25^{o}C (KJ/mole)	234.4
Heat of formation (liquid at 25^{o}C) (KJ/mole)	-151
Heat of vaporization at (KJ/mole)	42.8

2.2.1. Sources of furfural production

Normally, the source of furfural production was obtained from lignocellulosic biomass. Agricultural and agro-industrial residues are abundant sources of organic compounds and present large potential for use as raw material for the production of value-added compounds. This residue is composed of three main fractions, namely cellulose, Hemicellulose, and lignin (Mesa et al., 2014). Hemicellulose is the second most abundant polymer containing about 20–40 % of lignocellulose biomass (Roweell, 2013). It has branches with short lateral chains consisting of different types of sugars. These monosaccharide's include pentose's (xylose, rhamnose, and arabinose), Hexoses (glucose, mannose, and galactose), and uronic acids (4-O-methylglucuronic, D-glucuronic, and D-galactouronic acids) (Saha et al., 2003). A Hemicellulose can be any of several heteropolymers (matrix polysaccharides), present in almost all plant cell walls along with cellulose.

2.2.2. Xylose

Xylose is the second most abundantly available sugar in nature next to glucose. It is one of the hemicellulose based (C_5) sugars and is often discarded during the conversion of lignocellulosic biomass to biofuels (Satyavolu et al., 2021). Like most sugars, it can adopt several structures depending on conditions. With its free carbonyl group, it is a reducing sugar. D-Xylose is widely applied industries include pharmaceutical (as intermediate: in medicine manufacturing); food production (as sweetener in beverage and food); cosmetics (as humectant: in cleanser, beauty creams and lotions to maintain the moisture); human consumption; agriculture /animal feed, etc (Z. H. Liu & Chen, 2015). Moreover, xylose is a precursor to synthetic polymers, a solvent in industry and various chemicals such as furfural production (Ricciardi et al., 2021), xylitol (Cheng et al., 2011), Bioethanol production (Lamptey et al., 2019) and ethanol production (Matsushika et al., 2009). In addition, D-Xylose is widely applied industries include pharmaceutical (as intermediate: in medicine manufacturing); food production (as sweetener in beverage and food); cosmetics (as humectant: in cleanser, beauty creams and lotions to maintain the moisture); human consumption; agriculture /animal feed, etc (Sánchez-Moreno et al., 2019). Usually, Hemicellulose will be easily released xylose by hydrolysates of samples with acid catalysts. Figure 2.2 describes the structure of xylose.

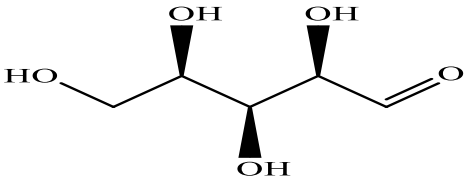

Figure 2. 2. Structure of D-xylose

2.3. Chemistry of furfural formation

Furfural is universally made from agricultural raw materials rich in pentosan. By aqueous acid catalysis, the pentosan is hydrolyzed to pentose, and this pentose is dehydrated to furfural in a unified process. The conversion of hemicellulose to furfural takes place through two steps. The first step is the hydrolysis of polysaccharide into simple sugar where xylan is broken down into the monomer xylose. Xylose is then converted to furfural in the second step through dehydration by removal of three molecules of water (shafeq et al., 2015; Zeitsch et al., 2000). The stochiometry of the two reactions reads as follows;

Pentosan + n×water $\longrightarrow$ n×pentose (2.1)

$(C_5H_8O_4)\ n + nH_2O \longrightarrow nC_5H_4O_2$

Pentose + 3water $\longrightarrow$ Furfural (2.2)

$C_5H_{10}O_5 + 3H_2O \longrightarrow C_5H_4O_2$

Thus, the overall reaction can be said to be,

Pentosan +2water $\longrightarrow$ Furfural (2.3)

2.3.1. Pentosan hydrolysis to pentose

Pentosan consists predominantly of rings linked by oxygen bridges (ether bridges). As shown in Figure, 2.3 protonation of oxygen link is the first step of hydrolysis of pentosan and carbon oxygen bond cleavage follows resulting in the formation of the hydroxyl group on one side Oxygen Bridge and carbonium ion is formed during the reaction on the other side. The addition of water molecule onto carbocation forms H_2O^+ group and then H_2O^+ group liberates hydrogen ion leaving a hydroxyl group behind. These steps of hydrolysis continue until the all oxygen bridge disappears (Gebre et al., 2015).

2.3.2. Dehydration of pentose to furfural

Numerous mechanisms for the conversion of xylose to furfural have been proposed but, most studies emphasis on the cyclodehydration mechanism removing three molecules of

water using heterogeneous catalysts. Figure 2.3 shows xylose dehydration to furfural with 1,2- eliminations via 1,4-elimination. In the 1,2, elimination, the H^+ attacks a non-bonding electron pair of a hydroxyl oxygen bound to a carbon atom, it creates a trivalent positively charged oxygen atom. Oxygen is more electronegative than carbon, so the positive charge immediately shifts to the neighboring carbon to produce a fission of the C=O bond, a positively charged carbon and the liberation of a water molecule. Under this situation, two electrons form a neighbor C=X bond are attracted to form a double C=C bond. During this step, the ring is opened and the liberated hydrogen seeks for another non-bonding electron pair. As well as in the first step, this liberates another water molecule and created another double carbon bond. In the last 1,4-elimination, the trivalent oxygen atom does not create another C=C bond, but it closes the opened ring due to the fact that atoms participating in double bonds form planar structures characterized by bond angles of 120^o (plane trigonal orbitals) and leading to the formation of furfural (Agirrezabal-Telleria et al., 2014).

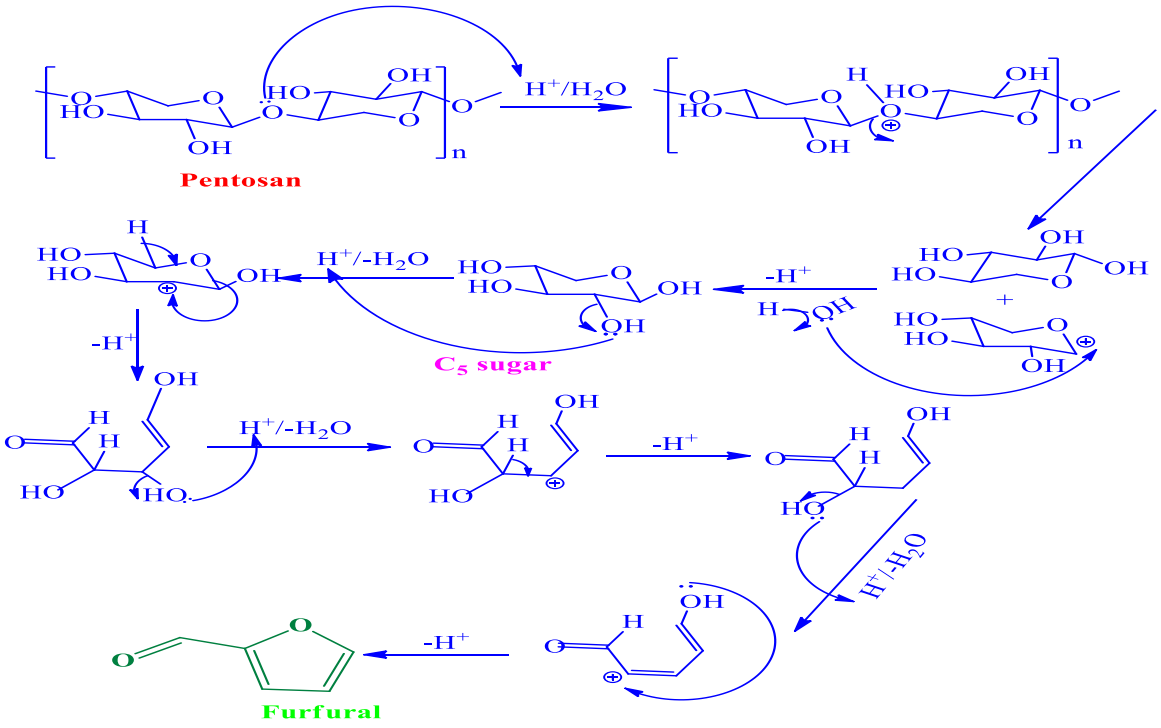

Figure 2. 3. Mechanism of hydrolysis of pentosan and dehydration of pentose

2.4. Application of furfural and its derivatives

Of the many actual and potential applications of furfural, the treatment is limited to a few fields where furfural is used as it is. It is merely noted that 65% of all furfural produced is converted to furfuryl alcohol. Furfural has several applications such as antacids, fertilizers, plastics, inks, fungicides, gasoline additives, pharmaceuticals, chemicals and biopolymers,

lubricants and resins, nematocides, adhesives and flavoring compounds (Zeitsch,2000). One of the different applications of furfural is on hydrocarbons purification technology of C_4 and C_5, which was developed during the II World War for butadiene fabrication in the United States for synthetic rubber production. Through extractive distillation with furfural, butadiene can be separated from other hydrocarbons C_4 and C_5 respectively (Machado et al., 2016). The main furfural derivatives and its applications are shown on Figure 2.4.

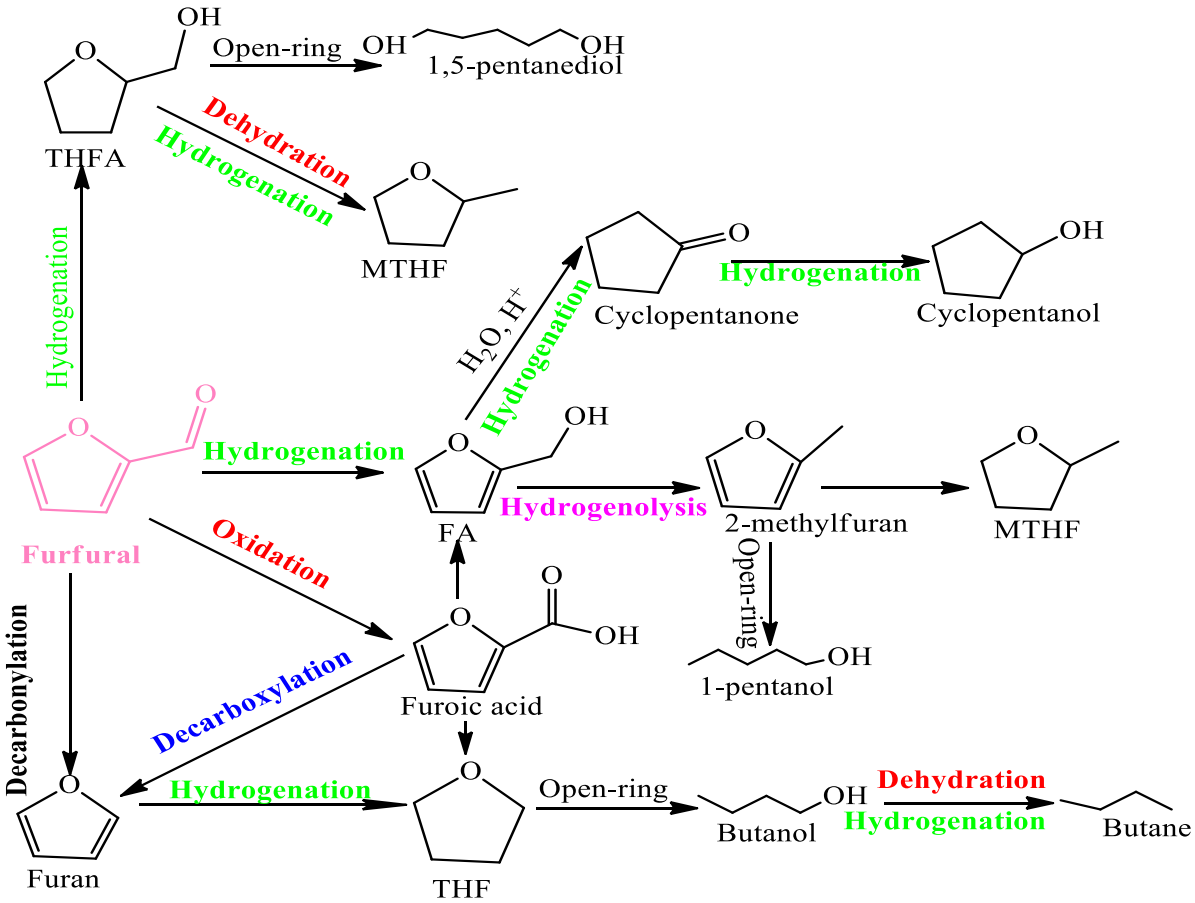

Figure 2. 4. Conversion of furfural into a number of high value added compounds

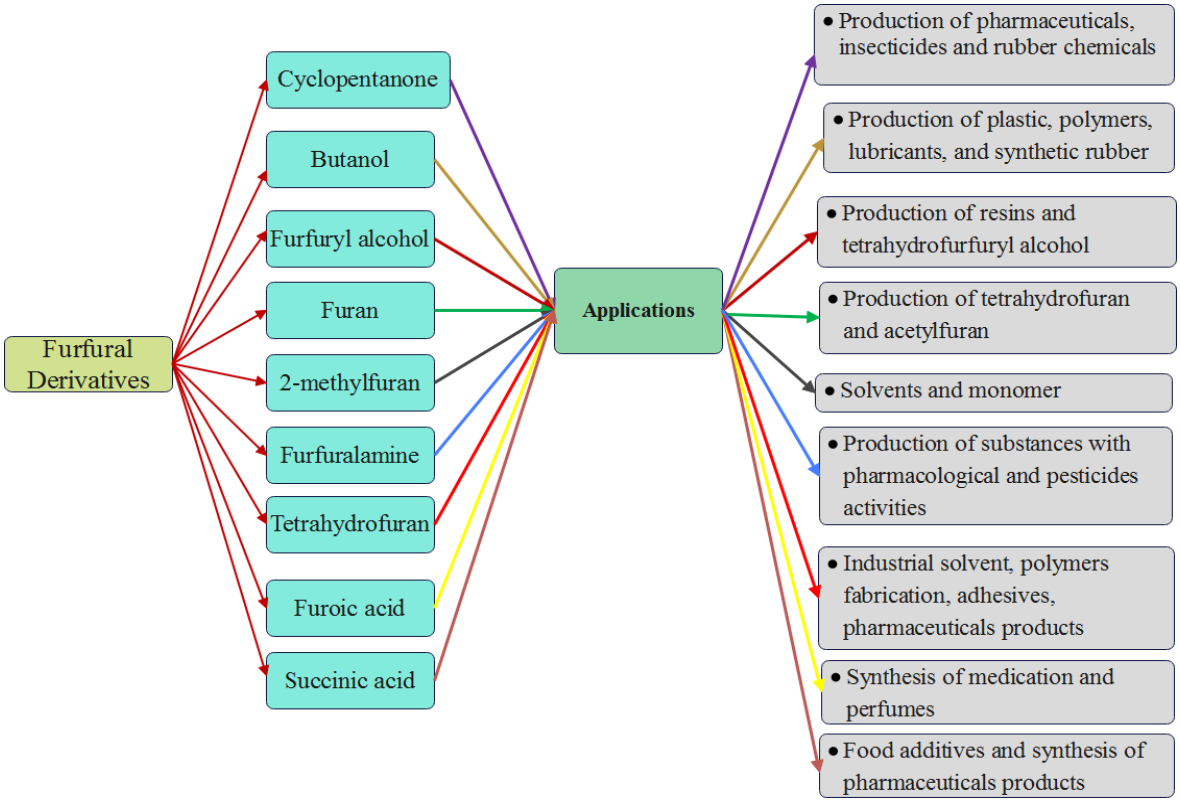

Figure 2. 5. The main derivatives of furfural and their applications

2.5. Catalyst

Catalysis is the process of speeding up a chemical reaction. The reactions are faster and require less activation energy. Generally, there are three types of catalysts homogeneous, heterogeneous, and enzyme catalysts. Enzyme catalysts are more expensive and require the purification of feed when compared to other catalysts. It is easier to recycle catalysts and to separate product from heterogeneous catalysts than homogeneous catalysts.

2.5.1. Homogenous catalyst

The homogeneous catalyst refers to the catalyst that can be dissolved in the reaction medium. In principle, there are no restrictions on the phase to be considered; the reaction can take place in either a gaseous or a liquid phase. There is a wide range of homogeneous catalysts available, ranging from Bronsted and Lewis acids, which are commonly used in organic synthesis, to metal complexes, metal ions, organometallic complexes, organic molecules, and biocatalysts (Enzymes, artificial enzymes, etc.). Unlike most heterogeneous catalysts, homogeneous catalysts usually do not need to be synthesized by researchers, and their catalytic performance is better than that of heterogeneous catalysts due to their uniform dispersion (Y. Zhao et al., 2021). In the last decades, comprehensive studies on the conversion of xylose into furfural have been performed instead of raw biomass for

simplification of analysis. Homogeneous catalysts, mineral acids, and metal chlorides have been investigated for furfural production. Among the mineral acids, sulfuric acid and hydrochloric acid are the most widely used catalysts for the commercial production of furfural. Yemiş & Mazza (2011) investigated and compared the catalytic activities of different acids including sulfuric acid, nitric acid, phosphoric acid, hydrochloric acid, acetic acid, and formic acid-targeting at the yield and conversion of furfural. Agirrezabal et.al investigated the effect of sodium chloride on the dehydration rate of xylose to furfural and achieved 76% furfural yield at 200 °C in a reaction time of 8 min (Agirrezabal-Telleria et al., 2013). However, the main drawbacks of homogenous catalysts are; high energy consumption, equipment corrosion, impractical catalyst recovery, environmental hazards, they cannot be effectively recycled after the reaction which makes it difficult to reduce the cost in industrial applications (L. Gong et al., 2019; Mishra et al., 2019).

Table 2. 2. Homogenous catalyzed onversion of xylose into furfural

Substrate	Catalyst	Reaction condition	solvent	Yield furfural	Reference
Xylose	Betaine-Formic acid	120^{o}C; 60min	CPME:H_2O	80%	(Delbecq et al., 2016)
Xylose	Iron chloride	170^{o}C; 20min	NaCl-H_2O-CPME	74%	(Guenic et al., 2015)
Xylan	Tin chloride	150^{o}C; 120min	2-MTHF/H_2O	78.1%	(W. Wang et al., 2015)
Xylose	Aluminum chloride	140^{o}C; 45min	THF-H_2O-NaCl	75%	(Y. Yang et al., 2012)
Xylose	$Sn_{0.625}Cs_{0.5}PW$	200^{o}C; 300min	DMSO-H_2O	63%	(X. Guo et al., 2018)
Xylose	Cupper chloride/HCl	140^{o}C; 120min	Toluene-water	76%	(Choudhary et al., 2012)

2.5.2. Heterogeneous catalyst

In chemistry, heterogeneous catalysis is catalysis where the phase of catalysts differs from that of the reactants. Heterogeneous catalysis typically involves solid phase catalysts and gas phase reactants. Heterogeneous catalysis is very important because it enables faster, large-scale production; the selective product formation and they can work at high temperatures by decreasing the reaction time which can favors the formation of required product instead of its decomposition during a prolonged reaction period (X. Hu & Yip, 2021). In addition to that, they are capable of adjusting the surface acidity to improve the selectivity of HMF and furfural, which will be very useful in the conversion of biomass, feedstocks. Solid acid catalysts have been the most widely employed heterogeneous catalysts in the petrochemical industry, particularly for organic reactions (Long et al., 2019). Heterogeneous catalytic reactions for furfural preparation are more complex than homogeneous reaction.

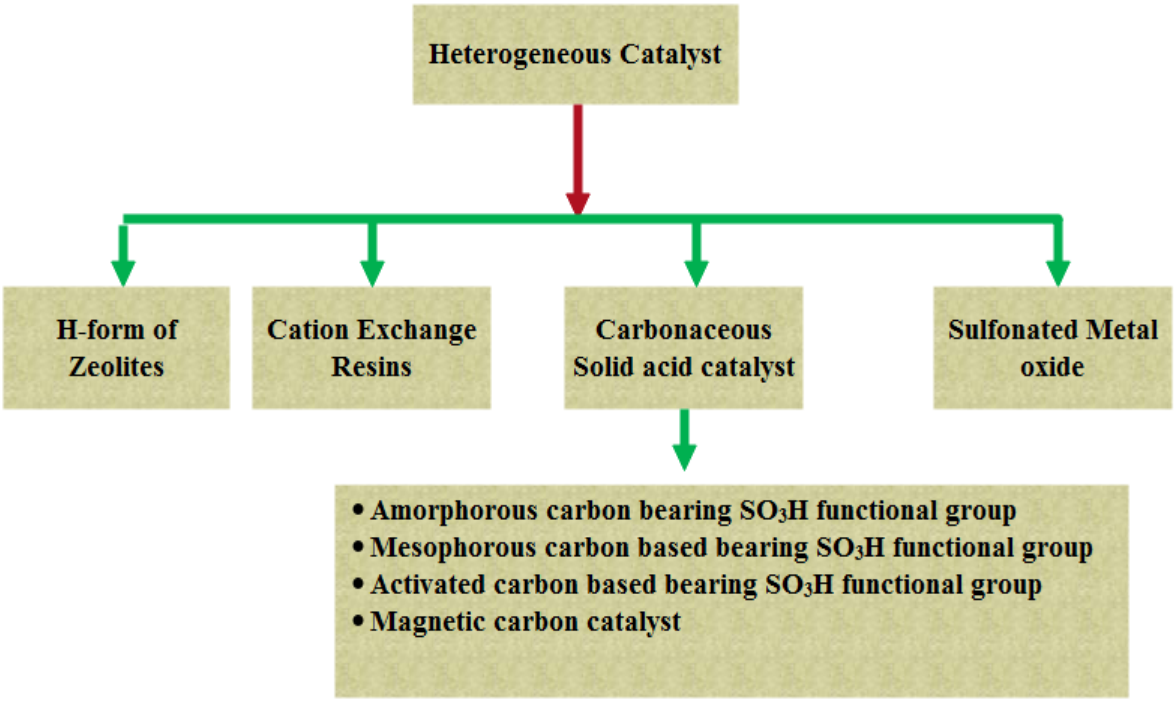

Figure 2. 6. Various types of a heterogeneous catalyst

A. H-form of zeolites

In a recent study, various solid acid catalysts such as sulfuric acid functionalized mesoporous SBA-15 materials, modified zeolites such as HUSY, H-Beta zeolite, H-mordenite, and MCM-41 are among heterogeneous solid catalysts that were developed for furfural production to solve the problems associated with the use of homogeneous catalysts. Arenesulfonic SBA-15 catalysts were prepared via co-condensation for the

dehydration for *d*-xylose to furfural (Agirrezabal-Telleria et al., 2014). High arenesulfonic-site and tight hexagonal pore configuration characterize these selective and hydrothermally stable catalysts. The activity of sulfonic acid functionalized mesoporous SBA-15 materials was investigated, with a focus on the catalyst's stability. They produced 82% furfural yield from d-xylose in water/toluene at 160 ^{o}C with 99 percent selectivity. Despite the fact that the solvent utilized in the study to extract furfural from water medium (toluene) is not a green chemical, arenesulfonic functionalized SBA-15 supports aged at higher temperatures exhibit increased stability and recyclability (Agirrezabal-Telleria et al., 2014). The most studied solid catalysts are zeolites, which are thermally and chemically stable, have tunable acidities and shape (Agirrezabal et.al, 2011). Furfural yield of lower than 40% was achieved on studies using a variety of H-zeolites (e.g., HYfaujasite, H-mordenite, and H-ferrierite) in water, water/methyl isobutyl ketone (MIBK), water/toluene and dimethyl sulfoxide (DMSO) in a batch reactor at 140–170 ^{o}C (Dias et al., 2005). However, these catalysts remain associated with one or more disadvantages like low acid density, small pore size, low porosity, fast deactivation, poor tolerance towards the water, poor stability and the high cost of synthesis (Xia et al., 2021). Their catalytic activity is very much lower than the bi-functionalized carbon based solid acid catalyst.

B. Cation-exchange resins

An ion-exchange sulfonic resin was used to catalyze the synthesis of furfural. 40-70% yield was achieved by using ion-exchange resins. The nature and qualities of the resins Amberlyst and Nafion, which have varied acidities, pore sizes, and thermal stabilities, allowed the dehydrated compounds to be produced depending on the method. The kinetic characteristics of furfural generation in a biphasic water-toluene system, with or without catalyst, at various reaction temperatures and times, as well as D-xylose loading and simultaneous nitrogen stripping, were investigated (Agirrezabal-Telleria et al., 2011). In this study, D-xylose provided 65% of the stripping furfural, and the condensate showed nearly 100% selectivity. Later, the effect of adding D-glucose to Xylose on furfural synthesis was investigated under various working conditions (Agirrezabal-Telleria et al., 2012). At 175 ^{o}C, adding D-glucose to D-xylose has a detrimental influence on furfural yield, but a favorable effect at 200 ^{o}C, which is referred to as a "entropy effect" at high reaction temperatures, resulting in slower side reactions. Furfural yields of up to 75 percent at 200 ^{o}C were achieved using a mixture of D-xylose and D-glucose in similar ratios to the genuine pentosan-rich biomass, and even 78 percent with lower D-xylose concentrations.

Amberlyst-70 with strong sulfonic acid sites had greater furfural selectivity than Nb_2O_5 supported catalyst, according to the same group (Agirrezabal-Telleria et al., 2013). A sulfated tin ion-exchanged montmorillonite (SO_4^{2-}/SnMMT) in 2 Methyltetrahydrofuran (2-MTHF)/NaCl-water showed high activity and reusability with furfural yield of 79.64% from xylose at 160 ℃ (Lin et al., 2017). Niobium-based catalysts combine acidic properties with high stability in aqueous medium, which has led to moderate furfural yields in biphasic media (around 60% in 6 h). Finally, acid resins like Nafion and Amberlyst have also received attention as catalysts for the dehydration of xylose. They are commercially available and inexpensive materials with high acidity and mechanical stability. Nevertheless, commercial resins typically feature low surface area (i.e., $<1 m^2/g$ and $0.02 m^2/g$ for Amberlyst-15 and Nafion respectively), which limits their use as catalyst. So far, a suitable combination of catalytic activity and transport properties, which is much needed to guarantee high yields and catalyst/reactor stability has not been reported (Krzelj et al., 2021).

C. Carbonaceous solid acid catalyst

Carbon-based solid acids can be made through incomplete carbonization of carbohydrates or lignocellulosic materials at high temperatures in a nitrogen environment, followed by a high-temperature sulfonation process of the carbon precursor. Sulfonation agents such as fuming sulfuric acid, chlorosulfonic acid, and concentrated sulfuric acid can be utilized. Three kinds of functional groups that were phenolic -OH, -COOH and -SO3H, -COOH that exist in sulfonated carbonaceous solid acid catalysts might be the main reason for efficient catalytic activity of the carbon material compared to the conventional solid acids that usually only had single functional groups. Based on the carbon sources and preparation processes, the carbon-based solid acids currently employed for biomass conversion can be split into two types.

- ✓ Solid acid catalyst prepared from biomass or biomass residues. Lignocellulosic biomass such as wood sawdust, corn cobs, flax straw, teff straw, miscanthus cassava, and water hyacinth were used as carbon sources
- ✓ Solid acid catalyst prepared by hydrothermal synthesis or aldol condensation, usually using biomass-derived monosaccharides or other small-molecule organic compounds as carbon sources.

Several studies have been reported on the investigation of carbon based solid acid catalysts. Typically, sulfonated process of carbon based solid acid catalyst can be produced in the two-step process. Z. Qi et al (2020) synthesized the magnetic carbon based solid acid catalyst by using iron chloride as the impregnation before carbonization at 350 ^{o}C for 1hr under nitrogen protection followed by sulfonation with the concentrated sulfuric acid (98% w/w), the solid –liquid ratio of 1:10 at 130 ^{o}C for 10 hours. Various carbon sources, acid functional groups, structures, and other additional qualities were developed in the recent development of carbon catalyst in the dehydration of xylose into furfural to boost selectivity and yields. The initial step is the carbonization of the raw biomass between 150 and 250 °C, which is followed by the sulfonation time from 4 to 8 hr. Teff straw was used to generate a sulfonated carbon-based catalyst, and the process yielded 62.4% of furfural at 170 ^{o}C for 30 minutes in a biphasic water/toluene system (Dulie, Woldeyes, & Demsash, 2021). similarly, the yield of furfural was achieved 80% at 170 ^{o}C for 60min with the conversion of xylose 100% using the solid acid catalyst prepared from the pectin and GVL used as the solvent (Xu et al., 2021). Zhang and their co-worker investigates the furfural yield of 78.5% at 170 ^{o}C for 30min in the GVL used as the media and their catalyst used can be prepared from the material which contains sucrose contents using 4-BDS as sulfonated agent (T. Zhang et al., 2016).

D. Sulfonated metal oxides

Sulfonated metal oxides were also used for the dehydration of xylose to produce furfural. Surface treatment of these oxides with acids such as sulfuric and phosphoric acids can also produce functionalized solid acid catalysts. Metal oxides such as TiO_2, ZrO_2, SnO_2, and Al_2O_3 were also studied and proved that SnO_2 gives the highest xylose conversion and furfural yield. $SO_4^{2-}/ZrO_2–TiO_2$ gave a higher yield than the selected zeolite catalysts (J. Zhang, Lin, et al., 2012). Ma et al (2019) reported the dehydration of xylose to furfural within the continuous process by water/1-butanol biphasic system at the 180 ^{o}C within 80min and achieved the 59% of furfural yield. Compared with the carbon-based solid acids, the sulfonated metal oxides have a more stable and clear structure and better catalytic performance, but the cost of raw materials is relatively higher and the catalyst preparation process is more complicated.

Table 2. 3. Heterogenous catalyzed conversion of xylose into furfural

Substrate	Catalyst	Reaction condition	Solvent	Yield furfural	Reference
Xylose	sulfonated sporopollenin	190^{o}C; 40min	H_2O-CPME	69%	(Y. Wang, Len, et al., 2017)
Xylose	Sn-MMT	180^{o}C; 30min	SBP/NaCl-DMSO	76.79%	(H. Li et al., 2015)
Xylose	Fe_3O_4@ Al_2O_3-(BAIL-Al)	140^{o}C; 180min	DMSO	67.5%	(Wu et al., 2017)
Xylose	OMC-SO_3H	200 ^{o}C; 45min	GVL/H_2O	76.7%	(X. Wang et al., 2021)
Xylose	SO_4^{2-} /Sn-DM	180 °C ; 180min	NaCl/DMSO/H_2O/toluene	80.97%	(Jia et al., 2019)
Xylose	MCM-41	170 ^{o}C; 180min	1-butanol/ H_2O	44.05%	(J. Zhang, Zhuang, et al., 2012)
Xylose	Lignin-Based Activated Carbon-Supported Iron	170^{o}C; 180min	H_2O-MIBK	57%	(Rusanen et al., 2020)
Xylose	SC-GCa-800	140 °C; 40 min	1,4-dioxane	76.9%	(T. Yang et al., 2020)
Xylose	CBSC	150 ^{o}C; 7hr	H_2O	20.36%	(Chung et al., 2020)
Xylose	SO_3H@Fe/MC	170 ^{o}C; 1hr	γ-valerolactone	45%	(Toumsri et al., 2021)
Xylose	sulfonated catalyst from Miscanthus giganteus	190 ^{o}C; 1hr	Water-CPME	60%	(Y. Wang, Delbecq, et al., 2017)
Xylose	SGO	200 ^{o}C; 35 min	H_2O	61%	(Lam et al., 2012)

2.6. Bi-Functional carbon based catalyst synthesis

Bi-functional solid acid catalyst contains both Lewis acid and bronsted acid active sites. Metal chloride impregnation on catalyst surfaces has several advantages, including low production costs, excellent stability, which leads to improved selectivity for target products, and high catalytic activity. Usually, metal chlorides such as chromium chloride, aluminum chloride, iron chloride, zinc chloride, cupper chloride, and magnesium chlorides are impregnated to the surface of the catalyst to improve the bi-functional solid acid catalyst for the production of furfural (B. Hu et al., 2021). From the trivalent chlorides, aluminum chloride has more catalytic efficiency to convert xylose into furfural when impregnated with biomass (Lopes et al., 2015). MIL-101(Cr)-SO_3H with both Lewis acid and Brønsted acid sites was developed to convert xylose into furfural in a biphasic cyclopentyl methyl ether (CPME)/H_2O-NaCl solvent system (figure 2.7). As high as a 70.8% furfural yield and 97.8% xylose conversion were obtained at 170 ◦C for 3 h in this catalytic system (Y. Liu et al., 2018).

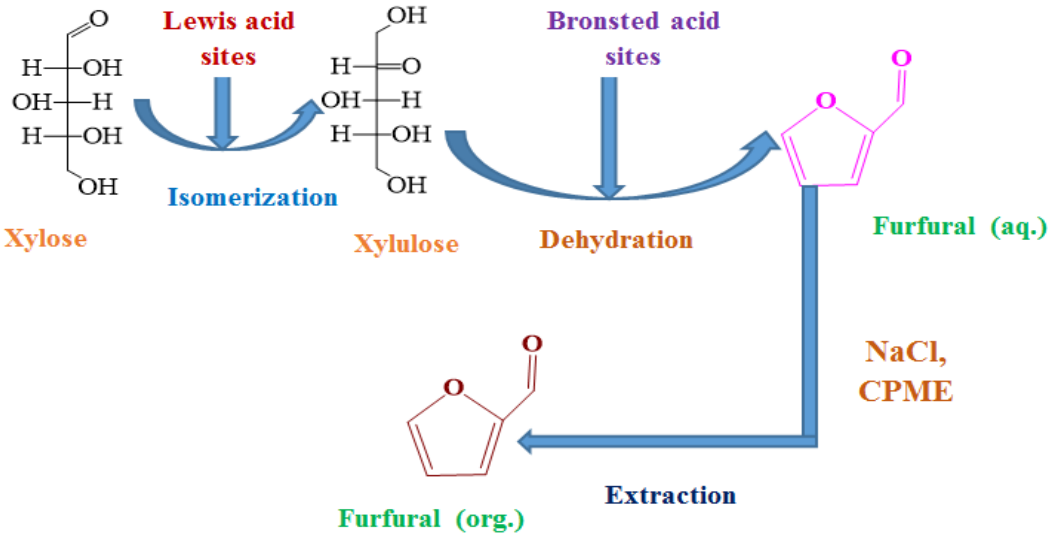

Figure 2. 7. Production of furfural from xylose in the presence of the MIL-101(Cr)-SO_3H

2.6.1. Lignocellulosic biomasses used for a catalyst support

Lignocellulose biomass is a generic terminology for describing the plants biomass. Lignocellulosic biomass is primarily composed of three main components such as cellulose, hemicellulose, and lignin (Parveen et al., 2017). These components in the lignocellulose materials have different functions and chemistries (Varanasi et al., 2013). And around 90 wt% of the dry matter in lignocellulosic biomass is made up of polymeric

carbohydrates (Figure 2.8) such as cellulose (20-60 wt%), hemicellulose (15-30 wt%) and lignin (10-25 wt%), and also (1-12 wt%) of extractives depends on the nature of the plant, and they occur in complex structure each other (Srivastava et al., 2021).

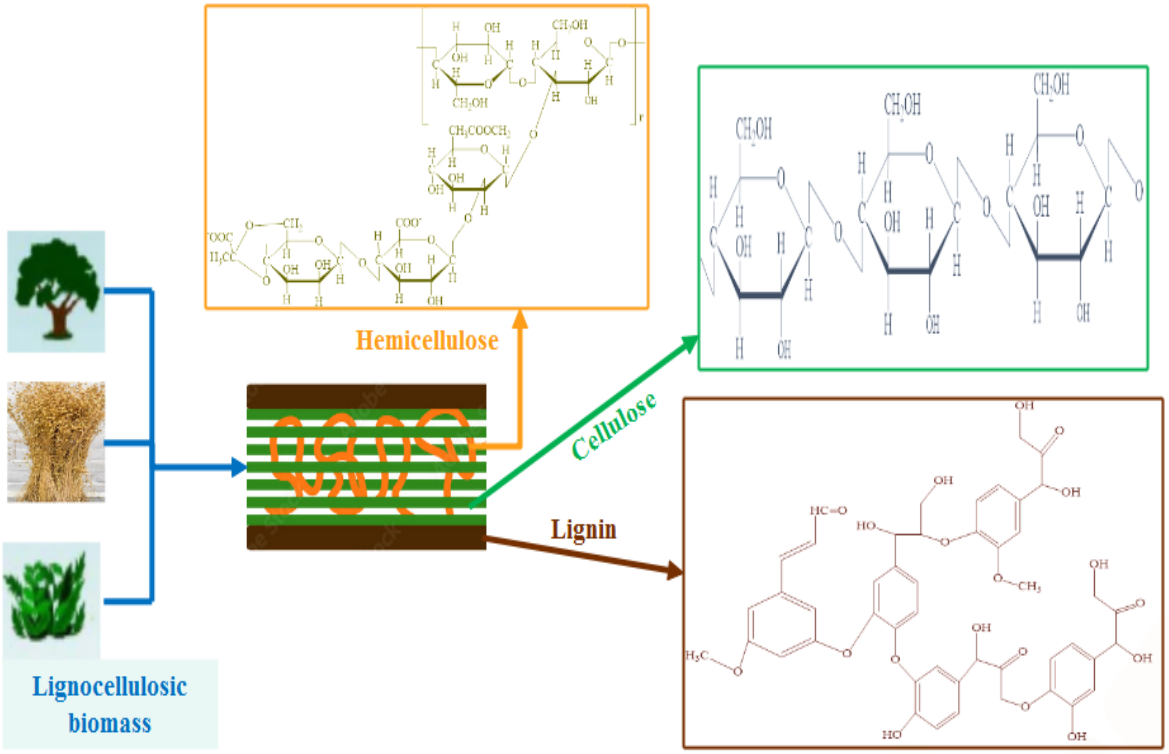

Figure 2. 8. Components of lignocellulosic biomass

Lignocellulosic biomass is a long-term alternative carbon source to fossil, and it could be used as raw material to prepare liquid fuels and valuable chemicals (Dai et al., 2017). Today, biomasses are the most abundantly used renewable materials on the earth, and so far, they are the most suitable and favorable materials used as a feedstock for biochar production. Platform compounds are mainly produced via the decomposition of lignocellulose, which mainly consist of cellulose, hemicellulose and lignin (Shi et al., 2018).

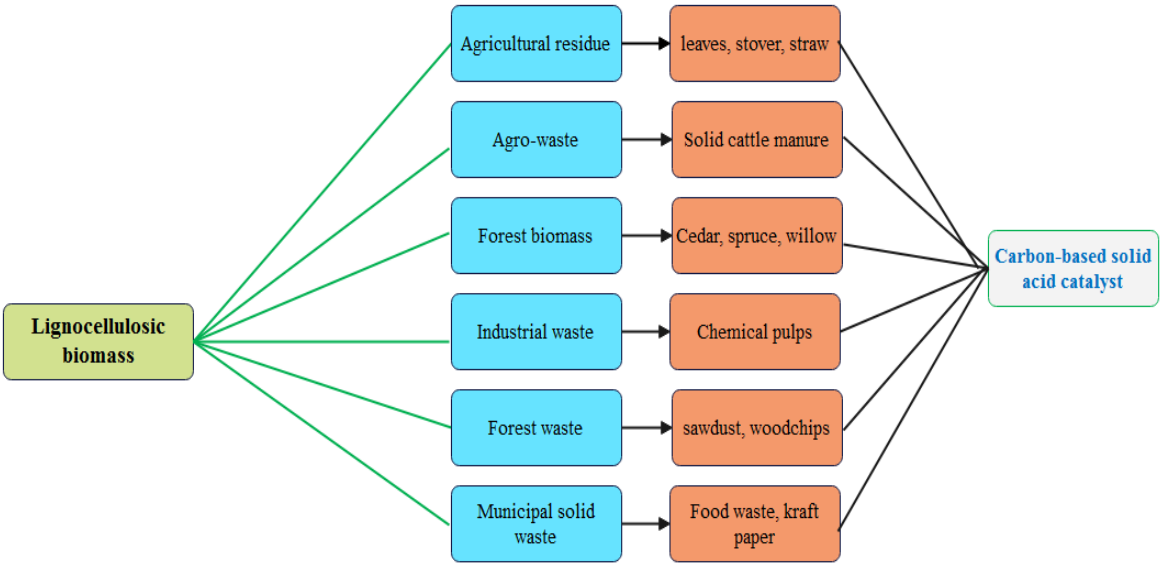

Figure 2. 9. Different sources of lignocellulosic biomasses used for catalyst support

2.6.2. Pretreatment of flax straw biomass as raw material for synthesis of carbon based catalyst

Lignocellulose biomass such as flax straw has a complex and inflexible structure. So, pretreatment is one of the most important process steps for synthesis of fine chemicals such as catalysts. The goal of pretreatment is to change or even destruct the lignocellulosic structure so that the effectiveness of the impregnation and carbonization process can be enhanced. On the whole, lignocellulosic biomass pretreatment methods can be classified into four common categories (Srivastava et al., 2021). These are, physical pretreatment, physicochemical pretreatment, and biological pretreatment. The most important lignocellulosic biomass pretreatment method used to enhance the effectiveness of carbonization is physical pretreatment. Physical pretreatment method includes size reduction by mechanical methods such as grinding /milling and drying. Reduction of particle size is required to make material handling easier, and to enhance uniform heat transfer during carbonization, and it can be done by grinding, milling and chipping (Aslanzadeh et al., 2014). On the other hand, this method of pretreatment needs a tremendously high amount of energy to reduce the size of the feedstock from large size to a particle size of a millimeter and fine particles of micrometers, which is undesirable from the engineering perception (S & P, 2019). From the physical treatment methods, grinding and milling methods are more operative at reducing the particle size. Drying is the easiest pretreatment process to reduce the moisture of feedstock to below 10%wt.

2.6.3. Preparation of Al-biochar

Impregnation and carbonization are one the most important to produce biochar composite with metal oxides. Impregnation is the most common and facile technique for the synthesis of supported catalysts for a variety of heterogeneous reactions. It consists of three basic steps: To begin with, a support with a high surface area is impregnated with a solution containing metal precursors; then, the solvent is evaporated at an elevated temperature; finally, the metal precursors are reduced under a designated environment to produce the catalysts (Tsao & Yang, 2018).

Carbonization is the complex process of concentrating and purifying carbon by denaturing organic matter with heat in the presence of little to no oxygen. It is a process that typically heats biomass feedstock in a kiln or retort (pyrolysis) at temperatures between 300 and 900°C to produce biochar, and bio-oil (Y. Zhang et al., 2019). The hemicellulose decomposes at 200– 260 °C, cellulose at 240–350 °C, and lignin at 280–500 °C (Salgado et al., 2018). Bio char is defined as a solid material obtained from the pyrolysis of biomass in an oxygen-limited environment. Pyrolysis can have classified into slow pyrolysis and fast pyrolysis depending on the heating rate and residence time. Fast pyrolysis involves the rapid thermal decomposition of organic compounds by heat in the absence of oxygen, producing high yields of bio-oil and low yields of bio char while slow pyrolysis, also known as conventional carbonization, involves heating biomass at a low heating rate and relatively long residence time (Xiu et al., 2017). Carbon material can be the result of biomass slow pyrolysis to that generate a highly cross-linked, multi-ringed aromatic structure anchored to lignin, that further can be functionalized to make it a strong solid acid catalyst (Rusanen et al., 2020).

2.6.4. Sulfonation methods

Sulfonation is the process in which sulfonic groups are usually introduced onto the carbon framework structure via chemical modification or functionalization by treating carbon black with $(NH_4)_2SO_4$/$(NH_4)_2SO_3$ and heating the resulting compound to a high temperature, sufficient to decompose the ammonium compounds or by treating carbon blacks with gaseous SO_3, oleum or fuming H_2SO_4 under ambient conditions. whereupon the sulfonic group density varies in the range of 0.05-7.3 mmol/g, depending on the sulfonation method used and the framework structure of the parent carbon support (Konwar, 2019.). Many researchers have reported that the sulfonated biomass contains Ph-

OH, -COOH, and SO_3H groups that can show greater catalytic activity amidst liquid-phase acid-catalyzed reactions in comparison to other solid acids (Pandian et al., 2020).

2.7. Factors that affect the catalytic performance of biochar based catalyst

2.7.1. Effects of carbonization temperature and time

The carbonization temperature and time at which bio char is produced have a significant impact on bio char-based catalysts. The carbonization temperature is an important parameter in catalyst synthesis because it can influence the carbon form structure and the amount of oxygen content in the carbon matrix of carbonaceous material, thereby indirectly affecting catalyst acid density (Zailan et al., 2020). During the carbonization process, the biomass's hemicellulose, cellulose, and lignin were slowly pyrolyzed to form numerous benzene rings with polycyclic aromatic hydrocarbon mesh skeleton structures through dehydration and condensation reactions. The majority of the organic components may have been removed at a higher temperature, making the catalyst support less flexible, owing to the growth and stacking of large polycyclic aromatic carbon sheets. Furthermore, mesoporous would expand to reduce pore density, resulting in fewer accessible active sites on the catalyst surface. Low carbonization temperature, on the other hand, improved the pore structure of the heterogeneous acid catalyst and reduced functional group deoxygenation. As a result, subsequent sulfonation can occur more efficiently and to a greater extent (Wong et al., 2020).

In addition, carbonization time is also one of the factors that affect the performance of solid acid catalysts by decreasing or increasing polycyclic aromatic carbon formation during the carbonization process. When the carbonization time is short, the carbonization degree is low, and the polycyclic aromatic hydrocarbons are not fully formed, which is disadvantageous for sulfonation. As the carbonization time increases, the structure of polyaromatic hydrocarbons becomes more complete. Thus, further increase beyond the appropriate time does not affect the formation of polycyclic aromatic carbons due to molecule structure variation (Zhou et al., 2016). Furthermore, as the pyrolysis time increased, the catalytic capacity of the biochar-based catalyst decreased due to the gradual decomposition of the phenolic compounds associated with the catalytic capacity.

2.7.2. Effects of sulfonation temperature and time

The temperature and time of sulfonation are important factors influencing the structure and activity of the carbon-derived catalyst as the sulfonation process introduces both oxygenated and sulfonic acid sites over the catalysts (da Luz Corrêa et al., 2020). The sulfonation conditions may also affect the composition of the functional groups on the surface of the catalysts, as the amounts of carboxylic COOH, sulfonic SO_3H, and phenolic OH groups attached to the surface of carbon based solid acid catalyst varies with different sulfonation parameters. Because of the high possibility of side reactions such as (condensation/ oxidation/ dehydrogenation) at high sulfonation temperatures which is an important factor in determining the SO_3H and phenolic OH site densities of the sulfonated carbon based catalyst (Ngaosuwan et al., 2016). Because of acid dehydration in the catalysts, the catalysts exhibit lower amounts of OH and SO_3H groups at high sulfonation temperatures. The optimal sulfonation temperature will provide the best balance of strong and weak acid densities for the sulfonated carbon-based catalyst, as too much acidity can result in severe catalyst deactivation. As the sulfonation temperature increased until it reached the optimum point, the total acid density of all the sulfonated carbon-based catalysts increased marginally but rapidly beyond the optimum point.

Sulfonation time can also be used to control the degree of sulfonation. The sulfonation time during the catalyst's functionalization also has a significant impact on the total acid density values of the sulfonated carbon-based catalyst. The acid densities of the catalysts increase with increasing sulfonation time, similar to the trend observed for sulfonation temperature until an optimal time is reached. Any further increase in sulfonation time after the optimal point does not affect the overall acid density values (R. Gong et al., 2019; Parreño et al., 2020). In general, the longer the contact time between SO_3H groups and the catalysts, and the greater the intensity and density of the acid sites, the longer the sulfonation time. As a result, highly active catalyst surface sites hold great promise for efficient catalytic performance.

2.8. Solvents systems

Several solvent solutions such as water, organic solvent, and biphasic solvent have been developed to improve furfural yield in a more environmentally friendly manner. Because water is the most environmentally benign and cost-effective solvent, it has been used in the industrial production of furfural. However, because water is a highly polar protic solvent,

the yield of furfural is quite low. The use of organic co-solvent lows an extraction of furfural from an aqueous phase and thus improves the yield by inhibiting the generation of undesired products.

Recently, various organic solvents are studied to recover the conversion of xylose into furfural. The optimum furfural yield in the GVL solvent solution was 57% after 2hrs at 170 ^{0}C. Despite the ease and cost of catalyst preparation, the procedure produced a low yield of furfural (T. Zhang et al., 2016). Zhu et al (2017) used 4-aniline sulfonic acid as a sulfonating agent to prepare a carbon-based solid acid catalyst for the conversion of xylose and corn Stover to furfural in GVL, and the highest FF yield of 78.5% was achieved at 170 ^{0}C in 30 min. The researchers looked at the conversion of xylose to furfural in 20 different solvents and found that dimethyl sulfoxide (DMSO) provides the best results. At 170 ^{0}C for 100 minutes, an optimum 75 percent furfural yield was obtained (X. Hu et al., 2014). Although DMSO preserves furfural better, it takes a long time (100 minutes) to reach the highest yield. Furthermore, the process is challenging to market due to the low efficacy of the downstream separation of furfural from DMSO (Roy Goswami et al., 2016). Concerning scaling up the process, to save energy and avoid furfural from the degradation of organic solvents, which have high boiling points, are not accepted. The conversion of xylose to furfural was effectively achieved in a water−MIBK biphasic solvent system over a synthesized magnetic carbon-based solid acid catalyst the result was gained 79.04 mol% at 190 ^{0}C for 10min (Z. Qi et al., 2020). However, MIBK is not a green solvent because of its toxicity, which has an impact on human health. In case of their toxicity, different researchers are used green solvents such as 2-MeTHF for synthesizing furfural from xylose. In a water-2MeTHF biphasic solvent system using a sulfated tin ion-exchanged montmorillonite ($SO4^{2-}$/Sn-MMT) solid acid catalyst, the conversion of xylose to furfural was accomplished and the furfural yield was obtained at 79.64% at 160 ^{o}C for 120 min (Lin et al., 2017). As a result; a more efficient biphasic system is sought. In this regard, the use of water immiscible 2- methyl Tetra Hydro Furan (2-MeTHF) as a low-cost extracting solvent for in situ extraction of furfural from the catalytic aqueous phase has been observed to be beneficial. Another significant advantage of 2-MeTHF is that its boiling point differs by 82 ^{o}C from that of furfural, making it ideal for future furfural separation. In general, bi-phasic solvents surpresses side reaction in several ways:-

- Reduced furfural conversion to humins and organic acids due to the limited presence of water

- Protection of furan derivatives aldehyde moiety through reversible derivatization or solvent interactions
- Simultaneously extraction of furan product from the reaction medium

2.9. Heating mechanism used for furfural production

Depending on the heating source, the heating mechanism can be categorized into conventional heating systems and microwave heating systems.

2.9.1. Conventional heating system

In conventional processing, the heat is generated from a source and then transmitted from the external to the internal section of the material by convection, conduction, and radiation, which is a sluggish and inefficient process (Jin et al., 2017). For the manufacturing of furfural, conventional heating techniques such as oil baths, sand baths, salt baths, and autoclave heating blocks are commonly used. Of those, the most commonly used tool is an oil bath. Mass transport in the reactive and extractive phases can be aided by heating and stirring. Conventional heating, on the other hand, frequently encountered the problem of long reaction times due to inefficient heat transfer (D. Hu et al., 2021). Furthermore, the rate of heat flow into the body of the materials from the surface, as indicated by its specific heat, thermal conductivity, density, and viscosity, limits the process duration. However, the technique is relatively developed and scale-up is simple.

2.9.2. Microwave heating

The improvement of heat and mass transport in chemical reaction processes has drawn a lot of attention to ultrasonic and microwave heating technologies. The cavitation phenomena that occur when sonication is used could result in localized hot and cold areas in the reaction system. Furthermore, microwaves caused polar molecules to vibrate and rotate, disrupted extensive hydrogen bonds in biomass molecules, and provided homogenous heat in a short period. Ultrasonic and microwave irradiation is a source of energy savings and a gentle way of generating furfural from xylose (D. Hu et al., 2021). In addition, the heating process can be controlled more accurately, resulting in higher yields and better quality in the least amount of time. It is, nevertheless, more expensive than conventional heating, and Process scale-up is not mature.

2.10. Factors affecting the furfural formation

2.10.1. Effect of reaction time

Reaction time is one important operating parameter that has a significant impact on ultimate product yield. In case of a shorter reaction time, the conversions of xylose into furfural lower due to the lower movement of the particles between the reactants. Increased reaction time will accelerate the movement of the particles. The movement of the particles causes heat transfer between particles and results in higher reaction temperature. D-Xylose conversion, furfural yield, and selectivity gradually increased with the time extension (Y. Wang, Delbecq, et al., 2017). The accumulation of by-products on the catalyst surface with increasing residence time may cause loading and subsequent partial deactivation by catalyst surface passivation (Dias et al., 2005). Moreover, excess reaction time will lead to a reduction of the product yield due to the formation of side reactions such as resinification.

2.10.2. Effect of reaction temperature

Another key component that influences reaction rate is reaction temperature. The reaction temperature has a significant impact on the activity of the used catalyst. Besides, raising the reaction temperature increases the particle's movement and increases the solubility of the reactants, resulting in higher furfural yield. However, a higher reaction temperature can decrease furfural yield due to the degradation of products and the formations of byproducts. The humin or the byproducts formed, in turn, affects the performance of solid acid catalysts, when deposited on the active sites, by preventing the reactants from accessing the active site The decreasing yield of furfural could also occur when xylose undergoes retro aldol fragmentation into acids, aldehydes, and ketones (Dulie, Woldeyes, & Demsash, 2021).

2.10.3. Effect of catalyst loading

The amount of catalyst used in the conversion of xylose to furfural can have an impact. Increased catalyst dosage is usually associated with higher furfural yield. Excess catalyst dose increases some yield loss of processes (fragmentation, condensation, and resinification) via humins generations or other byproducts that delay the recycling of the catalyst. This reduces the final product yield (W. Li et al., 2017). Furthermore, an increase in catalyst loading results in a decrease in the furfural yield.

2.11. Challenges for furfural production

The latest achievements on the production of furfural from xylose in various solvent systems, heating mechanisms, catalyst reuse and product purification over homogeneous and heterogeneous catalysts have been outlined and discussed in this review. Despite the fact that many positive results have been achieved, the industrial production of furfural still faces many significant challenges. In producing furfural, various technologies have been developed at the experimental level. For instance, the supercritical CO_2 extraction technology is one of the methods applied to separate furfural from the reaction mixture in view of getting a higher yield by suppressing reactions leading to furfural loss. But this technology is being applied only at the laboratory stage due to its high operating and material cost requirements to be applied on an industrial scale (Sato et al., 2019).

The main bottleneck in the preparation of furfural is the dehydration of xylose, but there are side reactions that occur. Theoretically, heterogeneous catalysts with a large specific surface area, proper pore size, and adjustable Bronsted and Lewis acid sites prepared from biomass are conducive to furfural preparation from xylose via a series of isomerization, and dehydration reactions. Thus, for furfural production, multifunctional solid acid catalysts with specific porosity, magnetic components, non-precious metals, and adjustable acidity are desirable. In addition, to reuse a catalyst for the next catalytic runs, separating it from the reaction mixture and regeneration may be required. But catalyst reuse is still a challenge for industrial applications due to reduced activity and deactivation of catalysts upon regeneration (T. Zhang et al., 2018).

Solvent recycling is one of the important processes in chemical industries for economical operations because it reduces the costs associated with waste stream management and chemical consumption (Z. Qi et al., 2020). Environmental pollution is a problem of high priority these days. Solvent released in waste streams from industries needs to be reduced to protect the environment. In addition, also to keep consistent operating conditions throughout the process in furfural production, the solvent used should be fully recovered and reused or makeup solvent is required. Generally, to reduce the amount of solvent required and to minimize the negative environmental impact associated with the disposal of solvents in waste streams, recovery and reuse of solvents is required. Recovery processes might be possible at a laboratory scale, but it would be tough for commercialization (Demsash, et al., 2021).

CHAPTER THREE

3. MATERIALS AND METHODS

3.1. Materials

3.1.1. Raw materials

The raw material flax straw (linseed straw) was collected from Holeta Agricultural Research Center (HARC). HARC is located in Holeta town Oromia regions special zone with latitude and longitude of 9°3′N 38°30′E & 9.050°N 38.500°E respectively, and an elevation of 2391 meters above sea level.

3.1.2. Chemicals and reagent used

The chemicals and reagents used in catalyst preparation, and furfural production are listed in Table 3.1.

Table 3. 1. List of chemicals and reagents used in the study

Chemicals and reagents	Chemical formula	Purity	Purpose
Distilled water	H_2O	-	Preparation of different solutions, solvents for furfural synthesis
D-xylose powder	$C_5H_{10}O_5$	99%	Reactants for furfural production
2-MeTHF	$C_5H_{10}O$	99%	Solvents for furfural synthesis
Sulfuric acid	H_2SO_4	98%	Sulfonating agent
Aluminum chloride pellets	$AlCl_3.H_2O$	99%	Impregnation agent
Sodium hydroxide pellets	NaOH	99%	Titrant for measurement of the acid density of synthesized catalyst
Sodium chloride pellets	NaCl	99%	Measurement of acid density of synthesized catalyst and extraction of furfural from the aqueous phase
Hydrochloric acid	HCl	37%	Titrant for measurement of the acid density of synthesized catalyst
Phenol	C_6H_6O	99%	The reagent used for xylose concentration determination

3.1.3. Apparatus/types of equipment used

The apparatus and types of equipment used in the study are presented in Table 3.2.

Table 3. 2. List of apparatus and types of equipment used in the study

Apparatus/ Equipments	Purpose
PH-meter	Measurement for PH-sample
Plastic bags	Used to store sample until next process needed
Mortar and pestle	Size reduction of biochar
Hot plate	Impregnation of flax straw with Aluminum chloride
Blender	Size reduction of flax straw
Siever	Sieving of flax straw and biochar
Desiccator	Cooling of sample
Muffle furnace	Carbonization of flax straw into biochar
Analytical balance	Measurement of sample weight
Oven	Drying of flax straw, biochar, synthesized catalyst, and heating of autoclave reactor
Stirrer	Mixing of solution
Crucible	Putting of sample for carbonization process
Different size beaker	Measurement of different volume samples and used as reactor during the impregnation process
Autoclave reactor	Used for sulfonation, and dehydration reaction
Conical and Erlenmeyer flasks	Used for titration of biochar, Al-biochar, and synthesized catalyst
Digital micro pipet	Used to measure different samples at the micro level
Filter paper	Used to separate liquid and solid
Aluminum foil	Used Temporary covering of instruments, shielding in vacuum equipment, packaging, wrapping, weighing boats

Centrifugal	Used to separate liquid based on their density
Separating funnel	Separation of furfural from remaining reactants
Rotary evaporator	Removing organic solvents from furfural

3.2. Overall research methodologies

The research process comprises a series of methodology with the main purpose of synthesizing a carbon based bi-functional solid acid catalyst for furfural production. The overall research plan can be divided into various successive components and the thesis was carried out according to the flow diagram illustrated in Figure 3.1.

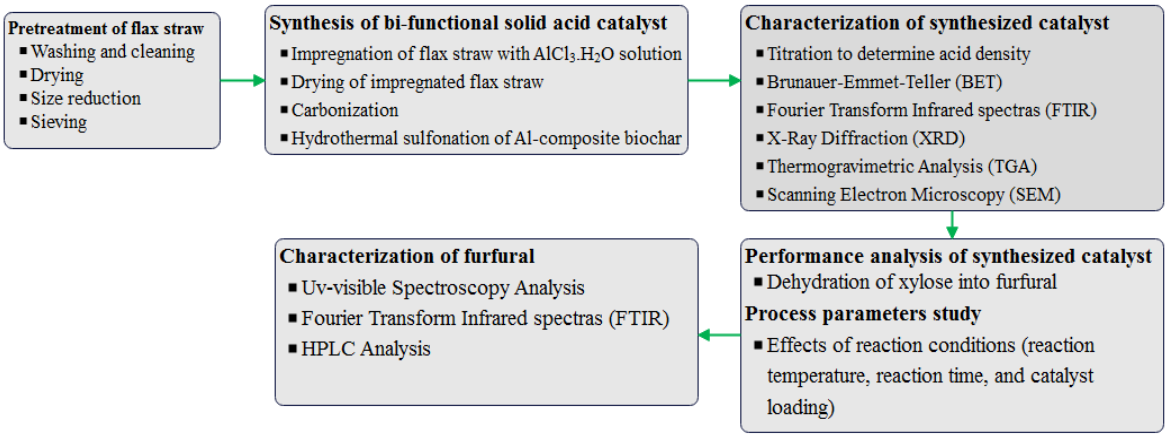

Figure 3. 1. Flow diagram of research methodology

3.2.1. Raw material preparation

The raw that is flax straw was collected and chopped using a knife into small pieces and washed with distilled water to remove dirt and dust particles from the surface of the straw. Then it was dried under the sun for 48 hr to remove moisture contents. The treated raw biomass (flax straw) was milled using a milling machine and sieved to obtain the desired size of flax straw powder (45-120 mesh). Finally, the sieved flax straw was dried using the oven drying at 105^{o}C for 8 hr until the moisture content of the powder flax straw reaches constant and then, it was stored in an airtight plastic bag for further experimental works.

Figure 3. 2. Raw material preparations

3.2.2. Proximate analysis of the flax straw

Proximate analysis of any biomass separates into four groups, such as moisture, volatile matter (consisting of gases and vapors driven off during pyrolysis), fixed carbon (the nonvolatile fraction of biomass), and ash (the inorganic residue remaining after combustion).

I. Moisture Content (MC)

The moisture content of the flax straw biomass sample was determined by measuring the weight loss of the sample after heating them above the boiling point of the water. An accurately weighed sample was taken into a Petri dish and oven-dried at 105^{o}C for 2hrs interval until constant weight was obtained. It was then cooled in a desiccator. The moisture content is expressed as a percentage of the samples (ASTM D-3172).

$$MC\% = \frac{w_1 - w_2}{w_1} \times 100\% \ldots\ldots\ldots\ldots\ldots\ldots\ldots\ldots\ldots\ldots\ldots\ldots 3.1$$

Where; MC is moisture content, w_1 is the weight of the sample plus Petri dish before drying (gm), and w_2 is the weight of the sample plus Petri dish after drying (gm).

II. Ash Content (AC)

The ash content of flax straw biomass was determined using a laboratory muffle furnace as per ASTM D-3174-02. After being weighed, the sample was placed in a crucible. The sample inside the crucible was opened and heated to 650^{o}C for 3hr in a muffle furnace. The crucible containing ash was cooled at room temperature, and the weight of the ash was calculated after the weighing crucible. The ash weight was expressed as the percentage of the weight of the whole sample.

$$AC\% = \frac{w_2}{w_1} \times 100\% \ldots\ldots\ldots\ldots\ldots\ldots\ldots\ldots\ldots\ldots\ldots\ldots\ldots\ldots\ldots\ldots\ldots\ldots\ldots\ldots\ldots\ldots 3.2$$

Where; AC is ash contents, w_1 is the weight of the sample (g), and w_2 is the weight of the ash (g).

III. Volatile Matter Content (VM)

The volatile matter of the flax straw sample was determined as the procedure given in ASTM D 3175-07. The sample was measured and placed in a closed crucible. It was then heated up to 950 $\pm$ 10^{o}C for 7 minutes in a muffle furnace. The sample was weighed after it has cooled. The percentage of the volatile matter (VM) of the sample was determined as;

$$VM\% = \frac{w_1 - w_2}{w_1} \times 100\% - Moisture\ (\%) \ldots\ldots\ldots\ldots\ldots\ldots\ldots\ldots\ldots\ldots\ldots\ldots\ldots\ldots\ldots 3.3$$

Where; VM is volatile matter, w_1 is the weight of the sample before heating, and w_2 is the weight of the sample after heating.

IV. Fixed Carbon Content

The fixed carbon content was determined by subtracting the sum of the percentage composition of volatile matter content, moisture contents and ash content from 100% according to ASTM D-388 standards. Wet basis content is the percentage amount of all material including water and the dry basis composition is the ratio of constitutes except for water.

Fixed carbon content (%) = 100-(VM+AC+MC) ……………..………………..……......3.4

3.3. Synthesis of catalyst

3.3.1. Preparation of Al-Biochar

The sample prepared was impregnated with aluminum chloride for surface modification of flax straw with aluminum oxides according to (Karnjanakom et al., 2019; Yu et al., 2019) with some modification. 30 gm (11% Al) of Aluminum chloride ($AlCl_3.H_2O$) were measured and added to 150ml of distilled water. After that, 10gm of flax straw was added to the solution of Aluminum chloride prepared, and then, it was stirred for 12hr at room temperature. Then, the sample having water was dried using an oven drier at 105^oC for 24 hrs. The dried Aluminum impregnated flax straw was placed in the crucible for introduced to the muffle furnace. The carbonization was performed at carbonization temperatures of 350^oC, 400^oC, and 450^oC with a reaction time of 30min, 60min, and 90 min. The carbonized impregnated flax straw was cooled and then, stored in desiccators for 1 hr. Al-biochar was washed with distilled water to remove the ash component on the surface of carbonized flax straw. The treated Al- biochar was filtered using a vacuum pump and dried at 105^oC for 12hr using an oven drier. Finally, the dried Al- biochar was sulfonated at fixed sulfonation temperature, sulfonation time, and bio char to sulfuric acid ratio to determine the amounts of SO_3H groups on the surface of Al-biochar. Finally, carbonization temperature and time were selected for the next process based on amounts of bronsted acidity or SO_3H catalyst.

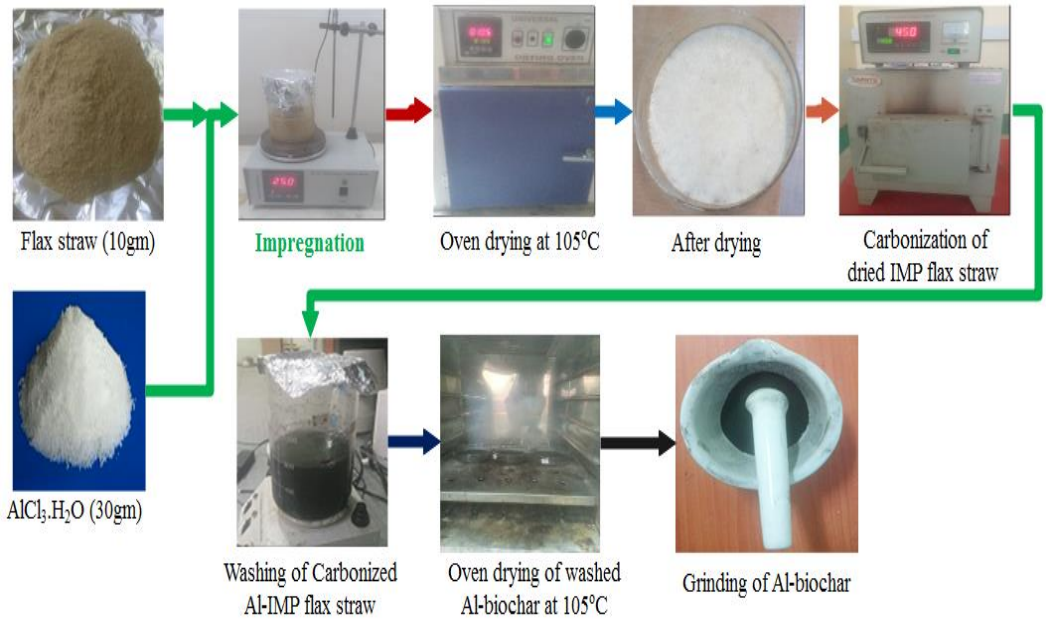

Figure 3. 3. Preparation of Al-bio char

3.3.2. Functionalization of Al-biochar with concentrated sulfuric acid

Catalyst functionalization was done to obtain a bi-functional solid acid catalyst by introducing SO_3H groups into polycyclic aromatic sheets of Al-biochar via sulfonation. The selected Al-biochar was sulfonated with concentric sulfuric acid at different sulfonation temperatures ranges (90^oC-200^oC) with the time (12 hr- 24 hr) in an autoclave reactor. The mass-to-volume ratio of Al-biochar to the concentration of sulfuric acid was taken in the ratio of 1:20 w/v according to (Bureros et al., 2019; Kang et al., 2014; Mateo et al., 2019; Ngaosuwan et al., 2016). Then, the black solid or catalyst was washed with hot distilled water $\geq 80^oC$ several times to remove sulfate ions attached to the surface of the catalyst, and then it was dried at 105^oC for 4hr to remove the water inside of the sulfonated Al-biochar catalyst.

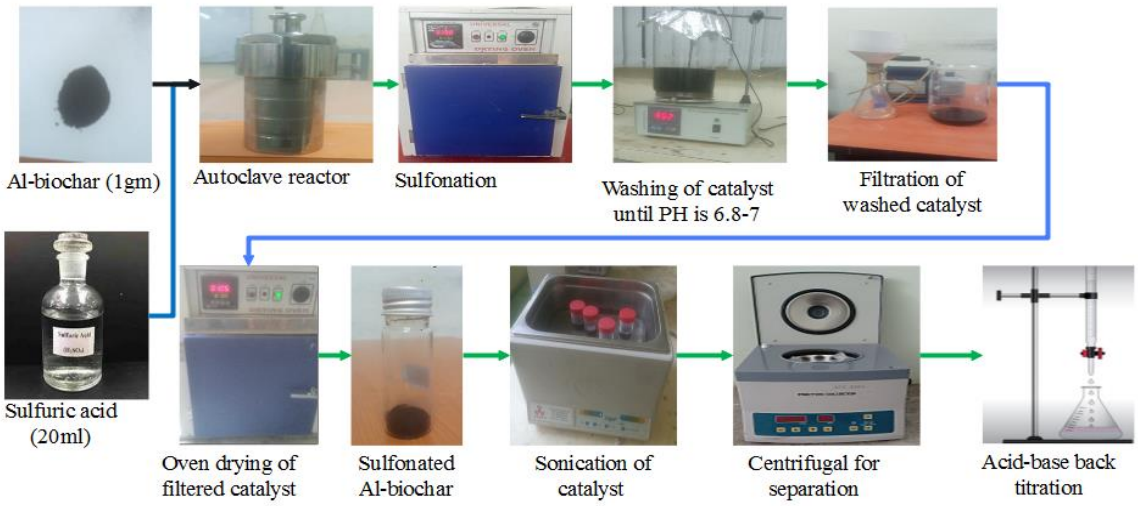

Figure 3. 4. Functionalization of Al-biochar with concentrated sulfuric acid

3.4. Catalyst characterization

3.4.1. Acid density of the catalyst

Total acid density and the sulfonic group were determined according to the literature (Dulie, Woldeyes, & Demsash, 2021; Mengstie & Habtu, 2020; Wong et al., 2020) with some modifications. Total acid density was determined using the standard acid-base back titration method. The catalysts were pre-dried in the oven at 105 °C for two hours before analysis. 0.05g of the sample catalyst were sonicated in 20ml of 0.05M a NaOH solution using an ultrasonic bath at room temperature for 1hr and titrated with 0.05M of HCl using phenolphthalein as an indicator.

Total acid density$= \frac{V_{NaOH} \times [NaOH] - V_{HCl} \times [HCl]}{Mass\ of\ catalyst}$ ……. 3.5

The sulfonic group density can be determined using the standard base direct titration method. The catalyst was pre-dried in the oven at 105°C for two hours before analysis. For sulfonic group determination, 0.05 g of catalyst was added into 20ml of 0.05M a NaCl and sonicate for 1hr. After sonication, solids were separated using centrifuge separation.

Then, the separated supernatant liquid was titrated against 0.05M NaOH solution using phenolphthalein as an indicator. When the color of the filtrate was turned from colorless to slightly pink, the end of titration was reached. Finally, the accurate acid density SO_3H was calculated as follows:

$$SO_3H\left(\frac{mmol}{l}\right) = \frac{Conc\ NaOH \times Volume\ of\ NaOH\ consumed\ in\ titration}{Mass\ of\ catalyst} \ldots\ldots\ldots\ldots 3.5$$

3.4.2. Experimental analysis instruments

Instruments used in both catalyst and product analysis are; FTIR, XRD, HPLC, SEM, UV-Visible, and TGA.

3.4.3. Brunauer-Emmett-Teller (BET) Analysis

The textural properties such as total surface area, pore volume, and pore size distribution were estimated using N_2 adsorption-desorption isotherm data that is obtained using a surface area analyzer (Quantachrome Instruments version 11.0). Samples were degassed initially at 300^{o}C for 8 hr. Then the isotherms were generated by contacting the clean samples with liquid N_2 at 77.3K. The Brunauer-Emmett-Teller (BET) theory was used to calculate the surface area.

3.4.4. Analysis of functional group

Fourier transform infrared spectroscopy (FTIR) is a technique that is used to obtain an infrared spectrum of absorption or emission of a solid, liquid, or gas. Fourier transform infrared spectroscopy was used to examine the framework vibration. The functional group of the catalyst was tested by Fourier transform infrared spectroscopy (FTIR) on Spectrum 65 FT-IR (PerkinElmer) with the resolution of 4 cm^{-1} and scanning range from 400 cm^{-1} to 4000cm^{-1} using the conventional KBr technique, and the functional group was determined based on the interpretation of the infrared spectrum obtained by comparing it with the standard spectrum group frequencies.

3.4.5. Analysis of catalyst structure

X-ray Diffraction (XRD) is an instrument used to identify the structure of the catalyst. In this technique, the catalyst sample is irradiated with an X-ray of a known wavelength (λ). The X-ray diffraction (XRD) patterns of sulfonated catalyst were obtained using MiniFlex 300/600, Japan operated at 40 kV and 15 mA, using Ni-filtered Cu-Kα radiation (1.54059-1.54441). The samples were placed on a sample holder made up of a silicon wafer and the measurements were taken continuously from 10^o to 80^o angles over the range of 2θ. The resultant intensity data were processed by using the in-built diffraction software Match! 3 to graph and analyze the peak position.

3.4.6. Analysis of thermal stability

The thermal stability of the catalyst was investigated through thermogravimetric analysis (TGA) on a thermogravimetric analyzer (TGA instrument, SDT Q600 V20.9 Build 20) in the temperature range of 50^oC - 800^oC with a heating rate of 20^oC / min where nitrogen (with the highest purity) was used as both the protection gas and reaction gas. The small amount of the sample (10mg) was placed in a vial, which is present in the TGA analyzer. Testing was carried out under an inert atmosphere (N_2) with a flow rate of 2 ml/min to remove all corrosive gases and avoid their oxidative degradation and the retention time of the sample at the maximum temperature.

3.4.7. Scanning Electron Microscopy Analysis

The surface morphology of the flax straw and acid functionalized flax straw was investigated by scanning electron microscopy (SEM, Hitachi S-3400N) at 20kv.

3.5. Catalytic dehydration of xylose into furfural

The catalytic performance of acid functionalized which is sulfonated Al-biochar was tested on the dehydration of D-xylose into furfural in water to 2-MeTHF (5:15 *v/v*) (T. Yang et al., 2017), with addition of 1.5 mmol of NaCl to extract furfural from the aqueous phase to organic phase. D-xylose (0.5 g), and with the catalyst dosage interval (0-0.4 g), were added into the 100ml of a stainless autoclave reactor. Then, the reaction mixture was performed at the temperature interval (150-190^oC) for the time range of (1-5) hr. Finally, the reaction was cooled down to room temperature, and then, the liquid product was collected and extracted from the system. After extraction, the upper layer contains organic phase, which contains furfural, and the lower one is aqueous phase that contains xylose

residues and other byproducts. Finally, the organic solvents containing furfural were separated using a rotary evaporator at 80^{o}C until the organic solvent was removed from the furfural.

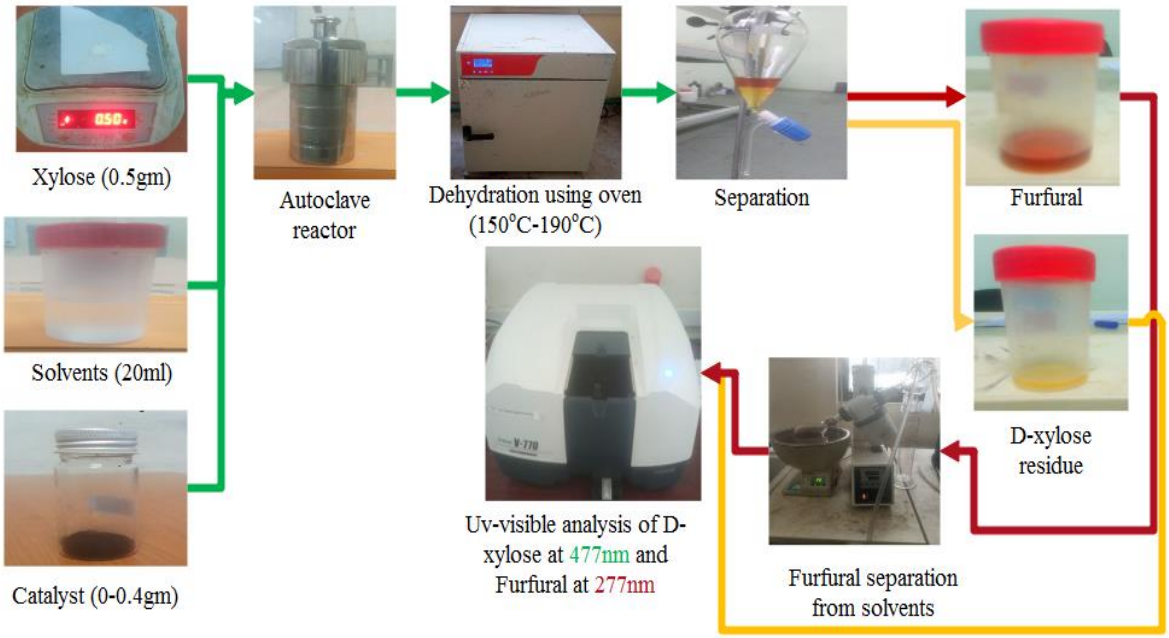

Figure 3. 5. Dehydration of xylose into furfural using sulfonated Al-biochar

3.5.1. Product analysis

3.5.1.1. UV-visible spectroscopy analysis

A. Furfural formation analysis

UV-VIS spectrophotometry was selected to study the appropriate conditions, such as the effects of temperature, time, and catalyst loading on the formation of furfural and conversion of xylose. To determine the concentration of furfural in the organic phase: 1ml of the organic phase was taken from the extracted sample solution and diluted with 300 ml of distilled water in the volumetric flask. After that, the solution was charged into a cuvette for the UV test. Finally, according to (Zhang et al., 2017), the formation of furfural was analyzed. The absorbance of the furfural sample was measured at 277nm using JASCO V-770 ultraviolet spectrum with the wavelength scanning range between 200nm-400nm.

3.5.1.2. UV-vis analysis of xylose

The xylose concentration left in the residues or unreacted xylose was determined by a **phenol-sulfuric acid method** using JASCO V-770 spectrophotometry at 477nm (Masawi & Manyere, 2018). The xylose-contained residues were measured using the pipette to

accurately deliver a known volume solution into a 25ml of volumetric flask. This was diluted to a specified range (within the xylose standards curve range) for measurement. To measure unreacted xylose, 20mg of xylose residues were taken from 1ml of sample diluted in 25ml of distilled water dissolved in the 100ml of volumetric flask. Then, 1ml of diluted xylose was taken from the prepared solution and added to 1ml of 5% phenol followed by 5ml of concentrated sulfuric acid. The absorbance was measured after 10 minutes at 477nm against blank and the concentration was calculated from the regression equation obtained from the calibration curve. The experiment was carried out in duplicate. Finally, the conversion of xylose can be calculated as followings:

$$Conversion = \frac{C_{in} - C_{out}}{C_{in}} \times 100\% \ldots\ldots\ldots\ldots\ldots\ldots\ldots\ldots\ldots\ldots\ldots\ldots\ldots\ldots\ldots\ldots\ldots\ldots\ldots\ldots\ldots 3.6$$

Where; C_{in} is the concentration of xylose in the solution

C_{out} is the final concentration of xylose in the solution

A blank solution was prepared by adding 1ml of 5% phenol to 1ml of deionized water, followed by 5ml of concentrated H_2SO_4. The standard solution was prepared as follows; from a 1000ppm stock solution of xylose prepared in deionized water, aliquots were taken to obtain xylose concentrations of 10-50mg/l in the 100ml of deionized water. 1ml of 5% phenol solution was added to 1ml of xylose solution followed by 5ml of concentrated H_2SO_4. The absorbance was measured after 10 minutes at 477nm against a blank.

3.5.1.3. HPLC analysis

The yield and selectivity of furfural in filtrates was analyzed by a high-performance liquid chromatography (HPLC) system equipped with a Jasco-AS-2050 autosampler and Jasco UV-2075 detector at 285nm using kinetic C18-XB150×4.6mm column (Phenomenex). The sample was analyzed after being diluted with an amount of water and centrifuged. Methanol/water (2:3 by volume ratio) was used as the mobile phase for furfural determination. To determine the yield and selectivity of the produced furfural, UV-visible analysis of the furfural produced at 180°C for 2 hr with a 0.2 gm catalyst was selected based on the maximum furfural formation.

$$Furfural\ yield = \frac{Concentration\ of\ furfural\ produced}{Initial\ concetration\ of\ xylose} \times 100\% \ldots\ldots\ldots\ldots\ldots\ldots 3.7$$

$$Furfural\ selectivity = \frac{Furfural\ yield}{xylose\ conversion} \times 100\% \ldots\ldots\ldots\ldots\ldots\ldots\ldots\ldots\ldots\ldots.\ldots\ldots\ldots\ldots 3.8$$

CHAPTER FOUR

4. RESULTS AND DISCUSSIONS

This chapter presented the outcomes of all laboratory experiments, including the characterization of raw flax straw proximate analysis (sample moisture percentage, and volatile component, ash content). It also includes different analysis and studies with the most operational parameters of bi-functional catalyst preparation condition (carbonization temperature and time, sulfonation temperature and time) which affects the acid density of the synthesized catalyst. It also includes various characterization results of sulfonated Al-biochar catalysts such as acid density determination, BET, FTIR, XRD, TGA, and SEM. Furthermore, various analyses and studies on the important reaction parameters that affect the formation of furfural and conversion of xylose were discussed. Product characterization using Uv-visible, FTIR, and HPLC are also included in this chapter.

4.1. Characterization of flax straw

The proximate analysis of flax straw was determined based on standard methods before it was carbonized to measure the four different values of raw flax straw such as; moisture content, ash contents, volatile matter, fixed carbon contents and compared with some others plants contents. As shown in Table 4.1, flax straw contains mostly moisture content of 7%, ash content of 3.3%, volatile matter of 76%, and fixed carbon contents of 13.7%. The results obtained from flax straw for proximate analysis are in agreement with those somewhere else literature (Azargohar et al., 2013; Naik et al., 2010). Flax straw had less moisture content as analysis made by this study when compared to oat straw and oil palm frond. The high moisture content can affect the surface properties of the biochar produced which indicates a less catalytic efficiency. Studies suggested that biomass with low moisture content favors biochar production, while those with high moisture content favor bio-oil production (Yadav & Jagadevan, 2020).

Table 4. 1. Proximate analysis of flax straw and other plants

Plant types	Moisture Contents (%)	Volatile Matters (%)	Fixed Carbon (%)	Ash Contents (%)	Reference
Flax straw	7	76	13.7	3.3	Current study
microalgae	5.5±0.4	61.2±5.4	21.2±1.8	12.1±0.8	(Jiménez Toro et al., 2019)
Oil palm frond	7.6±0.17	70.24±0.72	18±1.49	4.16±0.18	(Abdullah et al., 2019)
Oat straw	7.2	74.48	17.71	5.99	(Mani et al., 2011)
Teff straw	6.33±0.36	43.27±0.63	41.19±1.02	9.21±0.26	(Dulie, Woldeyes, & Demsash, 2021)

The mineral component of lignocellulosic material is generally indicated as ash content. Biomass ash content is classified as low (<5%), medium (5-10%) and high (>10%) (Stella Mary et al., 2016). Based on this classification, the flax straw considered in this study has low ash content (3.3%) which would result in minimal effect of inorganic impurities during carbonization. The ash content of flax straw (current study) was markedly higher than that of microalgae, oil palm frond, oat straw and teff straw. The ash content determines the number of mineral contents in the biochar such as silica, iron, magnesium, calcium, and mineral salts. These mineral salts are considered as impurities that block the pores and part of concentrated sulfuric acid was consumed owing to reactions between inorganic salts and concentrated sulfuric acid. This implies the reduction on concentration of concentrated sulfuric acid which is not beneficial to the secondary sulfonation of aromatics (Yue et al., 2020).

In the synthesis of carbon-based catalysts from biomass, an important consideration is the fixed carbon (FC) content of the catalyst. The fixed carbon content of the flax straw used in this study (i.e. 13.7%) was within the range of values (9.53 -35.2%) of fixed carbon contents of the other biomass residues that were studied as raw material for the synthesis of carbon based catalysts (Hirano et al., 1998). The fixed carbon (FC) content of raw flax

straw obtained in this study was 13.7% relatively higher than some other biomasses used in the previous study (Hanis et al., 2016). The proximate analysis result of flax straw, reveals a significant amount of fixed carbon content (13.7%) when compared to other biomass residues, which is enough for developing carbonaceous support, providing the chosen precursor material suitable for attachment of sulfonate group during sulfonation. In addition, the higher the content of volatiles implies the longer devolatilization time and ensures effective carbonation product (Merwe et al., 1986). However, biomass with higher volatile content produces many porous materials that used to graft sulfonate groups during the sulfonation process.

4.2. Parameters that affect the performance of Al-biochar based catalyst

4.2.1. Effects of carbonization temperature and time on the total acid density of Al-biochar based catalyst

Carbonization is important to facilitate the formation of the biomass carbon structure in the favor of -SO_3H loading by sulfonation reaction, the process of grafting -SO_3H active functional groups into the carbon skeleton (Bureros et al., 2019; Hara et al., 2004). The combined effects of carbonization temperature and time on the total acid density were studied maintaining other catalyst preparation conditions constant (IMP ratio of flax straw to the solution of $AlCl_3.H_2O$ (1/15 *w/v*), Mass of Al-biochar to the sulfuric acid ratio (1/20 *w/v*), Sulfonation temperature 145^oC, Sulfonation time 18 hr). Figure 4.1, which was tabulated from Table 1 appendix B2 showed that the effects of carbonization temperatures and time on the total acid density of Al-biochar-based catalyst. As can be seen in the figure, during carbonization temperature of 450^oC, the total acid density decreased as the carbonization time increased from 30 min to 90 min. But, at 350^oC and 400^oC of carbonization temperature, it increased with time and then drops after reaching maximum value. This may be due to saturation of the active sites adsorption and gradual distraction of the carbon structure by excessive carbonization temperature and time. An increase in carbonization temperature leads to an increase the degradation of hemicellulose, cellulose, and lignin which favors more formation of -OH and –COOH functional groups. Therefore, the maximum total acid density was obtained at carbonization temperature 450^oC and carbonization time of 30 min, which is 4.233$\pm$0.22 mmol/g.

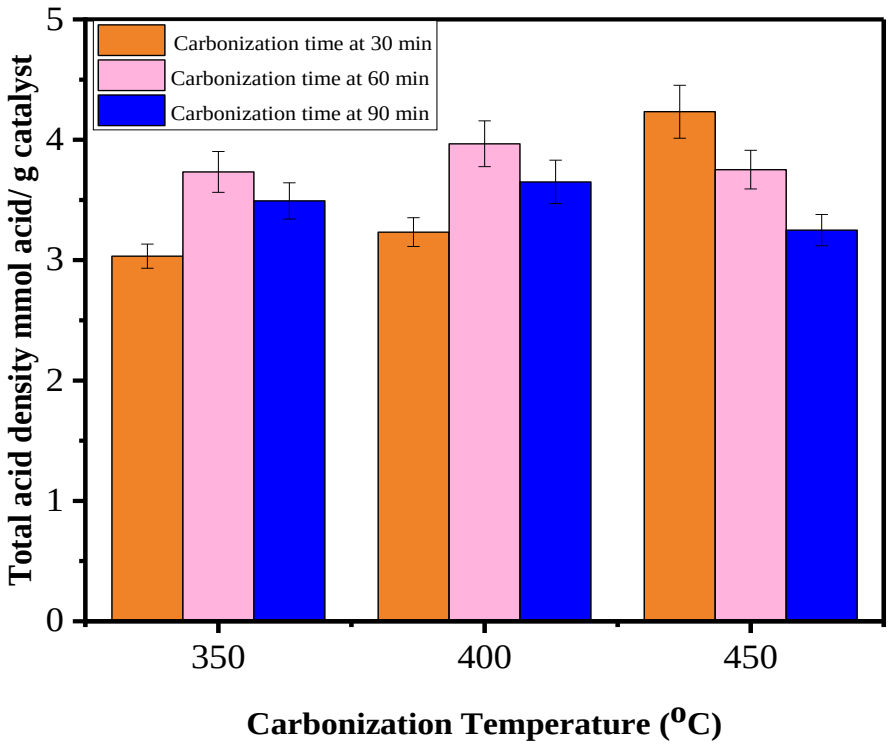

Figure 4. 1. The total acid density of sulfonated Al-biochar-based catalyst

In addition, carbonization temperature and time were also had great impact on the content of the SO_3H group (Dong et al., 2016). As can be seen from Figure 4.2, at 450°C, carbonization temperature, the SO_3H density was higher but as carbonization time increased the SO_3H density reduced slight difference between the carbonization time of 60 min and 90 min. But at relatively lower carbonization temperatures i.e., 350°C and 400°C, the SO_3H varied slightly with the carbonization time. Therefore, it can be concluded from this result the highest sulfonic acid density can be obtained at relatively higher temperature and short carbonization time. High sulfonic acid loading at higher temperature is probably due to incomplete amorphous carbonized structures, –OH, and -COOH was successfully formed onto the carbon skeleton (X. L. Zhang et al., 2020). Furthermore, low sulfonic acid charging at lower carbonization temperature and higher carbonization time due to the formation of macromolecular fused ring aromatic planar carbon, which deceases their binding ability with the sulfonic acid groups (X. L. Zhang et al., 2020). Therefore, the maximum SO_3H group density (0.967$\pm$ 0.09 mmol/g) was obtained at a carbonization time of 30 min, carbonization temperature 450°C, sulfonation temperature 145°C, sulfonation time of 18 hr, and mass ratio of Al-biochar to the concentrated sulfuric acid ratio (1/20 *w/v*).

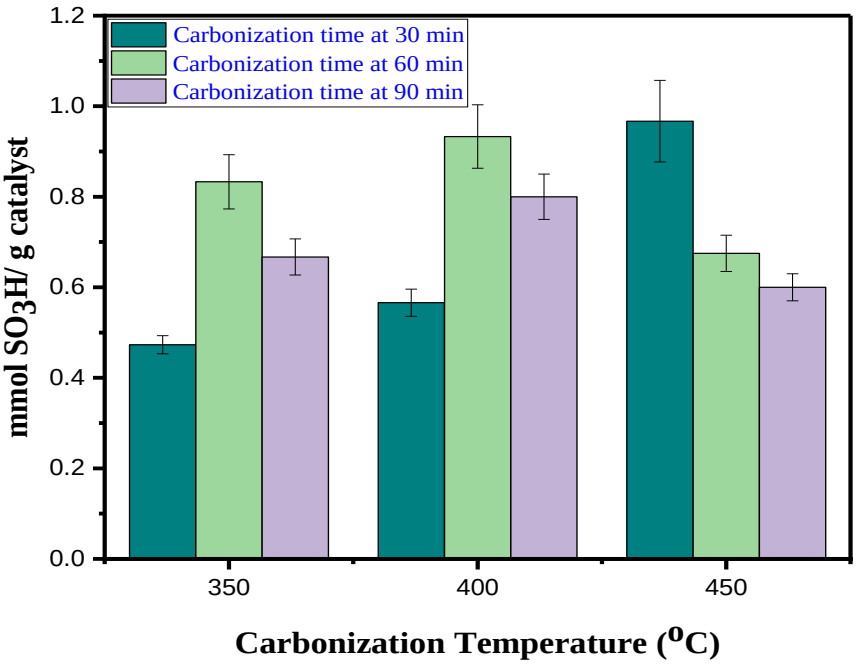

Figure 4. 2. The sulfonic acid density of the sulfonated Al-biochar based catalyst

4.2.2. Effects of sulfonation time on SO_3H group Al-biochar based catalyst

One parameter at a time analysis was conducted on the factors that affect the degree of sulfonation (temperature and time). Figure 4.3, which was tabulated from Table 2 under appendix B2, showed that the effects of sulfonation time were studied by varying the time between (12-24) hr at maintained other parameters (sulfonation temperature (145^{o}C), carbonization temperature (450^{o}C), carbonization time (30 min), the mass ratio of Al-biochar to sulfuric acid ratio (1/20 *w/v*)) on the SO_3H group acid density. As shown in the figure, the SO_3H acid density increased obviously with the time up to 18 hr. Further extending the sulfonation time leads to reduction of acid density (SO_3H). This is may be due to the carbon surface saturation of the catalyst happened at prolonged sulfonation time which protects the anchoring of SO_3H groups (Hussain & Kumar, 2018). Therefore, the maximum sulfonation time of 18 hr was obtained for the sulfonated carbon catalysts with a given study range. Similar results were presented by other researchers, in which the SO_3H group acid density decreased when the sulfonation time increased after reaching its maximum point and the maximum sulfonation time was also consistent with this work (X. L. Zhang et al., 2020). Therefore, a sulfonation time of 18 hr was selected for the subsequent preparation of catalyst.

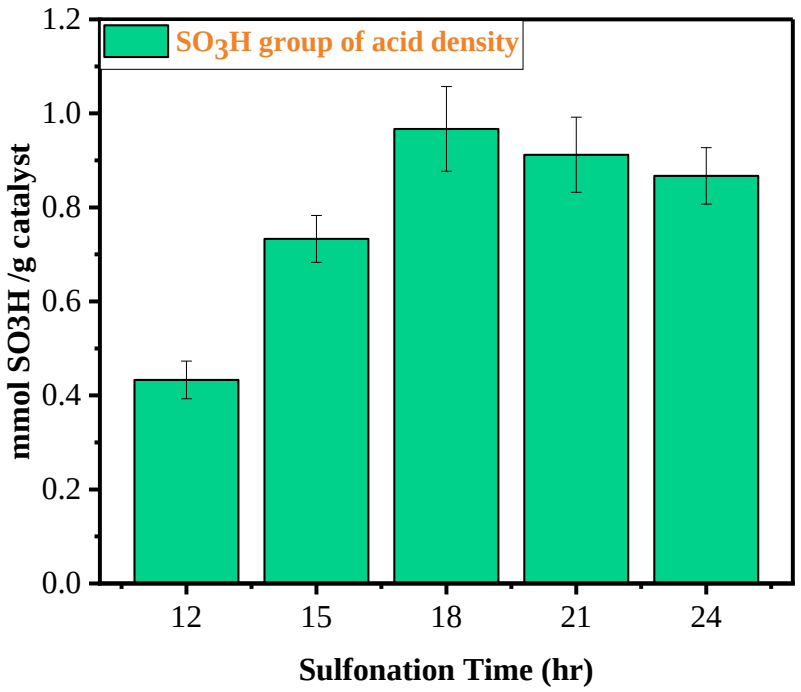

Figure 4. 3. Effect of sulfonation time on the sulfonic acid density

4.2.3. Effects of sulfonation temperature on SO_3H group Al-biochar-based catalyst

Sulfonation temperature is also one of the parameters that affect the amounts of SO_3H group of acid density. As it can be seen in Figure 4.4, which is tabulated from Table 2 of appendix B2, the SO_3H group of acid density first increased with increasing sulfonation temperature up to 120^{o}C and then, decreased when the temperature is above 120^{o}C, mostly resulting from the occurrence of side reactions such as sulfone and multi-sulfonation (Gowri & Fei-Ling, 2021). On the other hand, the lower SO_3H acid density results in lesser active sites for the reactions. Low sulfonation temperature favored the attachment of sulfonic acid groups to the Al-biochar, resulting in higher sulfonic group acid density. This was in agreement with other sulfonation processes performed by other research study under the temperature range of 50 to 200℃ (Jiménez Toro et al., 2019). However, it has been found that the sulfonation temperature below 100^{o}C is not sufficient to promote the formation of chemical bonds (interactions) between the sulfonating agent and the biochar, resulting in a decrease in the sulfonation rate, so the amount of sulfonic acid groups produced (SO_3H) catalyst is insufficient. Therefore, the maximum sulfonation temperature is 120°C for the sulfonated Al-biochar catalysts maintaining other conditions constant (carbonization temperature 450°C, carbonization time 30 min, sulfonation time 18 hr, mass

ratio of Al-biochar to a concentrated sulfuric acid ratio (1/20 *w/v*)). The maximum acid density obtained at this is around 1.033±0.1mmol/g.

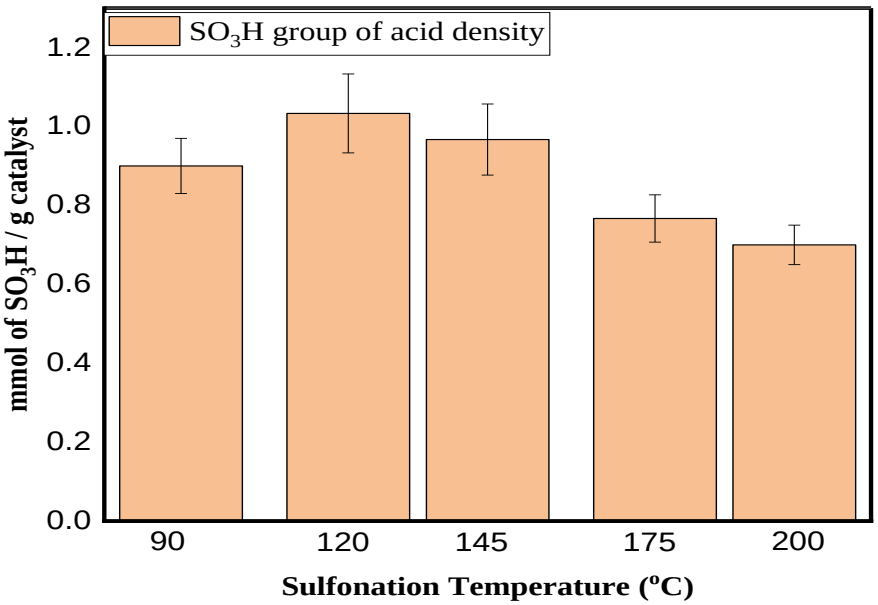

Figure 4. 4. Effect of sulfonation temperature on the sulfonic acid density

4.3. Characterization of sulfonated Al-biochar catalyst

4.3.1. Acid density determination

To measure the acid density characteristics of biochar, Al-biochar, and sulfonated Al-biochar acid-base back titration was used. The total acid density of Al-biochar (3.734±0.18 mmol/g) is higher than that of biochar (2.567±0.12 mmol/g), as indicated in Table 4.2. This showed that Al incorporation contributes to the total of acid sites. Additionally, the presence of metal oxides can positively affect the mechanism of biomass pyrolysis (Norouzi & Di Maria, 2018). Likewise, the total acid density of 4.767±0.23 mmol/g was obtained after treating Al-biochar with concentrated sulfuric acid. This indicates the incorporation of SO_3H acid densities, which act as the bronsted acid.

Table 4. 2. Total acid densities and SO_3H acid sites of the prepared catalyst

Sample	Total acid densities (mmol/g)	SO_3H acid densities (mmol/g)
Biochar	2.567±0.12	n.d
Al-biochar	3.734±0.18	n.d
Sulfonated Al-biochar	4.767±0.23	1.033±0.1

4.3.2. Brunauer-Emmett-Teller (BET) Analysis

The specific surface area of biochar, Al-biochar, and sulfonated Al-biochar catalyst samples were measured using N_2 physisorption analysis. Accordingly, the surface area of biochar, Al-biochar, and sulfonated Al-biochar samples are shown in Table 4.3. As shown in the table, the surface area of biochar is higher than that of Al-biochar and sulfonated Al-biochar catalyst. On the other hand, the surface area of Al-biochar is less than that of biochar due to the surface dispersion of aluminum oxides on the flax straw during the impregnation process. Moreover, sulfonated Al-biochar has a lower surface area compared to the other due to surface loading of Lewis acidity during the impregnation of flax straw and SO_3H group acid density grafted on the surface of Al-biochar during the sulfonation process. Therefore, the surface area of the sulfonated products was lower as compared to the others.

Table 4. 3. Surface area characterization of biochar, Al-biochar, and SABBC

Sample name	BET or surface area (m^2/g)
Biochar	553.51
Al-biochar	543. 25
SABBC	516. 03

4.3.3. Fourier Transform Infrared (FT-IR) Spectroscopy

The FTIR spectrum of biochar, Al-biochar, and Sulfonated Al-biochar are shown in Figure 4.5. The FTIR analysis of flax straw biochar, which was carbonized at 450 ^oC for 30 min, is shown in Figure 4.5 for comparison with the result of Al-biochar and synthesized catalyst. As shown in the figure, the spectra of biochar presented at a wavenumber of 3434 cm^{-1} indicate the presence of an OH functional group. In addition, the characteristic bands found at the peaks of 2917 cm^{-1} and 2849 cm^{-1} showed the vibration bands of the carboxylic acid functional group (-COOH). Furthermore, the bands formed at 1629 cm^{-1} and 1543 cm^{-1} wavenumber implies the presence of C=C and C=O functional group of the biochar respectively. The other peaks presented at 567 cm^{-1}, 494 cm^{-1}, 450 cm^{-1}, and 426 cm^{-1} wavenumbers are shows the presence of C-H (aromatic) out-of-plane bending vibrations (Sevilla & Fuertes, 2009).

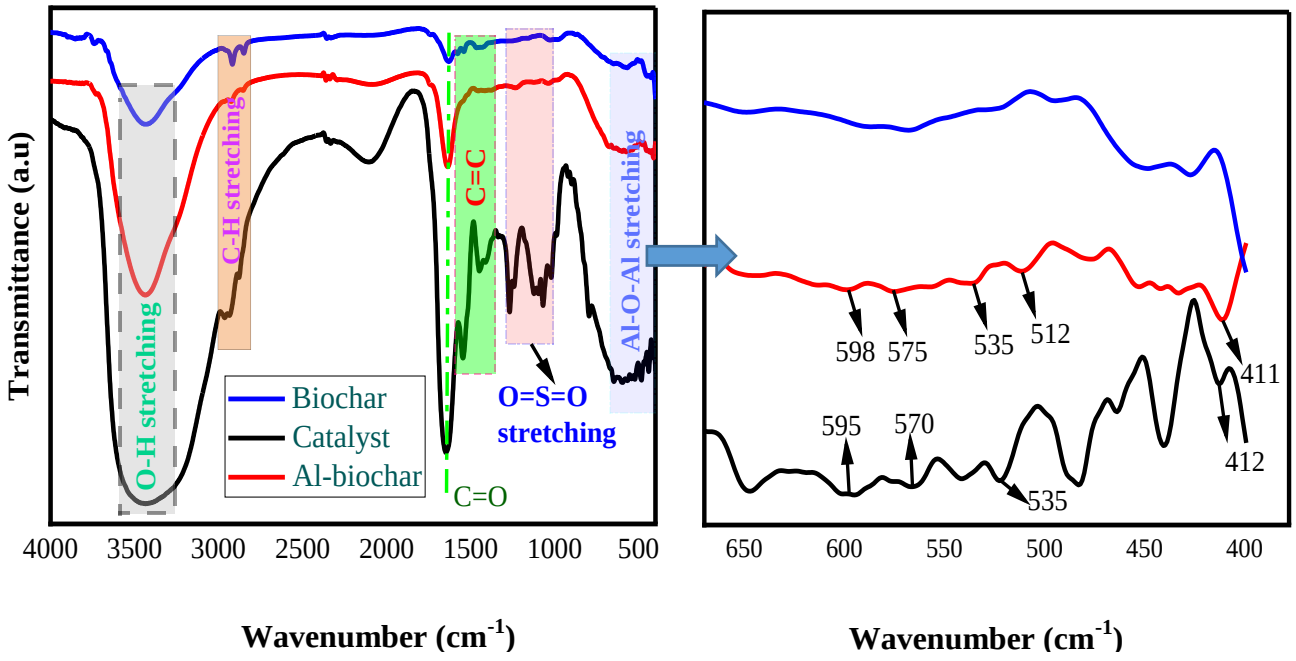

Figure 4. 5. FTIR spectra of biochar, Al-biochar, and Sulfonated Al-biochar

For Al-biochar the stretching mode of conjugated C=C bond at 1547 cm^{-1} and a band at 2925 cm^{-1}, 2854 cm^{-1} are attributable to saturated C-H stretching vibration, it was attributable to the aromatic ring formed as a result of incomplete carbonization of carbonaceous materials (X. Liu et al., 2017). The band 1642 cm^{-1} was C=O stretching vibration peak and 3429 cm^{-1} belonged to the O-H stretching vibration peak (W. Qi et al., 2018). In addition, peaks observed in spectra indicated there were plentiful oxygen-containing groups such as phenolic, hydroxyl, ester, ether, and carboxylic groups in the polycyclic aromatic skeleton. According to Nila (2018) the Al-O-Al stretching vibration lies between 400-900cm^{-1}. As shown in Figure 4.5 the peaks at 598cm^{-1}, 575 cm^{-1}, 535 cm^{-1}, 512 cm^{-1}, and 412cm^{-1} are demonstrating the Al-O-Al stretching vibration. Therefore, these FTIR results confirmed that Al was incorporated on the surface of flax straw during the impregnation process.

The FTIR spectra result of sulfonated Al-biochar is shown in Figure 4.5. After treatment with sulfuric acid, the stretching vibration peak located at 3429 cm^{-1}, 2962 cm^{-1}, 2879 cm^{-1}, 1642 cm^{-1}, and the functional groups of –OH, -CH_2 –COOH is dramatically increased as compared to Al-biochar, which means that significant changes have taken place in the structure of sulfonated Al-biochar catalyst. In addition, the new peaks observed around 1547cm^{-1} (C=C stretching vibration) show that the sulfonation process favors the formation

of carboxylic groups on the surface of the material (da Luz Corrêa et al., 2020). The new bands formed at 1267 cm^{-1}, 1122 cm^{-1}, 1069 cm^{-1}, and 1022 cm^{-1} are attributed to the group of SO_3H acid density of the prepared catalyst. From these, the peaks at 1267 cm^{-1}, and 1122 cm^{-1} shows that the asymmetric stretching of the O=S=O functional group of SO_3H acid density. Similar results have been reported by (Ryu et al., 2018; Trung et al., 2020). However, the peaks formed at 1069 cm^{-1}, and 1022 cm^{-1} depict the symmetric stretching of the O=S=O functional group of SO_3H acid density. This study also agreed with the literature studies (FA et al., 2018; Lin et al., 2017; Mazzotta et al., 2014). Furthermore, Al-O-Al stretching vibration peaks have been confirmed at 595cm^{-1}, 570 cm^{-1}, 535 $cm^{-1,}$ and 412cm^{-1}, which indicate the presence of Al after the sulfonation process. Therefore, the FTIR results confirmed that the presence of four different kinds of acid cities (e.g. -OH, -COOH, SO_3H, and Lewis acid sites in the form of Al-O-Al) in the carbon framework of the catalysts.

4.3.4. XRD analysis of catalyst

Figure 4.6, shows the XRD patterns of biochar, Al-biochar and the sulfonated Al-biochar based catalyst.

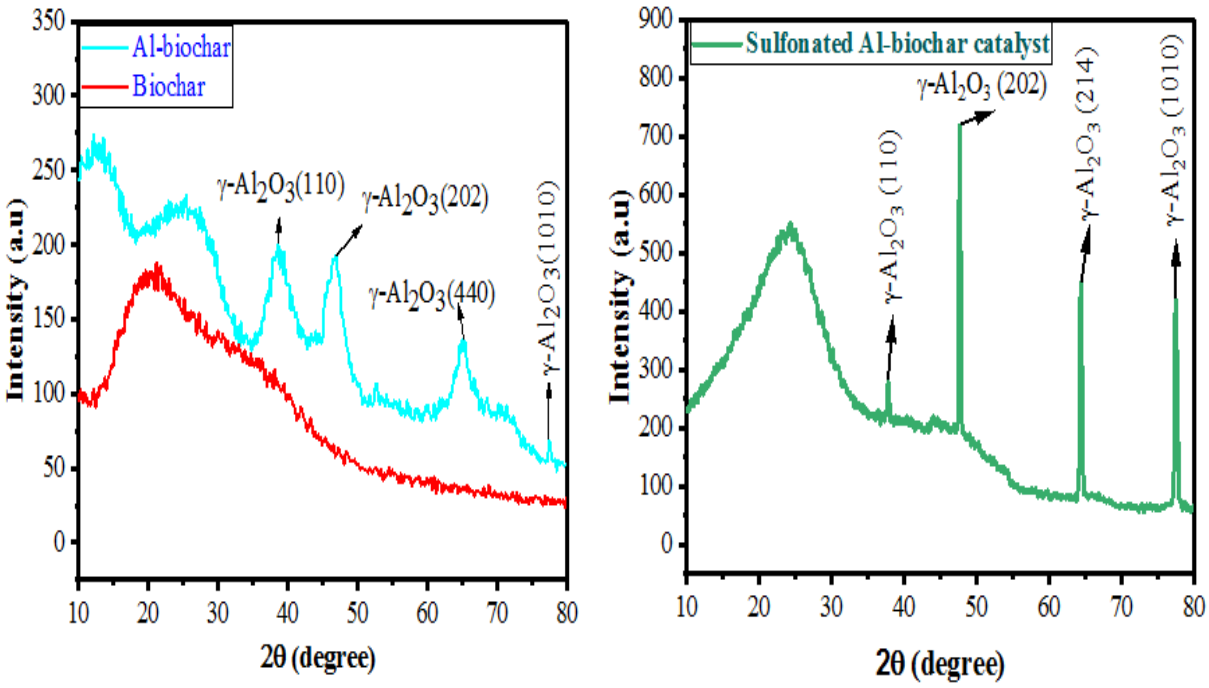

Figure 4. 6. XRD pattern of biochar, Al-biochar, and sulfonated Al-biochar catalyst

As shown in Figure 4.6, the broad peaks were observed between the 2-theta of 20^o-30^o for biochar obtained at 450 ^oC at 30 min, which indicates a highly amorphous structure was

formed. No other kinds of peaks were observed. Whereas in the case of Al-biochar in the presence of Al in form of gamma Al_2O_3 on the surface of biochar. Especially the peaks found at 37.76^o, 46.57^o, 66.76^o, and 77.50^o confirms the crystallinity structure of Aluminum composite biochar (Alam & Ansari, 2015; Omar, 2015; Selpiana et al., 2022). Furthermore, no $AlCl_3$ or Al metal were detected, indicating that the $AlCl_3$ was completely removed or bonded to the oxygen functional groups on the carbon support under the applied carbonization temperature.

Likewise, as shown in Figure 4.6, sulfonated Al-biochar displayed a broad range diffraction peak within 2-theta of 10^o - 30° assigned to amorphous carbon and was understood to be the reflection of aromatic carbon composed of aromatic carbon sheets oriented significantly at random (L. Wang et al., 2014). Additionally, the XRD pattern for sulfonated Al-biochar based catalyst showed sharp peaks at 37.76^o, 46.57^o, and 77.50^o when compared to Al-biochar (Shen et al., 2014). Furthermore, based on the XRD analysis of sulfonated Al-biochar catalyst, the diffractograms pattern of gamma aluminum oxide showed the same peaks with Al-biochar except one peak observed at 64.963^o (214) which also demonstrates the presence of gamma-Al_2O_3 on the surface of catalyst (Nila, 2018).

4.3.5. Thermogravimetric Analysis (TGA)

Thermogravimetric analysis (TGA) curves were used to observe the change in thermal stability of synthesized catalyst caused by surface modification of biochar. The TGA curves for the biochar, Al-biochar, and sulfonated Al-biochar based catalyst (SABBC) were shown in Figure 4.7 and Table 4.4 compiles the weight losses determined from TGA profiles at different temperature ranges.

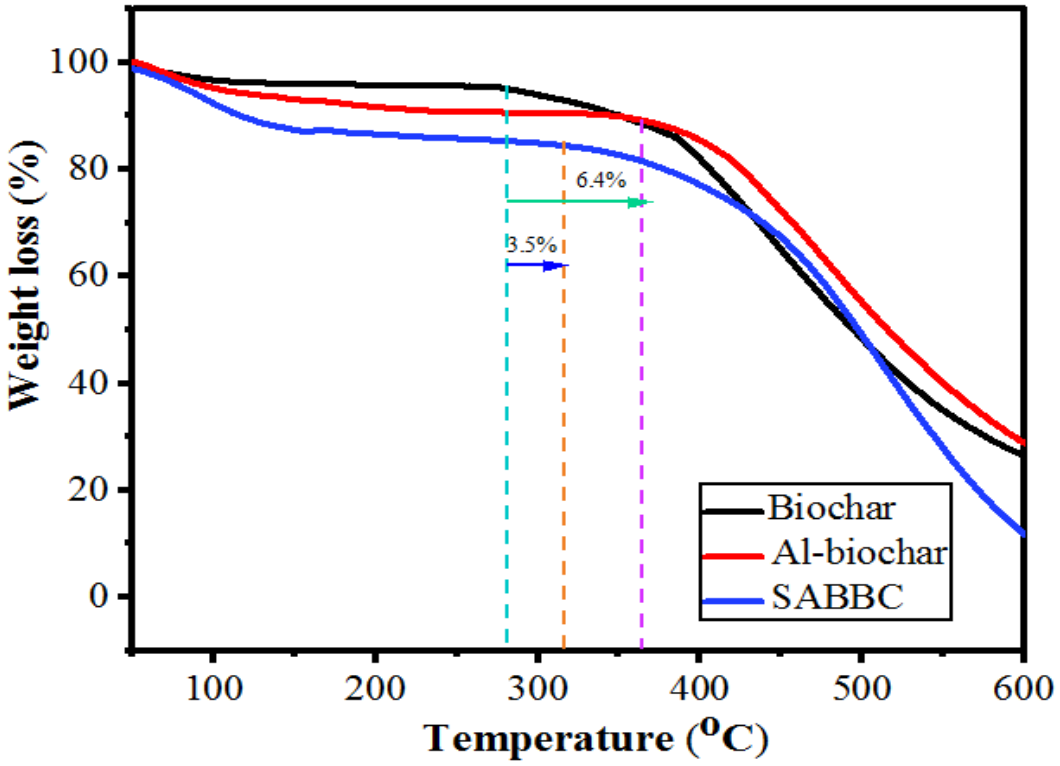

Figure 4. 7. TGA curve of biochar, Al-biochar, and sulfonated Al-biochar based catalyst (SABBC)

Table 4. 4. Sample weight loss during TGA analysis

Sample	Temperature (°C)	Weight loss due to moisture (%)
Biochar	50-100	3.83
Al-biochar	50-150	6.71
SABBC	50-150	12.48

As it can be seen in the figure, the thermal decomposition behavior of biochar, Al-biochar, and sulfonated Al-biochar based catalyst attributes to a marginal weight loss 3.83%, 6.71%, and 12.48% were observed in the temperature range of biochar (50-108 °C), and Al-biochar (50°C -150°C) and SABBC (50°C -150°C), respectively. This is probably due to the thermo-desorption of the physical adsorbed material. The moisture content is depicted as the loss of water molecules present in the catalyst, which is being adsorbed from the environment due to the hydrophilic properties of biomaterial. This process did not change the chemical structure of the sample.

Similarly, as it can be seen in the figure of biochar, Al-biochar, and sulfonated Al-biochar based catalysts are stable within 108-279^{o}C, 150-365^{o}C, and 150-315^{o}C temperature range, respectively. As compared to that of Al-biochar, sulfonated Al-biochar based catalyst showed an extra weight loss (around 3.5%) 315^{o}C-365^{o}C temperature range. This phenomenon could be due to decomposition of sulfonic acid group (-SO_3H) in this temperature range, and this would eventually cause the decline of its catalytic activity. Therefore, the synthesized sulfonated Al-biochar thermally stable up to 315^{o}C. The dehydration reaction should not exceed 315 ^{o}C, to prevent the deactivation of the catalyst.

The final weight loss, which is 49.05%, observed between 279^{o}C and 500^{o}C for biochar may be due to the removal of the surface functional group, which is leading to the formation of aromatized residue (L. Zhao et al., 2010). While compared to that of biochar, the TGA curve of the Al-biochar indicated extra stability or weight stage, which is, 6.4% in the 279^{o}C- 365^{o}C temperature range (Figure 4.7). This indicates that the thermal stability of Al-biochar is more than that of biochar due to Al-species appear in stable forms, such as oxides or strong Al-carbon interactions (Yu et al., 2019).

4.3.6. SEM analysis of catalyst

The surface morphology of the biochar, Al-biochar, and sulfonated Al-biochar catalyst were evaluated by scanning electron microscopy.

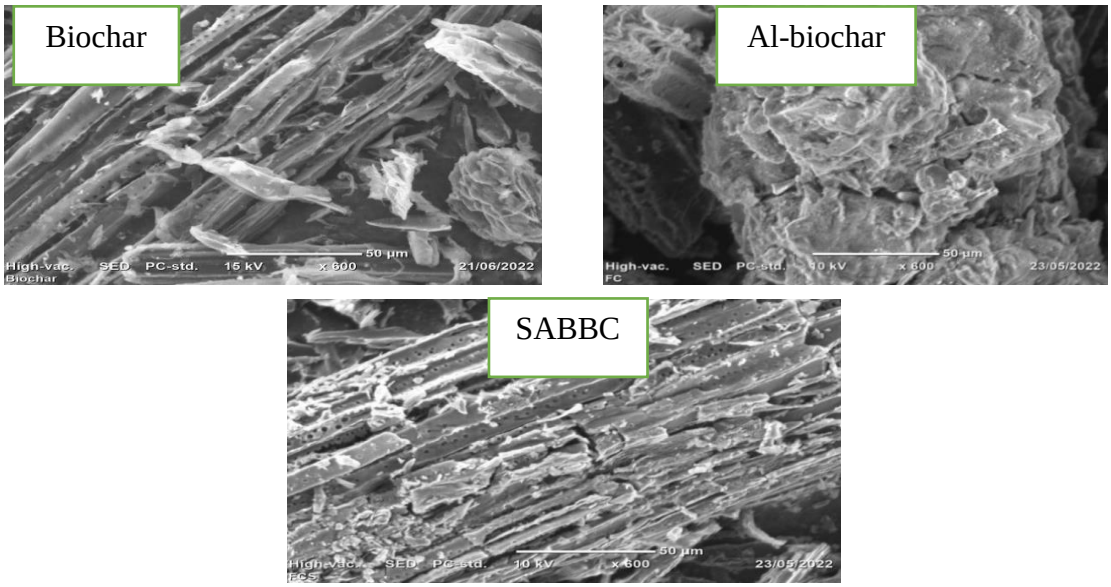

Figure 4. 8. SEM images of biochar, Al-biochar, and Sulfonated Al-biochar based catalyst (SABBC)

As shown in Figure 4.8, the carbonized flax straw displayed longitudinal fibrous structures probably arising from the cellulosic structures of flax straw, and some irregular pores begin forming due to the elimination of volatile content during carbonization at 450^{o}C. On the surface of carbonized flax straw, some unidentified fragments with tiny pores were also observed, which might be the remains of tarry compounds created during the carbonization stage. This was supported by a prior study in which the char products of surface porosity increased during the carbonization process, producing a huge surface area (Thanapal et al., 2014).

In Figure 4.8, the SEM micrographs of Al-biochar show the formation of an amorphous and porous structure. It was identified that the pores formed on the Al-biochar surface were reduced after acid treatment using sulfuric acid as shown in SEM image analysis of SABBC. The decreases in cavity in the sulfonated Al-biochar based catalyst were probably due to the process of functionalization with concentrated sulfuric acid, which is a strong sulfonating agent (Endut et al., 2017). The surface structure was also changed from an amorphous to an irregular shape into a fibrous structure.

4.4. Performance analysis for dehydration of xylose into furfural

The sulfonated Al-biochar contains (Lewis acid Al^{3+}), Bronsted acid sites (-SO_3H, -COOH, –OH functional groups). The total impact of these functional groups provides the catalysts with better catalytic performance. Lewis acid sites favor the xylose-xylulose-furfural route instead of xylose to furfural direct conversion and Bronsted acid sites catalyze the conversion of xylulose to furfural. The -SO_3H and -COOH act as Bronsted acid in the formation of furfural. The -SO_3H group protonates the hydroxyl group on xylose to form furfural via cyclodehydration upon release of water molecules. The hydrophilic nature of -OH and -COOH groups favor the accessibility active site of the catalyst by facilitating the adsorption of the reactant. Functionalization of the carbon structure with -COOH and -OH groups provides a hydrophilic nature to the hydrophobic carbon surfaces.

4.4.1. Reaction mechanism

Figure 4.10 shows the predicted reaction mechanism of xylose isomerization to xylulose followed by xylulose dehydration to furfural using a bi-functional-based solid acid catalyst. The reaction pathway of the bronsted acid catalyzed xylose dehydration might differ from that in the presence of Lewis acid and bronsted acid catalyzed xylose conversion into furfural.

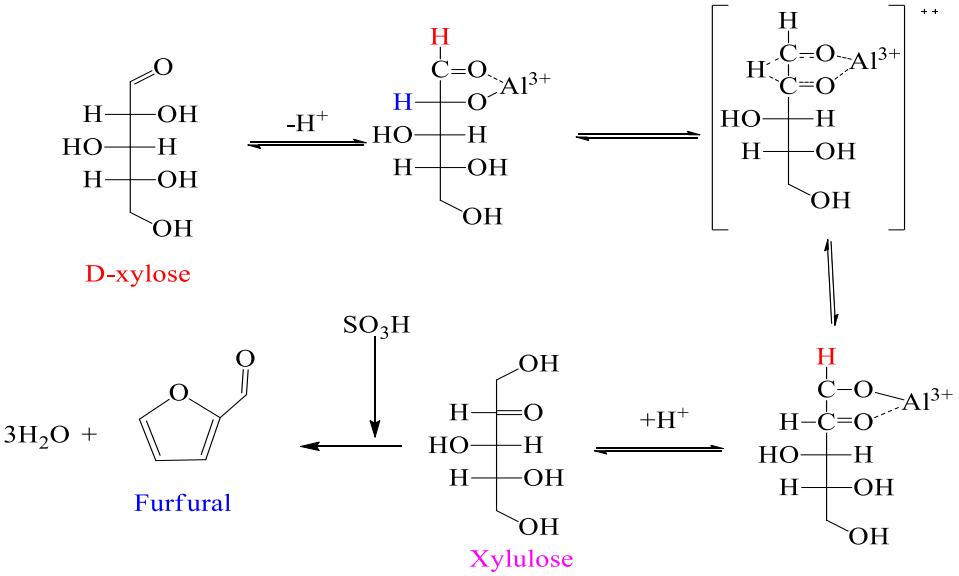

Figure 4. 9: Xylose dehydration into furfural reaction mechanism

The xylose to xylulose reaction path is analogous to the glucose to fructose isomerization proposed by (Román-Leshkov et al., 2010). As can be seen in Figure 4.9, the xylose isomerization to xylulose requires hydrogen transfer from O2 to O1 and C2 to C1. The hydrogen transfer from C2 to C1 is hydride transfer and it is activated by a proton donation from O2 to a solvation water molecules. This initial proton donation from O2 allows the formation of aluminum ion chelate with the O2 and O1 oxygens of the saccharide molecule, the hydride transfer ensues and proton back donation to O1 oxygen completes the isomerization. Alternatively, bronsted acid can dehydrates xylulose molecules into furfural by losing three molecules of water and forming furfural.

4.4.2. Performance analysis of with no catalyst (Blank), Al-biochar, and sulfonated Al-biochar catalyst on dehydration of xylose into furfural

The performance analysis without catalyst (Blank), Al-biochar, and sulfonated Al-biochar were evaluated during conversion of xylose into furfural at reaction conditions of (reaction temperature: 180 ^{o}C, reaction time: 2 hr and 0.2 gm of catalyst loading). Furfural formation was also analyzed using UV-visible analysis (Figure 4.10).

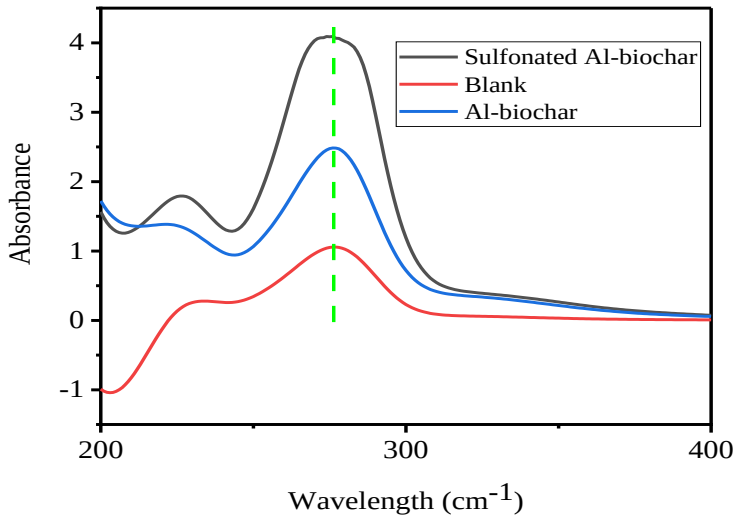

Figure 4. 10. Comparisons of blank (no catalyst), Al-biochar, and Sulfonated Al-biochar catalyst on furfural formation (reaction temperature: 180 ^{o}C, reaction time: 2 hr and 0.2 gm of catalyst loading)

The result revealed that high amount of furfural was synthesized by using Al-biochar as the catalyst as compared to blank (no catalyst) dehydration reaction condition. As well, the formation of furfural was enhanced further when sulfonated Al-biochar was used because more acid sites were loaded on the surface of Al-biochar. Relatively 38.9 % more furfural was produced using sulfonated Al-biochar catalyst as compared to Al-biochar catalyst. Whereas, more than 73.9% furfural was produced using sulfonated Al-biochar catalyst as compared to no catalyst (blank) reaction condition.

4.5. Determination of xylose conversion and furfural formation

The xylose residue and furfural formation were determined using the Uv-visible spectrophotometry. The residue of xylose left after the reaction was determined using calibration curve generated using **phenol-sulfuric acid** method. Thus, standard xylose concentration and their absorbance in Uv-visible spectrophotometry were reported in Table 1 under Appendix E. Using origin software, the calibration curve of the xylose standard was plotted and the linear equation produced from the plot was used for the determination of unknown xylose as follows;

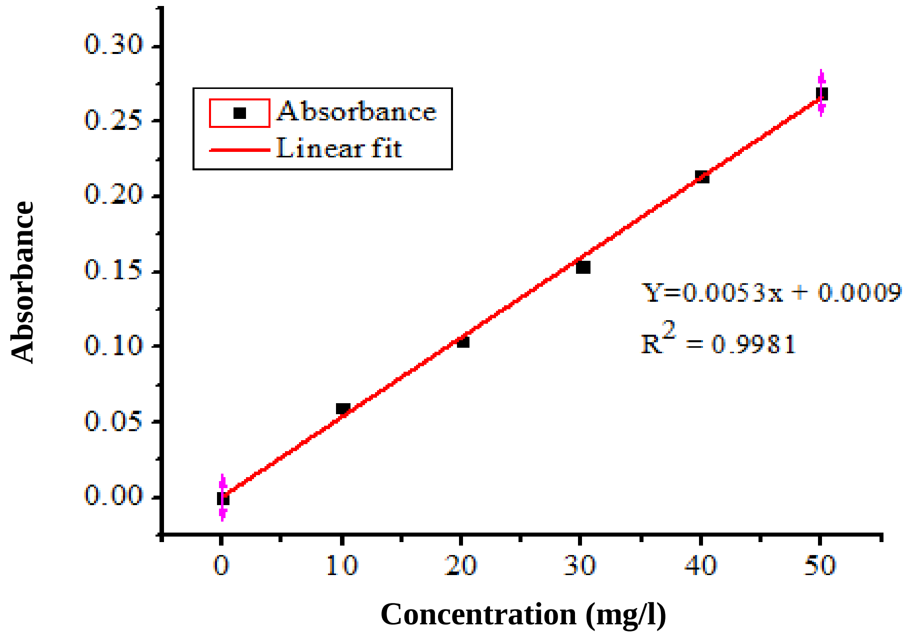

Figure 4. 11. Calibration curve of standard xylose for determination of xylose concentration

$$Y = mx + b \ldots\ldots\ldots\ldots\ldots\ldots\ldots\ldots\ldots\ldots\ldots\ldots\ldots\ldots 4.1$$

Where; Y is absorbance, m is slope of the line, x is concentration xylose, and b is intercept.

From the graph above intercept is 0.0009 and slope is 0.0053, then the equation Y=0.0053x+0.0009 with R-square 0.9981. The unknown concentration of xylose was determined as follows;

$$X = \frac{Y - 0.0009}{0.0053} \ldots\ldots\ldots\ldots\ldots\ldots\ldots\ldots\ldots\ldots\ldots\ldots 4.2$$

Finally, the total concentration of unreacted xylose determined by ‘‘X’’ multiplied dilution factor. Then, final concentration of xylose determined based equation 4.2 multiplied by dilution factor were stated in Table 2 under Appendix E.

4.5.1. Parameters that affect furfural synthesis from xylose

4.5.1.1. Effects of reaction temperature

The effect of reaction temperatures on the formation of furfural from xylose were investigated in the presence of a prepared catalyst. The investigation were performed in the temperature ranges 150^{o}C-190^{o}C using 2 hr time, 0.2 g SABBC, 0.5 g xylose, 1.5mmol NaCl, 20 ml water/2-MeTHF systems (5 ml water and 15 ml 2-MeTHF). As shown in Figure 4.12 (a) the formation of furfural increased with the increase in reaction temperature

up to 180^{o}C. However, for temperatures exceeding 180^{o}C the activity decreased and lower furfural formation was obtained. The lower furfural formation might be due to the degradation of products and the formation of byproducts. Furfural formed is converted to by-products, mainly to humins, when exposed to higher temperatures (D. R. Hua et al., 2016). The humin, deposited on the surface of solid acid catalysts affects the performance of the catalysts by preventing the reactants from accessing the active site (Kang et al., 2018). The researchers also carried out experimental studies on the behavior of furfural concerning its degradation at varied temperatures above 180 ℃ and found decreasing amounts of furfural in both the reactions with and without catalysts (Ershova et al., 2015). Various works by different researchers also revealed the same diminishing trend in furfural formation at higher temperatures after reaching the maximum (F. Guo et al., 2019; Z. Qi et al., 2020; Vo et al., 2016). In addition, in Figure 4.12 (b), at the lowest temperature of 150 ^{o}C, the conversion of D-xylose using SABBC was achieved 30.09%, whereas practically any furfural was produced. The catalyst can partially dehydrate D-xylose, even at very low temperatures; however, it was not fully generated furfural. Further increasing reaction temperature, and conversion of xylose increases indicates that most of the molecules of xylose could be converted into furfural and byproducts of furfural.

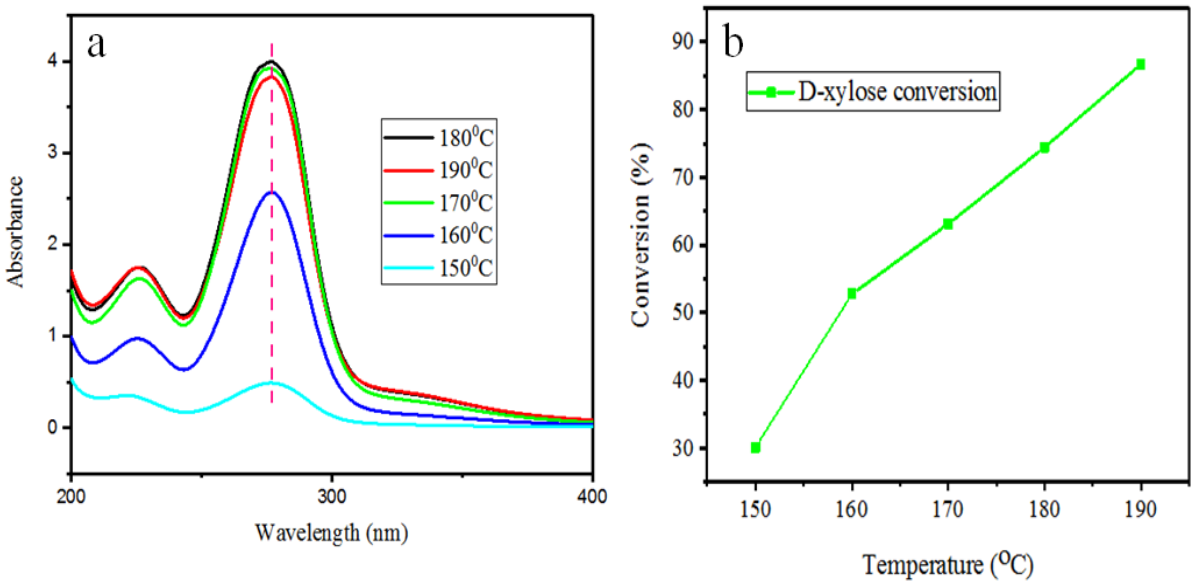

Figure 4. 12. Effect of reaction temperature on the furfural formation/a and xylose conversion/b

4.5.1.2. Effects of reaction time

After determining the best temperature reaction condition (180 ^{o}C) for the formation of furfural, the effect of the reaction time (1 – 5 hr) was studied on the furfural formation and

xylose conversion as shown in Figure 4.13 (a, b). The other parameters were unchanged using D-xylose (0.5 g), SABBC (0.2 g), NaCl (1.5 mmol), and biphasic solvents (5 ml water and 15 ml of 2-MeTHF). For the first 2 hr, the degree of dehydration increases, and hence the formation of the product increased. However, the formation of furfural decreased for the reaction time greater than 2 hr as illustrated in Figure 4.13 (a), which may also be due to degradation of furfural upon further treatment beyond 2 hr. The decreasing of furfural formation could also occur when furfural undergoes retro aldol fragmentation into acids, aldehydes, and ketones (Wu et al., 2014). The fragmentation of furfural results in the formation of lactic and formic acids and various aldehydes such as glyceraldehyde, formaldehyde, pyruvaldehyde, glycolaldehyde, and acetaldehyde (Peleteiro et al., 2016).

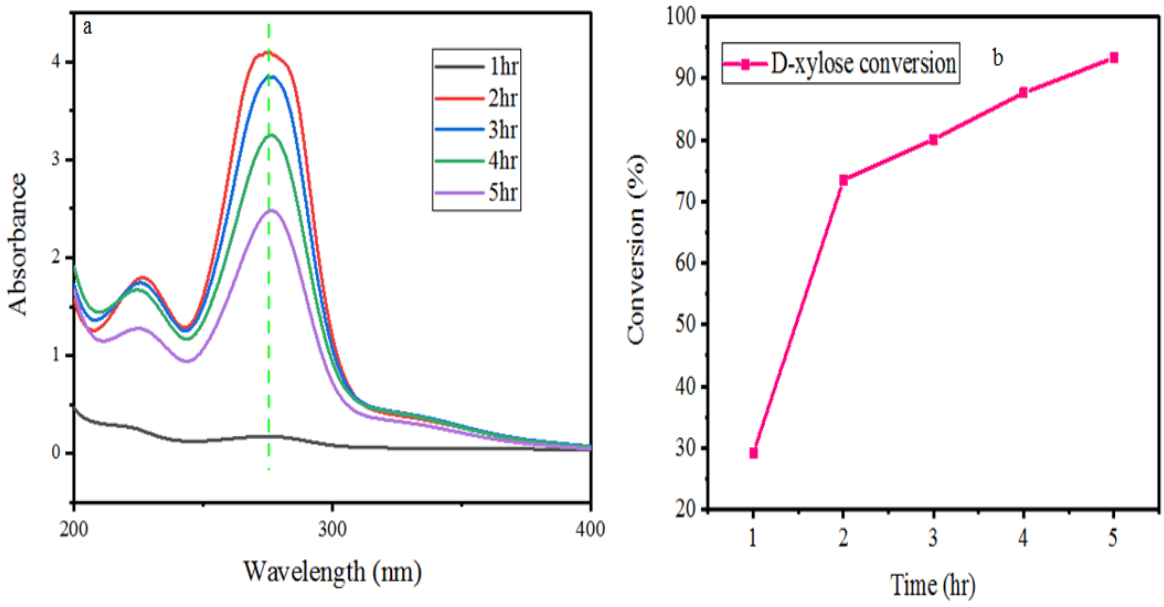

Figure 4. 13. Effect of reaction time on the furfural formation /a and xylose conversion /b

4.5.1.3. Effects of catalyst loading

The catalyst loading was one of the major parameters that affect the formation of furfural. The influence of the catalyst dosage on xylose conversion and furfural formation at 180 ^{o}C for 2 hr in biphasic solvents water/2-MeTHF ratio (5:15, *v/v*) was investigated by varying the amount of SABBC from 0 to 0.4 g. The other reaction conditions were consistent with previous experiments As shown in Figure 4.14 (a) very low furfural formation was recorded for the conversion test without catalyst and increased formation of furfural was observed with the increase in the amount of catalyst up to 0.2 g. Moreover, xylose conversion increased from 38.58% to 89.52% (Figure 4.14 (b)) when catalyst loading increased from 0 to 0.4g. Surprisingly, the furfural formation reached a relatively high

value and 61.23% of xylose conversion using only 0.1 g catalyst, which also suggests the high performance of the SABBC. Further increasing the catalyst dosage to 0.4 g, almost similar furfural formations were observed. As the amount of the catalyst added to the reaction system increases, sufficient catalytically active sites will be available for xylose dehydration to furfural, and therefore the formation of furfural increases. However, the overloading of the catalysts would lead to side reactions such as fragmentation, condensation, and resinification, which limits the final formation of products (L. Zhang et al., 2019). The adsorption of furfural is also possible (Doiseau et al., 2014) as a strong hydrogen bond may probably be formed between the -OH and -COOH functional groups on the catalyst and the aldehyde group of furfural (Lin et al., 2019). These phenomena include both reversible and irreversible adsorption (Doiseau et al., 2014).

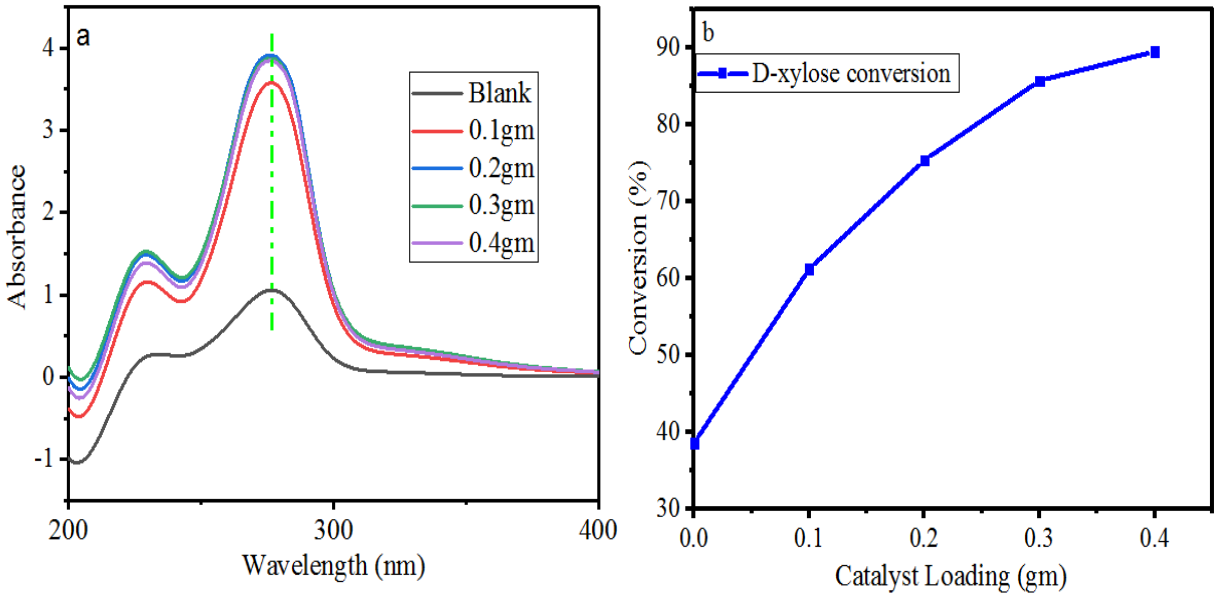

Figure 4.14. Effect of catalyst loading on the furfural formation /a and xylose conversion/b

4.5.2. Catalyst reusability on the formation of furfural

One of the distinctive advantages of heterogeneous acid catalysts over liquid acids is that the used catalyst can be easily recovered from the reaction mixture and can be potentially regenerated and reused (Ryu et al., 2018). The catalyst was checked for its recyclability by filtering and washing after being used in each catalytic run. The filtered catalyst was washed with ethanol and hot water. Then, the catalysts were dried at 105^{o}C for 12 hr using an oven drier and used for the next reaction. The furfural formation in each run were shown in Figure 4.15 using maximum parameters obtained from the study (5:15 H_2O/2-MeTHF ratio, 0.2 gm of catalyst, 0.5 gm of xylose, 180 ^{o}C reaction temperature, 2 hr reaction time and 1.5mmol of NaCl). As it can be seen in figure, the furfural formation has

slightly decreased from the initial to 4th cycles of catalyst reusability. The reason for the decrease in formation of furfural of may be caused by the following factors. First, during the reaction process, the sulfonic acid functional groups are dissociated or reacted with the reaction byproducts to form insoluble residues, which leads to the decrease of acid concentration on the catalyst surface (Wu et al., 2014). Second, the insoluble byproducts are continuously deposited on the catalyst surface and in the pores during the reaction process, which leads to the coverage and blockage of the active sites of the catalyst (Xu et al., 2021). Nevertheless, the reused catalysts still demonstrate better performance than the reaction with no catalyst.

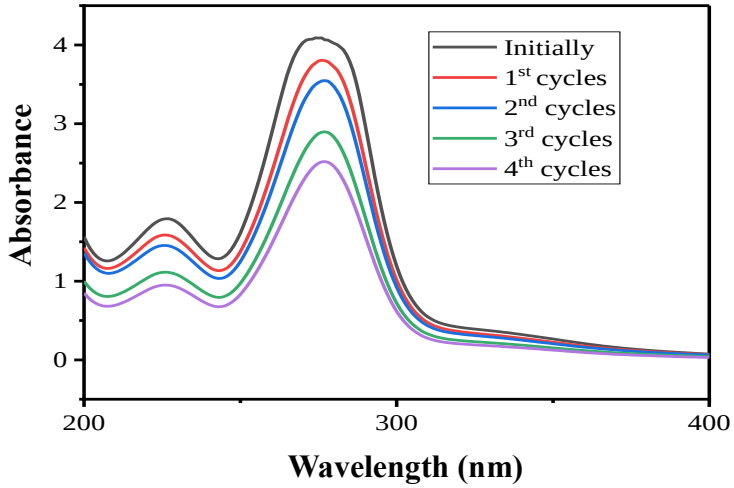

Figure 4. 15. Reusability of sulfonated Al-biochar catalyst on the formation of furfural

4.5.2.1. FTIR analysis of recycled sulfonated Al-biochar catalyst

Figure 4.16 shows the FTIR analysis of reused catalyst obtained from the spent fourth recycled sulfonated Al-biochar catalyst and initial or fresh sulfonated Al-biochar based catalyst. As it can be seen in the figure, the spectrum of the spent catalyst intensity of O=S=O (1243 cm^{-1}, 1118 cm^{-1}, 1054 cm^{-1}) stretching was decreased as compared to the initial prepared catalyst. The other peak was observed at 412 cm^{-1} confirm the presence of Al-O-Al stretching on the spent catalyst. However, the peaks observed at 595 cm^{-1}, 570 cm^{-1} and 535 cm^{-1} on the surface of sulfonated Al-biochar catalyst were removed after the 4th recycling of the sulfonated Al-biochar catalyst. This may be due to the fact that the cycle experiments were caused by ethanol washing, which resulted in the leaching of the Lewis acid and bronsted acid sites groups from the polycyclic aromatic hydrocarbons to deactivate the reusable catalyst (Lu et al., 2019). Additionally, the water used as the reactions solvent may be a contributing factor in the catalysts declining activity because heterogeneous acid catalysts find it difficult to maintain the desired acidity in a highly

protic and polar solvent such as water due to the solvents surface interaction and coordination properties (Molina et al., 2015).

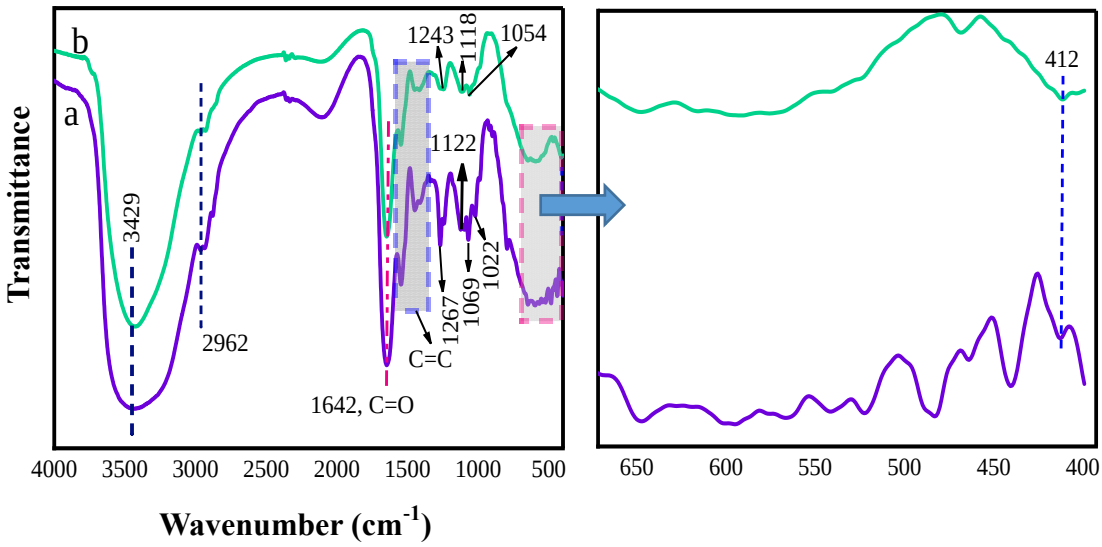

Figure 4. 16: FTIR analysis of fresh sulfonated Al-biochar catalyst (a) and recycled sulfonated Al-biochar catalyst (b)

4.6. Characterization of furfural

4.6.1. Physical characterization of furfural

The color and physical appearance of the produced furfural are compared to the standard furfural as shown in Table 4.5.

Table 4. 5. Physical properties of produced furfural

Physical property	The produced furfural	Standard furfural
Color	Reddish-brown	Appears as colorless to pale yellow or as reddish-brown
Physical state	Liquid	Liquid
Odor	Penetrating odor	Characterizing almond-like odor

4.6.2. Validation of furfural compound with FTIR spectroscopy

FTIR analysis with a wave number range of 400 cm^{-1} to 4000 cm^{-1} was performed to identify different functional groups available on the furfural compound. Although the physical characterizations of the produced furfural had been done, the presence of furfural

in the product can be confirmed by using FTIR spectroscopy based on functional group similarities with pure furfural Infrared spectra. As can be seen from Figure 2.1 and Figure 4.17, the structure of furfural is mainly characterized by the presence of an aldehyde group with C=O stretch, C-H stretch off C=O, and C=C, as well as aromatic ring furan consisting of C=C-H asymmetric stretch.

Table 4. 6. FTIR absorption spectrum of standard furfural

Characteristic wavenumber (cm^{-1})	Types of vibration
900–600	C-H-bonded
1140-1070	C-O-C
1620–1560	Aromatic -C=C-
1750–1625	Aldehyde –C=O
2900-2700	Aldehyde C-H
3060-3010	Aromatic C-H
3500–3200	Mono-substituted rings for aromatic ring

Figure 4.17 displays the produced furfural Fourier Transform Infrared Spectroscopy (FT-IR) spectrum and its distinctive wavelength. According to FTIR Table 4.6 above the furfural spectrum was examined (Iriany et al., 2021; Mohamad et al., 2020).

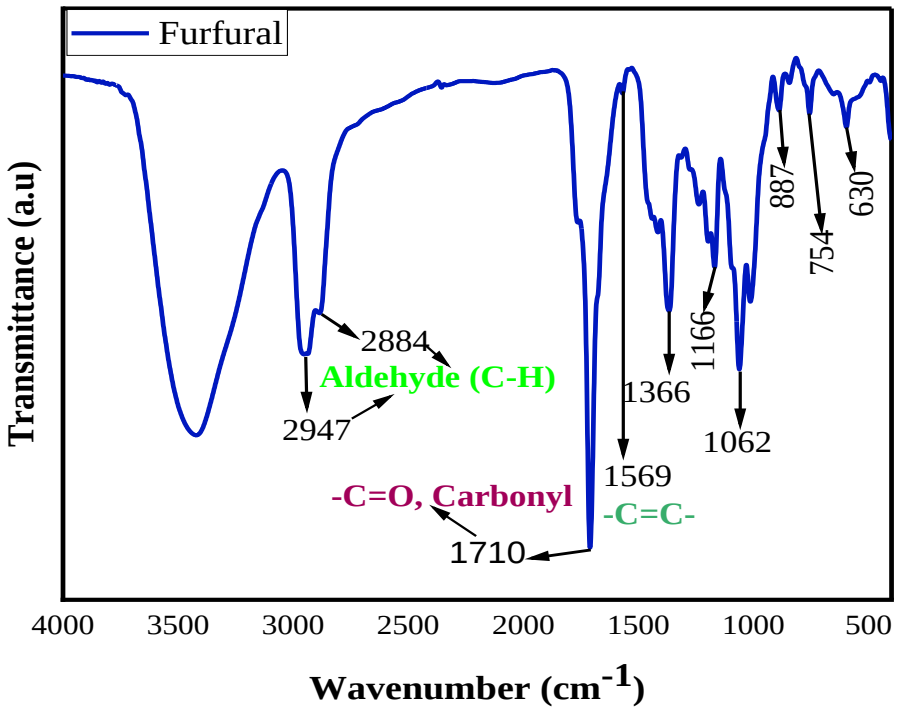

Figure 4. 17. FTIR analysis of the product containing furfural

As shown in the figure, the aldehyde group and aliphatic C-H stretches are responsible for the moderate intensity of the band established at 2947 cm^{-1} and 2884 cm^{-1} in the liquid

product furfural (Mohamad et al., 2020). The presence of a strong absorption at 1,710 cm^{-1} corresponds to the absorption of conjugated carbonyl (C=O) which occurs in conjugated aldehydes and not the ketone group. The C=O absorption is lower than the usual absorption of aldehyde due to internal hydrogen bonding which occurs in conjugated unsaturated aldehyde and conjugation lowers the vibrational frequency of carbonyl compounds (Ambalkar & Talib, 2012). The Strong peaks obtained at 1569 cm^{-1} and 1366 cm^{-1} show the stretching of -C=C- from the aromatic ring (Iriany et al., 2021). The peaks at 1,166 cm^{-1} and 1062 cm^{-1} correspond to the C-O stretching vibration. The aromatic ring and its derivatives are attributed to the C-H stretching and are detected by spectral ranges of 887 cm^{-1}, 754 $cm^{-1,}$ and 630 cm^{-1} that indicating the out-of-plane bending vibration. The presence of substituted aromatic groups is detected by the presence of peaks between 900–675 cm^{-1} (Ong & Sashikala, 2007).

4.6.3. HPLC Analysis of Furfural

Agilent 1100Series HPLC with UV detector was used to analyze and quantify furfural in the liquid product. For identification of the produced furfural using HPLC was carried out by comparing retention times (tR), and the peak of known standard furfural in the range of 50-300 ppm assay. The standard furfural sample is calibrated before the analysis of the produced furfural sample. The peak identification was based on the retention time and the ultraviolet spectrum was compared with the standard furfural. The matching between the occurrence of peaks at a retention time of the standard furfural and the component peak at the same retention time confirms the identity of the produced furfural.

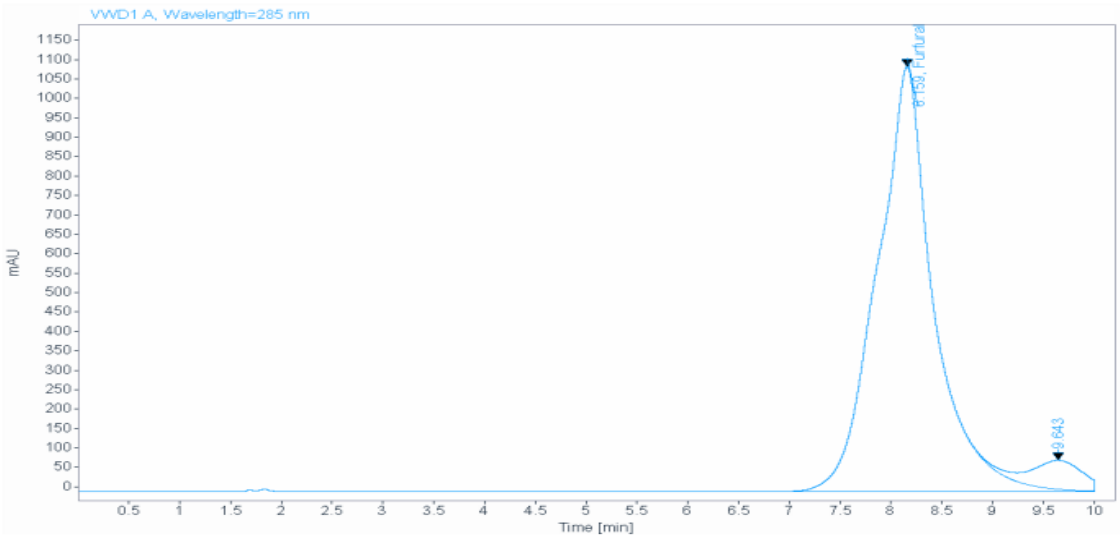

Figure 4. 18. HPLC analysis of standard furfural

Chromatogram Figure 4.18 shows the peak and retention time of the standard furfural, while Figure 4.19 shows the peak and the retention time of the produced furfural with respect to the standard furfural sample. The retention time is the time in which furfural took to travel through the column to the detector. This time is measured from the time at which the sample is injected to the point at which the display shows a maximum peak height. It is the characteristic of the furfural under operating conditions.

Figure 4.19 illustrates the HPLC analysis of furfural produced at 180 ^{o}C, under reaction conditions lasting 2hr, with 0.2 gm of catalyst loading to ascertain the quantitative and qualitative percentage of furfural synthesized from the xylose. By comparing the chromatographic peak regions and the retention times of the created furfural against the injection of a known quantity of standard furfural, the identification of the produced furfural was verified. The regular furfural has an 8.159 min retention time on average. The produced furfural is detected using this reference retention time, with a peak height of 1448.93 and a retention time of 8.159 min.

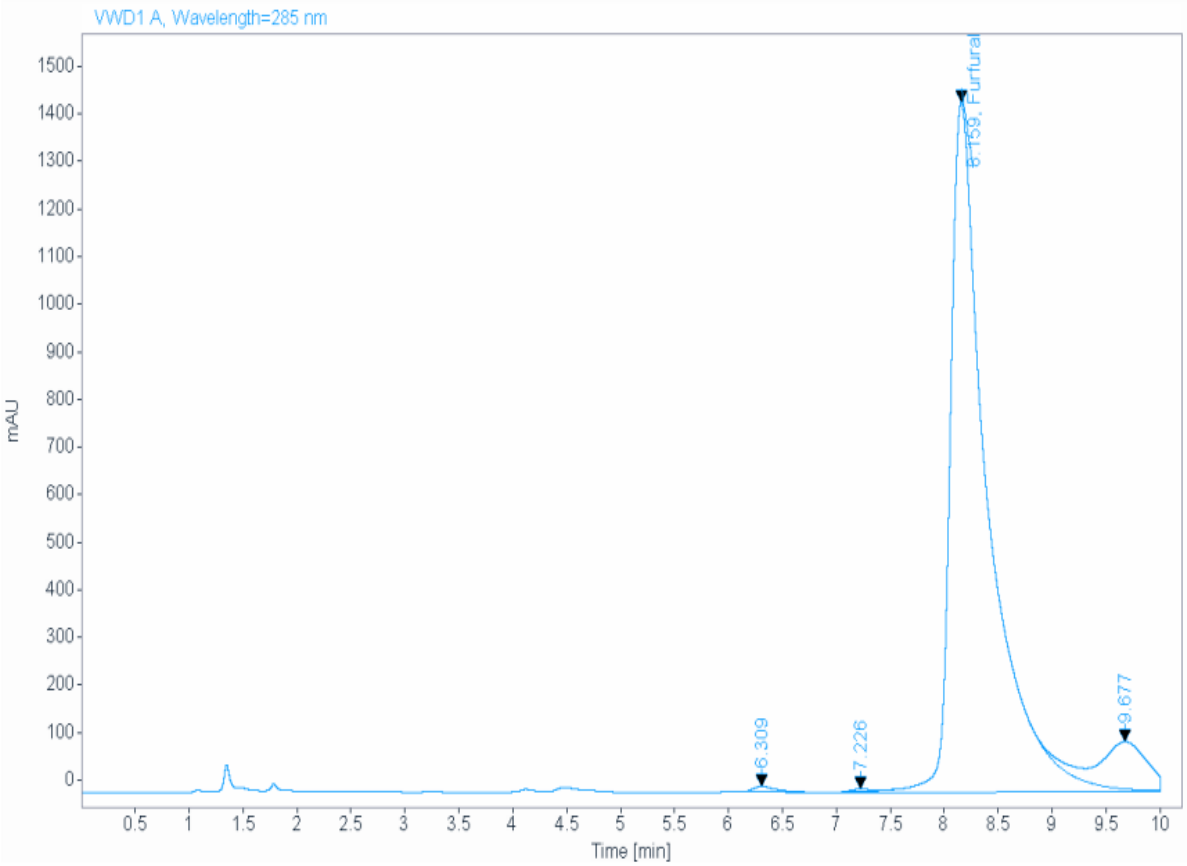

Figure 4. 19. HPLC analysis of produced furfural

CHAPTER FIVE

5. CONCLUSION AND RECOMMENDATION

5.1. Conclusion

In this study, carbon based bifunctional solid acid catalyst was used as an green, cheap, and recyclable heterogeneous catalyst for furfural synthesis. It has been prepared via impregnation-carbonization-sulfonation methods. The effects of catalyst preparation conditions (carbonization temperature and time, sulfonation temperature and time) on acid density were studied. The maximum total acid density (4.767 $\pm$ 0.23 mmol/g) and sulfonic acid density (1.033 $\pm$ 0.1 mmol/g) were achieved at maximum catalyst preparation conditions (Carbonization temperature of 450^{o}C, carbonization time of 30 min, sulfonation temperature of 120^{o}C, and sulfonation time of 18 hr). The specific surface area of synthesized catalyst had also reached 516.04 m^2/g. The presence of different functional groups (-OH, -COOH, SO_3H, Al-O-Al) on the surface of sulfonated Al-biochar based catalyst was confirmed by FTIR. Furthermore, XRD results also revealed that the presence of Al in the form of gamma- aluminum oxide on the surface of the prepared catalyst. The sulfonated Al-biochar based catalyst also showed thermally stable temperature between 150- 315^{o}C based on thermogravimetric analysis.

The synthesized bi-functional carbon based solid acid catalyst was responsible for the higher activity of isomerization and dehydration of xylose into furfural. The reaction was intensified with water-2-MeTHF a biphasic solvent by the addition of NaCl in the reaction medium to create an interface between the organic and water phases. The conversions of xylose and furfural formation were affected by sulfonated Al-biochar catalyst loading, temperature, and reaction time. The experimental results show that high reaction temperature, reaction time and catalyst loading were beneficial to increase the conversion of xylose in the early stage of the reaction, while high these reaction conditions would lead to a decrease in the formation of furfural. The conversion of xylose (73.5%), yield of furfural (64.7%), and selectivity of furfural (88.0%) were achieved at the reaction conditions (reaction temperature of 180^{o}C, reaction time of 2 hr, catalyst loading 0.2 gm). The functional groups exist in furfural were detected using FTIR and the results revealed the presence of conjugated carbonyl groups at a band intensity of 1710 cm-1 and aldehyde functional groups at wavelengths of 2884 cm^{-1} and 2947 cm^{-1}. In general, the synthesized

sulfonated Al-biochar catalyst showed a good performance in conversion of xylose into furfural as compared to other carbonaceous based solid acid catalyst.

5.2. Recommendation

Based on the findings of the present study and limitations, the following points were recommended.

- The current study looked at the effects of catalyst preparation parameters including carbonization temperature and time, as well as sulfonation temperature and time, on acid densities. However, to enhance the contents of acid densities, optimization of these catalyst preparation conditions were need to be further investigation.
- In addition, further study is required to investigate the effect of percent Al loading on the acid density of the catalyst. Further characterizations technique such as SEM-EDX to determine the amount of Al present in the produced catalyst.
- The current study additionally looked at how reaction parameters including catalyst loading, reaction time, and reaction temperature affect the conversion of xylose and furfural formation. It is recommended to investigate the effect initial substrate (xylose) concentration and solvent ratio on the conversion of xylose into furfural.

AKNOWLEDGEMENTS

This research thesis was funded by Adama Science and Technology University under the grant number ASTU/SM-R/581/22, Adama, Ethiopia.

6. REFERENCES

Abdullah, S. H. Y. S., Lananan, F., & Endut, A. (2019). *Catalyst Activity of Solid Acid Catalyst Derived From Agricultural Biomass for Biodiesel Production From Waste Cooking Oil*. *12*, 1031–1036.

Agirrezabal-Telleria, I., Gandarias, I., & Arias, P. L. (2013). Production of furfural from pentosan-rich biomass: Analysis of process parameters during simultaneous furfural stripping. *Bioresource Technology*, *143*, 258–264.

Agirrezabal-Telleria, I., Gandarias, I., & Arias, P. L. (2014). Heterogeneous acid-catalysts for the production of furan-derived compounds (furfural and hydroxymethylfurfural) from renewable carbohydrates: A review. *Catalysis Today*, *234*, 42–58.

Agirrezabal-Telleria, I., Larreategui, A., Requies, J., Güemez, M. B., & Arias, P. L. (2011). Furfural production from xylose using sulfonic ion-exchange resins (Amberlyst) and simultaneous stripping with nitrogen. *Bioresource Technology*, *102*(16), 7478–7485.

Agirrezabal-Telleria, I., Requies, J., Güemez, M. B., & Arias, P. L. (2012). Furfural production from xylose + glucose feedings and simultaneous N 2-stripping. *Green Chemistry*, *14*(11), 3132–3140.

Alam, M. T., & Ansari, A. H. (2015). X-Ray Diffraction Analysis and Microstructural Examination of Al-Sic Composite Fabricated By Stir Casting Technique. *International Journal of Science Technology & Management*, *4*(01), 941–955. www.ijstm.com

Ambalkar, V. U., & Talib, M. I. (2012). Synthesis of Furfural from Lignocellulosic Biomass as Agricultural Residues : A Review. *The International Journal of Engineering And Science.*, *1*(1), 30–36. www.theijes.com

Aslanzadeh, S., Ishola, M. M., Richards, T., & Taherzadeh, M. J. (2014). An Overview of Existing Individual Unit Operations. In *Biorefineries: Integrated Biochemical Processes for Liquid Biofuels*. Elsevier B.V.

Azargohar, R., Jacobson, K. L., Powell, E. E., & Dalai, A. K. (2013). Evaluation of properties of fast pyrolysis products obtained, from Canadian waste biomass. *Journal of Analytical and Applied Pyrolysis*, *104*, 330–340.

Biomass, L., Jiang, Z., Hu, D., Zhao, Z., Yi, Z., Chen, Z., & Yan, K. (2021). Mini-Review on the Synthesis of Furfural and Levulinic Acid from Lignocellulosic Biomass. *Processes*, *9*(7), 1234.

Bureros, G. M. A., Tanjay, A. A., Cuizon, D. E. S., Go, A. W., Cabatingan, L. K., Agapay, R. C., & Ju, Y. H. (2019). Cacao shell-derived solid acid catalyst for esterification of oleic acid with methanol. *Renewable Energy*, *138*, 489–501.

Chen, Z., Zhang, W., Xu, J., & Li, P. (2015). Kinetics of xylose dehydration into furfural in acetic acid. *Chinese Journal of Chemical Engineering*, *23*(4), 659–666.

Cheng, H., Wang, B., Lv, J., Jiang, M., Lin, S., & Deng, Z. (2011). Xylitol production from xylose mother liquor: A novel strategy that combines the use of recombinant Bacillus subtilis and Candida maltosa. *Microbial Cell Factories*, *10*, 1–12.

Choudhary, V., Sandler, S. I., & Vlachos, D. G. (2012). Conversion of xylose to furfural using Lewis and Brønsted acid catalysts in aqueous media. *ACS Catalysis*, *2*(9), 2022–2028.

Chung, N. H., Hoai, N. T. T., & Dien, L. Q. (2020). Synthesis of furfural from Acacia mangium wood sawdust-derived xylose by continuous distillation method using sulfonated carbonaceous catalyst from the same source. *Vietnam Journal of Chemistry*, *58*(4), 494–499.

Cortés Ortiz, W. G., Campos-Rosario, A. M., & Piñeros-castro, Y. (2013). Conversion of d-xylose into furfural with aluminum and hafnium pillared clays as catalyst. *Dyna*, *180*, 105–112.

da Luz Corrêa, A. P., Bastos, R. R. C., Rocha Filho, G. N. da, Zamian, J. R., & Conceição, L. R. V. da. (2020). Preparation of sulfonated carbon-based catalysts from murumuru kernel shell and their performance in the esterification reaction. *RSC Advances*, *10*(34), 20245–20256.

Dai, J., Zhu, L., Tang, D., Fu, X., Tang, J., Guo, X., & Hu, C. (2017). Sulfonated polyaniline as a solid organocatalyst for dehydration of fructose into 5-hydroxymethylfurfural. *Green Chemistry*, *19*(8), 1932–1939.

Dalvand, K., Rubin, J., Gunukula, S., Clayton Wheeler, M., & Hunt, G. (2018). Economics of biofuels: Market potential of furfural and its derivatives. *Biomass and Bioenergy*, *115*(August 2017), 56–63.

Dawale, K., Chavan, S., Dhole, G., & Bagal, M. V. (2020). *PREPARATION OF FURFURAL FROM AGRICULTURAL WASTE*. *7*(6), 1123–1131.

Delbecq, F., Wang, Y., & Len, C. (2016). Conversion of xylose, xylan and rice husk into furfural via betaine and formic acid mixture as novel homogeneous catalyst in biphasic system by microwave-assisted dehydration. *Journal of Molecular Catalysis A: Chemical*, *423*, 520–525.

Dias, A. S., Pillinger, M., & Valente, A. A. (2005). Dehydration of xylose into furfural over micro-mesoporous sulfonic acid catalysts. *Journal of Catalysis*, *229*(2), 414–423.

Doiseau, A. C., Rataboul, F., Burel, L., & Essayem, N. (2014). Synergy effect between solid acid catalysts and concentrated carboxylic acids solutions for efficient furfural production from xylose. *Catalysis Today*, *226*, 176–184.

Dong, X., Jiang, Y., Shan, W., & Zhang, M. (2016). A novel highly ordered mesoporous carbon-based solid acid for synthesis of bisphenol-A. *RSC Advances*, *6*(21), 17118–17124.

Dulie, N. W., Woldeyes, B., & Demsash, H. D. (2021). Synthesis of lignin-carbohydrate complex-based catalyst from Eragrostis tef straw and its catalytic performance in xylose dehydration to furfural. *International Journal of Biological Macromolecules*, *171*, 10–16.

Dulie, N. W., Woldeyes, B., Demsash, H. D., & Jabasingh, A. S. (2021). An Insight into the Valorization of Hemicellulose Fraction of Biomass into Furfural: Catalytic Conversion and Product Separation. *Waste and Biomass Valorization*, *12*(2), 531–552.

Elias, S., Rabiu, A. M., Okeleye, B. I., Okudoh, V., & Oyekola, O. (2020). Bifunctional heterogeneous catalyst for biodiesel production from waste vegetable oil. *Applied Sciences (Switzerland)*, *10*(9).

Endut, A., Abdullah, S. H. Y. S., Hanapi, N. H. M., Hamid, S. H. A., Lananan, F., Kamarudin, M. K. A., Umar, R., Juahir, H., & Khatoon, H. (2017). Optimization of biodiesel production by solid acid catalyst derived from coconut shell via response surface methodology. *International Biodeterioration and Biodegradation*, *124*, 250–257.

Ershova, O., Kanervo, J., Hellsten, S., & Sixta, H. (2015). The role of xylulose as an intermediate in xylose conversion to furfural: insights via experiments and kinetic modelling. *RSC Advances*, *5*(82), 66727–66737.

FA, D., OO, A., OC, O., AA, I., AE, A., & MO, O. (2018). Development of Solid Acid Catalyst from Biomass Obtained from Cake of Vitellaria paradoxa and Its Application in Biodiesel Production Via a TwoStep Reaction System. *Industrial Chemistry*, *04*(02).

Gabriel, J. B., Oliveira, V., Souza, T. E. De, Padula, I., Oliveira, L. C. A., Gurgel, L. V. A., Baêta, B. E. L., & Silva, A. C. (2020). New Approach to Dehydration of Xylose to 2-Furfuraldehyde Using a Mesoporous Niobium-Based Catalyst. *ACS Omega*, *5*(34),

21392–21400.

Gebre, H., Fisha, K., Kindeya, T., & Gebremichal, T. (2015). Synthesis of Furfural from Bagasse. *International Letters of Chemistry, Physics and Astronomy*, *57*(August 2015), 72–84.

Gong, L., Xu, Z. Y., Dong, J. J., Li, H., Han, R. Z., Xu, G. C., & Ni, Y. (2019). Composite coal fly ash solid acid catalyst in synergy with chloride for biphasic preparation of furfural from corn stover hydrolysate. *Bioresource Technology*, *293*(June).

Gong, R., Ma, Z., Wang, X., Han, Y., Guo, Y., Sun, G., Li, Y., & Zhou, J. (2019). Sulfonic-acid-functionalized carbon fiber from waste newspaper as a recyclable carbon based solid acid catalyst for the hydrolysis of cellulose. *RSC Advances*, *9*(50), 28902–28907.

Gowri, K. S., & Fei-Ling, P. (2021). Synthesis of Oil Palm Empty Fruit Bunch Derived Magnetic Solid Acid Catalyst for Levulinate Production. *IOP Conference Series: Earth and Environmental Science*, *749*(1).

Guenic, S. Le, Delbecq, F., Ceballos, C., & Len, C. (2015). Microwave-assisted dehydration of D-xylose into furfural by diluted inexpensive inorganic salts solution in a biphasic system. *Journal of Molecular Catalysis A: Chemical*, *410*, 1–7.

Guo, F., Jia, X., Liang, S., Zhou, N., Chen, P., & Ruan, R. (2019). Development of biochar-based nanocatalysts for tar cracking/reforming during biomass pyrolysis and gasification. *Bioresource Technology*, 122263.

Guo, X., Guo, F., Li, Y., Zheng, Z., Xing, Z., Zhu, Z., Liu, T., Zhang, X., & Jin, Y. (2018). PT. *"Applied Catalysis A, General."*

Hanis, S., Sayid, Y., Hanis, N., Hanapi, M., & Azid, A. (2016). *A review of biomass-derived heterogeneous catalyst for a sustainable biodiesel production*. *September 2015*.

Hazmi, B., Rashid, U., Kawi, S., Mokhtar, W. N. A. W., Ahangar, F. A., Yaw, T. C. S., Tsubota, T., Alharthi, F. A., & Ngamcharussrivichai, C. (2022). A Heterogeneous Bifunctional Carbon Nanocatalyst from Plastic Waste to Efficiently Catalyze Waste Cooking Oil into Biodiesel. *Catalysts*, *12*(8), 874.

He, Q., Lu, Y., Peng, Q., Chen, W., Fan, G., Chai, B., & Song, G. (2021). Synthesis of 5-hydroxymethylfurfural from fructose catalyzed by sulfonated carbon-based solid acid. *Biomass Conversion and Biorefinery*, *0123456789*.

Hirano, A., Hon-Nami, K., Kunito, S., Hada, M., & Ogushi, Y. (1998). Temperature effect on continuous gasification of microalgal biomass: Theoretical yield of methanol

production and its energy balance. *Catalysis Today*, *45*(1–4), 399–404.

Hu, B., Xie, W. luan, Wu, Y. ting, Liu, J., Ma, S. wei, Wang, T. peng, Zheng, S., & Lu, Q. (2021). Mechanism study on the formation of furfural during zinc chloride-catalyzed pyrolysis of xylose. *Fuel*, *295*(March), 120656.

Hu, D., Zhang, M., Xu, H., Wang, Y., & Yan, K. (2021). Recent advance on the catalytic system for efficient production of biomass-derived 5-hydroxymethylfurfural. *Renewable and Sustainable Energy Reviews*, *147*(November 2020).

Hu, S., Zhu, J., Wu, Y., Xie, R., Wu, K., & Yang, M. (2018). Preparation of packing type catalysts AAO@Al/Meso-SiO2-SO3H for the dehydration of xylose into furfural. *Microporous and Mesoporous Materials*, *262*, 112–121.

Hu, X., Westerhof, R. J. M., Dong, D., Wu, L., & Li, C. Z. (2014). Acid-catalyzed conversion of Xylose in 20 solvents: Insight into interactions of the solvents with Xylose, furfural, and the acid catalyst. *ACS Sustainable Chemistry and Engineering*, *2*(11), 2562–2575.

Hu, X., & Yip, A. C. K. (2021). Heterogeneous Catalysis: Enabling a Sustainable Future. *Frontiers in Catalysis*, *1*(March), 1–3.

Hua, D., Ding, H., Liu, Y., Li, J., & Han, B. (2021). Dehydration of Xylose to furfural over imidazolium-based ionic liquid with phase separation. *Catalysts*, *11*(12), 13–16.

Hua, D. R., Wu, Y. L., Liu, Y. F., Chen, Y., Yang, M. De, Lu, X. N., & Li, J. (2016). Preparation of furfural and reaction kinetics of xylose dehydration to furfural in high-temperature water. *Petroleum Science*, *13*(1), 167–172.

Hussain, Z., & Kumar, R. (2018). Synthesis and characterization of novel corncob-based solid acid catalyst for biodiesel production. *Industrial and Engineering Chemistry Research*, *57*(34), 11645–11657.

Iriany, Taslim, Bani, O., & Pratama, A. J. (2021). Potential of lime as a green catalyst in the manufacture of furfural from Mikania micrantha. *IOP Conference Series: Earth and Environmental Science*, *713*(1).

Ji, L., Tang, Z., Yang, D., Ma, C., & He, Y. C. (2021). Improved one-pot synthesis of furfural from corn stalk with heterogeneous catalysis using corn stalk as biobased carrier in deep eutectic solvent–water system. *Bioresource Technology*, *340*(July), 1–8.

Jia, Q., Teng, X., Yu, S., Si, Z., Li, G., Zhou, M., Cai, D., Qin, P., & Chen, B. (2019). Production of furfural from xylose and hemicelluloses using tin-loaded sulfonated diatomite as solid acid catalyst in biphasic system. *Bioresource Technology Reports*,

6(February), 145–151.

Jiménez Toro, M. J., Dou, X., Ajewole, I., Wang, J., Chong, K., Ai, N., Zeng, G., & Chen, T. (2019). Preparation and Optimization of Macroalgae-Derived Solid Acid Catalysts. *Waste and Biomass Valorization*, *10*(4), 805–816.

Jin, S., Guo, C., Lu, Y., Zhang, R., Wang, Z., & Jin, M. (2017). Comparison of microwave and conventional heating methods in carbonization of polyacrylonitrile-based stabilized fibers at different temperature measured by an in-situ process temperature control ring. *Polymer Degradation and Stability*, *140*, 32–41.

Kang, S., Chang, J., & Fan, J. (2014). One step preparation of Sulfonated solid catalyst and its effect in esterification reaction. *Chinese Journal of Chemical Engineering*, *22*(4), 392–397.

Kang, S., Fu, J., & Zhang, G. (2018). From lignocellulosic biomass to levulinic acid: A review on acid-catalyzed hydrolysis. *Renewable and Sustainable Energy Reviews*, *94*(March 2017), 340–362.

Karnjanakom, S., Maneechakr, P., Samart, C., & Guan, G. (2019). A facile way for sugar transformation catalyzed by carbon-based Lewis-Brønsted solid acid. *Molecular Catalysis*, *479*(September), 110632.

Kim, S. B., You, S. J., Kim, Y. T., Lee, S., Lee, H., Park, K., & Park, E. D. (2011). *Dehydration of D-xylose into furfural over H-zeolites*. *28*(3), 710–716.

Konwar, L. J. (n.d.). *SO 3 H - Containing Functional Carbon Materials : Synthesis , Structure , and Acid Catalysis*.

Krzelj, V., Ferrandez, D. P., & Neira D'Angelo, M. F. (2021). Sulfonated foam catalysts for the continuous dehydration of xylose to furfural in biphasic media. *Catalysis Today*, *365*(July 2020), 274–281.

Lam, E., Chong, J. H., Majid, E., Liu, Y., Hrapovic, S., Leung, A. C. W., & Luong, J. H. T. (2012). Carbocatalytic dehydration of xylose to furfural in water. *Carbon*, *50*(3), 1033–1043.

Lamptey, O., Naa, I., & Farzad, S. (2019). *Comparative Kinetic Analysis of Furfural Production From Xylan and Xylose*. *April*. http://hdl.handle.net/10019.1/105904

Laohapornchaiphan, J., Smith, C. B., & Smith, S. M. (2017). One-step Preparation of Carbon-based Solid Acid Catalyst from Water Hyacinth Leaves for Esterification of Oleic Acid and Dehydration of Xylose. *Chemistry - An Asian Journal*, *12*(24), 3178–3186.

Lathiya, D. R., Bhatt, D. V., & Maheria, K. C. (2018). Synthesis of sulfonated carbon

catalyst from waste orange peel for cost effective biodiesel production. *Bioresource Technology Reports*, *2*, 69–76.

Li, H., Ren, J., Zhong, L., Sun, R., & Liang, L. (2015). Production of furfural from xylose, water-insoluble hemicelluloses and water-soluble fraction of corncob via a tin-loaded montmorillonite solid acid catalyst. *Bioresource Technology*, *176*, 242–248.

Li, W., Zhu, Y., Lu, Y., Liu, Q., Guan, S., Chang, H. min, Jameel, H., & Ma, L. (2017). Enhanced furfural production from raw corn stover employing a novel heterogeneous acid catalyst. *Bioresource Technology*, *245*, 258–265.

Lin, Q., Li, H., Wang, X., Jian, L., Ren, J., Liu, C., & Sun, R. (2017). SO42−/Sn-MMT solid acid catalyst for xylose and xylan conversion into furfural in the biphasic system. *Catalysts*, *7*(4), 1–14.

Lin, Q. xuan, Zhang, C. hui, Wang, X. hui, Cheng, B. gui, Mai, N., & Ren, J. li. (2019). Impact of activation on properties of carbon-based solid acid catalysts for the hydrothermal conversion of xylose and hemicelluloses. *Catalysis Today*, *319*, 31–40.

Liu, X., Zhang, L., Sun, W., Zhang, M., & Yu, S. (2017). One-step preparation of sulfonated carbon-based solid acid from distillers' grain for esterification. *Research on Chemical Intermediates*, *43*(10), 5917–5932.

Liu, Y., Ma, C., Huang, C., Fu, Y., & Chang, J. (2018). Efficient Conversion of Xylose into Furfural Using Sulfonic Acid-Functionalized Metal-Organic Frameworks in a Biphasic System. *Industrial and Engineering Chemistry Research*, *57*(49), 16628–16634.

Liu, Z. H., & Chen, H. Z. (2015). Xylose production from corn stover biomass by steam explosion combined with enzymatic digestibility. *Bioresource Technology*, *193*, 345–356.

Long, J., Xu, Y., Zhao, W., Li, H., & Yang, S. (2019). Heterogeneous Catalytic Upgrading of Biofuranic Aldehydes to Alcohols. *Frontiers in Chemistry*, *7*(July).

Lopes, M., Dussan, K., & Leahy, J. J. (2015). *Chloride Salts as Co-Catalysts for the Conversion of D-Xylose to Furfural with Formic Acid*. *July*.

Lu, H., Tang, W., Ji, J., Liang, X., & Ji, G. (2019). Preparation of Granular Carbon-Based Solid Acid Catalyst from White Poplar and the Catalytic Activities in Esterification. *ChemistrySelect*, *4*(30), 8855–8859.

Ma, J., Li, W., Guan, S., Liu, Q., Li, Q., Zhu, C., Yang, T., Ogunbiyi, A. T., & Ma, L. (2019). Efficient catalytic conversion of corn stalk and xylose into furfural over sulfonated graphene in γ-valerolactone. *RSC Advances*, *9*(19), 10569–10577.

Machado, G., Leon, S., Santos, F., Lourega, R., Dullius, J., Mollmann, M. E., & Eichler, P. (2016). Literature Review on Furfural Production from Lignocellulosic Biomass. *Natural Resources*, *07*(03), 115–129.

Mani, T., Murugan, P., & Mahinpey, N. (2011). Pyrolysis of oat straw and the comparison of the product yield to wheat and flax straw pyrolysis. *Energy and Fuels*, *25*(7), 2803–2807.

Masawi, D., & Manyere, S. (2018). *Production of Xylose from Brewers Spent Grain by Dilute Hydrochloric Acid Hydrolysis.*

Mateo, W., Leix, H., Villota, E., Qian, M., Zhao, Y., Huo, E., Zhang, Q., Lin, X., Wang, C., & Huang, Z. (2019). Synthesis and Characterization of Sulfonated Activated Carbon as a Catalyst for Bio-jet Fuel Production from Biomass and Waste Plastics. *Bioresource Technology*, 122411.

Matsushika, A., Inoue, H., Kodaki, T., & Sawayama, S. (2009). Ethanol production from xylose in engineered Saccharomyces cerevisiae strains: Current state and perspectives. *Applied Microbiology and Biotechnology*, *84*(1), 37–53.

Mazzotta, M. G., Gupta, D., Saha, B., Patra, A. K., Bhaumik, A., & Abu-Omar, M. M. (2014). Efficient solid acid catalyst containing lewis and brønsted acid sites for the production of furfurals. *ChemSusChem*, *7*(8), 2342–2350.

Mengstie, M. A., & Habtu, N. G. (2020). Synthesis and Characterization of 5-Hydroxymethylfurfural from Corncob Using Solid Sulfonated Carbon Catalyst. *International Journal of Chemical Engineering*, *2020*.

Merwe, G. W. Van Der, Everson, R. C., & Bunt, J. R. (1986). *The influence of particle size and density on the combustion of Highveld coal* .

Mesa, L., Morales, M., González, E., Cara, C., Romero, I., Castro, E., & Mussatto, S. I. (2014). Restructuring the processes for furfural and xylose production from sugarcane bagasse in a biorefinery concept for ethanol production. *Chemical Engineering and Processing: Process Intensification*, *85*, 196–202.

Mishra, R. K., Kumar, V. B., Victor, A., Pulidindi, I. N., & Gedanken, A. (2019). Selective production of furfural from the dehydration of xylose using Zn doped CuO catalyst. *Ultrasonics Sonochemistry*, *56*(July 2018), 55–62.

Mohamad, N., Abd-Talib, N., & Kelly Yong, T. L. (2020). Furfural production from oil palm frond (OPF) under subcritical ethanol conditions. *Materials Today: Proceedings*, *31*(February), 116–121.

Molina, M. J. C., Granados, M. L., Gervasini, A., & Carniti, P. (2015). Exploitment of

niobium oxide effective acidity for xylose dehydration to furfural. *Catalysis Today*, *254*, 90–98.

Naik, S., Goud, V. V., Rout, P. K., Jacobson, K., & Dalai, A. K. (2010). Characterization of Canadian biomass for alternative renewable biofuel. *Renewable Energy*, *35*(8), 1624–1631.

Ngaosuwan, K., Goodwin, J. G., & Prasertdham, P. (2016). A green sulfonated carbon-based catalyst derived from coffee residue for esterification. *Renewable Energy*, *86*, 262–269.

Nila, A. S. S. (2018). Synthesis and XRD, FTIR Studies of Alumina Nanoparticle using Co-precipitation Method. *International Journal for Research in Applied Science and Engineering Technology*, *6*(3), 2493–2496.

Norouzi, O., & Di Maria, F. (2018). Catalytic effect of functional and Fe composite biochars on biofuel and biochemical derived from the pyrolysis of green marine biomass. *Fermentation*, *4*(4).

Omar, H. D. (2015). The Effect of the Difference Time Grinding on the Structure and Morphology of Aluminum Oxide (Al_2O_3). *International Letters of Chemistry, Physics and Astronomy*, *58*, 62–65.

Ong, H. K., & Sashikala, M. (2007). Identification of furfural synthesized from pentosan in rice husk. *Journal of Tropical Agriculture and Food Science*, *35*(2), 305–312.

Paksung, N., Pfersich, J., Arauzo, P. J., Jung, D., & Kruse, A. (2020). Structural Effects of Cellulose on Hydrolysis and Carbonization Behavior during Hydrothermal Treatment. *ACS Omega*, *5*(21), 12210–12223.

Pandian, S., Saravanan, A. S., Sivanandi, P., Santra, M., & Booramurthy, V. K. (2020). 4. Application of heterogeneous acid catalyst derived from biomass for biodiesel process intensification: a comprehensive review. In *Refining Biomass Residues for Sustainable Energy and Bioproducts*. Elsevier Inc.

Parreño, R. P., Liu, Y. L., Beltran, A. B., & Carandang, M. B. (2020). Effect of a direct sulfonation reaction on the functional properties of thermally-crosslinked electrospun polybenzoxazine (PBz) nanofibers. *RSC Advances*, *10*(24), 14198–14207.

Parveen, F., Gupta, K., & Upadhyayula, S. (2017). Synergistic effect of chloro and sulphonic acid groups on the hydrolysis of microcrystalline cellulose under benign conditions. *Carbohydrate Polymers*, *159*, 146–151.

Peleteiro, S., Rivas, S., Alonso, J. L., Santos, V., & Parajó, J. C. (2016). Furfural production using ionic liquids: A review. *Bioresource Technology*, *202*, 181–191.

Pérez, J., Muñoz-Dorado, J., De La Rubia, T., & Martínez, J. (2002). Biodegradation and biological treatments of cellulose, hemicellulose and lignin: An overview. *International Microbiology*, *5*(2), 53–63.

Qi, W., He, C., Wang, Q., Liu, S., Yu, Q., Wang, W., Leksawasdi, N., Wang, C., & Yuan, Z. (2018). Carbon-Based Solid Acid Pretreatment in Corncob Saccharification: Specific Xylose Production and Efficient Enzymatic Hydrolysis. *ACS Sustainable Chemistry and Engineering*, *6*(3), 3640–3648.

Qi, Z., Wang, Q., Liang, C., Yue, J., Liu, S., Ma, S., Wang, X., Wang, Z., Li, Z., & Qi, W. (2020). Highly Efficient Conversion of Xylose to Furfural in a Water-MIBK System Catalyzed by Magnetic Carbon-Based Solid Acid. *Industrial and Engineering Chemistry Research*, *59*(39), 17046–17056.

Ricciardi, L., Verboom, W., Lange, J. P., & Huskens, J. (2021). Selective Extraction of Xylose from Acidic Hydrolysate-from Fundamentals to Process. *ACS Sustainable Chemistry and Engineering*, *9*(19), 6632–6638.

Román-Leshkov, Y., Moliner, M., Labinger, J. A., & Davis, M. E. (2010). Mechanism of glucose isomerization using a solid lewis acid catalyst in water. *Angewandte Chemie - International Edition*, *49*(47), 8954–8957.

Roy Goswami, S., Mukherjee, A., Dumont, M. J., & Raghavan, V. (2016). One-Pot Conversion of Corn Starch into 5-Hydroxymethylfurfural in Water-[Bmim]Cl/MIBK Biphasic Media. *Energy and Fuels*, *30*(10), 8349–8356.

Rusanen, A., Kupila, R., Lappalainen, K., Kärkkäinen, J., Hu, T., & Lassi, U. (2020). Conversion of xylose to furfural over lignin-based activated carbon-supported iron catalysts. *Catalysts*, *10*(8).

Ryu, Y. J., Kim, Z. H., Lee, S. G., Yang, J. H., Shin, H. Y., & Lee, C. G. (2018). Development of carbon-based solid acid catalysts using a lipid-extracted alga, dunaliella tertiolecta, for esterification. *Journal of Microbiology and Biotechnology*, *28*(5), 732–738.

S, R., & P, B. (2019). The potential of lignocellulosic biomass precursors for biochar production: Performance, mechanism and wastewater application—A review. *Industrial Crops and Products*, *128*(May 2018), 405–423.

Sádaba, I., Lima, S., Valente, A. A., & López Granados, M. (2011). Catalytic dehydration of xylose to furfural: Vanadyl pyrophosphate as source of active soluble species. *Carbohydrate Research*, *346*(17), 2785–2791.

Saha, B. C. (2003). Hemicellulose bioconversion. *Journal of Industrial Microbiology and*

Biotechnology, *30*(5), 279–291.

Salgado, M. D. F., Abioye, A. M., Junoh, M. M., Santos, J. A. P., & Ani, F. N. (2018). Preparation of activated carbon from babassu endocarpunder microwave radiation by physical activation. *IOP Conference Series: Earth and Environmental Science*, *105*(1).

Sánchez-Moreno, I., Benito-Arenas, R., Montero-Calle, P., Hermida, C., García-Junceda, E., & Fernández-Mayoralas, A. (2019). Simple and Practical Multigram Synthesis of d-Xylonate Using a Recombinant Xylose Dehydrogenase. *ACS Omega*, *4*(6), 10593–10598.

Sato, O., Mimura, N., Masuda, Y., Shirai, M., & Yamaguchi, A. (2019). The Journal of Supercritical Fluids E ff ect of extraction on furfural production by solid acid-catalyzed xylose dehydration in water. *The Journal of Supercritical Fluids*, *144*(July 2018), 14–18.

Satyavolu, J., Tadimeti, J. G. D., & Thilakaratne, R. (2021). Xylose production and the associated integration for biocoal production. *Energy Conversion and Management: X*, *10*, 100073.

Selpiana, S., Bahrin, D., Yunita, R. R., Ningsih, B., Akbar, A. H., & Permatasari, A. (2022). *Synthesis and Characterization Catalyst γ-Al 2 O 3 and Al / γ-Al 2 O 3 Using XRD Analysis*. *February*, 26–31.

Sevilla, M., & Fuertes, A. B. (2009). Chemical and structural properties of carbonaceous products obtained by hydrothermal carbonization of saccharides. *Chemistry - A European Journal*, *15*(16), 4195–4203.

Shafeeq, A., Muhammad, A., Sarfaraz, S., Akram, Z., Saeed, H. M. U., & Farooq, U. (2015). Effect of Acid Concentration on the Extraction of Furfural from Corn Cobs. *International Journal of Chemical Engineering and Applications*, *6*(5), 381–384.

Shen, S., Wang, C., Han, Y., Cai, B., & Li, H. (2014). Influence of reaction conditions on heterogeneous hydrolysis of cellulose over phenolic residue-derived solid acid. *Fuel*, *134*, 573–578.

Shi, X. L., Hu, Q., Chen, Y., Wang, F., & Duan, P. (2018). Conversion of biomass components to methyl levulinate over an ultra-high performance fiber catalyst in impellers of the agitation system. *Journal of Industrial and Engineering Chemistry*, *65*, 264–271.

Srivastava, N., Shrivastav, A., Singh, R., Abohashrh, M., Srivastava, K. R., Irfan, S., Srivastava, M., Mishra, P. K., Gupta, V. K., & Thakur, V. K. (2021). Advances in the

structural composition of biomass: Fundamental and bioenergy applications. *Journal of Renewable Materials*, *9*(4), 615–636.

Sun, S., Yu, Q., Li, M., Zhao, H., Wang, Y., & Ji, X. (2020). Effect of carbonization temperature on characterization and water vapor adsorption of coffee-shell activated carbon. *Adsorption Science and Technology*, *38*(9–10), 377–392.

Suzuki, T., Yokoi, T., Otomo, R., Kondo, J. N., & Tatsumi, T. (2011). Dehydration of xylose over sulfated tin oxide catalyst: Influences of the preparation conditions on the structural properties and catalytic performance. *Applied Catalysis A: General*, *408*(1–2), 117–124.

Thanapal, S. S., Chen, W., Annamalai, K., Carlin, N., Ansley, R. J., & Ranjan, D. (2014). Carbon dioxide torrefaction of woody biomass. *Energy and Fuels*, *28*(2), 1147–1157.

Torres Ortega, J. A. (2012). Sulfonation/Sulfation Processing Technology for Anionic Surfactant Manufacture. *Advances in Chemical Engineering*, *Figure 1*.

Toumsri, P., Auppahad, W., Saknaphawuth, S., Pongtawornsakun, B., Kaowphong, S., Dechtrirat, D., Panpranot, J., & Chuenchom, L. (2021). Facile preparation protocol of magnetic mesoporous carbon acid catalysts via soft-template self-assembly method and their applications in conversion of xylose into furfural. *Philosophical Transactions of the Royal Society A: Mathematical, Physical and Engineering Sciences*, *379*(2209).

Trung, T. Q., Thinh, D. B., Anh, T. N. M., Nguyet, D. M., Quan, T. H., Viet, N. Q., Tuan, T. T., Dat, N. M., Nam, H. M., Hieu, N. H., & Phong, M. T. (2020). Synthesis of furfural from sugarcane bagasse by hydrolysis method using magnetic sulfonated graphene oxide catalyst. *Vietnam Journal of Chemistry*, *58*(2), 245–250.

Tsao, K. C., & Yang, H. (2018). Oxygen reduction catalysts on nanoparticle electrodes. In *Encyclopedia of Interfacial Chemistry: Surface Science and Electrochemistry*. Elsevier.

Varanasi, P., Singh, P., Auer, M., Adams, P. D., Simmons, B. A., & Singh, S. (2013). Survey of renewable chemicals produced from lignocellulosic biomass during ionic liquid pretreatment. *Biotechnology for Biofuels*, *6*(1), 1–9.

Vo, A. T. H., Lee, H., Kim, S., & Cho, J. K. (2016). Clean and Efficient Synthesis of Furfural From Xylose by Microwave-Assisted Biphasic System using Bio-Based Heterogeneous Acid Catalysts. *Clean Technology*, *22*(4), 250–257.

Wang, L., Dong, X., Jiang, H., Li, G., & Zhang, M. (2014). Preparation of a novel carbon-based solid acid from cassava stillage residue and its use for the esterification of free

fatty acids in waste cooking oil. *Bioresource Technology*, *158*, 392–395.

Wang, W., Ren, J., Li, H., Deng, A., & Sun, R. (2015). Direct transformation of xylan-type hemicelluloses to furfural via SnCl4 catalysts in aqueous and biphasic systems. *Bioresource Technology*, *183*, 188–194.

Wang, X., Qiu, M., Tang, Y., Yang, J., Shen, F., Qi, X., & Yu, Y. (2021). Synthesis of sulfonated lignin-derived ordered mesoporous carbon for catalytic production of furfural from xylose. *International Journal of Biological Macromolecules*, *187*(June), 232–239.

Wang, Y., Delbecq, F., Kwapinski, W., & Len, C. (2017). Application of sulfonated carbon-based catalyst for the furfural production from D-xylose and xylan in a microwave-assisted biphasic reaction. *Molecular Catalysis*, *438*, 167–172.

Wang, Y., Len, T., Huang, Y., Diego Taboada, A., Boa, A. N., Ceballos, C., Delbecq, F., Mackenzie, G., & Len, C. (2017). Sulfonated Sporopollenin as an Efficient and Recyclable Heterogeneous Catalyst for Dehydration of d -Xylose and Xylan into Furfural. *ACS Sustainable Chemistry and Engineering*, *5*(1), 392–398.

Wei, Z., Xiong, D., Duan, P., Ding, S., Li, Y., Li, L., Niu, P., & Chen, X. (2020). Preparation of carbon-based solid acid catalysts using rice straw biomass and their application in hydration of α-pinene. *Catalysts*, *10*(2).

Wong, W. Y., Lim, S., Pang, Y. L., Shuit, S. H., Chen, W. H., & Lee, K. T. (2020). Synthesis of renewable heterogeneous acid catalyst from oil palm empty fruit bunch for glycerol-free biodiesel production. *Science of the Total Environment*, *727*, 138534.

Wu, C., Chen, W., Zhong, L., Peng, X., Sun, R., Fang, J., & Zheng, S. (2014). Conversion of xylose into furfural using lignosulfonic acid as catalyst in ionic liquid. *Journal of Agricultural and Food Chemistry*, *62*(30), 7430–7435.

Wu, C., Yuan, W., Huang, Y., Xia, Y., Yang, H., Wang, H., & Liu, X. (2017). Conversion of Xylose into Furfural Catalyzed by Bifunctional Acidic Ionic Liquid Immobilized on the Surface of Magnetic γ-Al2O3. *Catalysis Letters*, *147*(4), 953–963.

Xia, Q., Peng, H., Zhang, Y., Fu, G., Liu, Y., Xiao, Z., Huang, L., & Bi, H. (2021). Microwave-assisted furfural production from xylose and bamboo hemicellulose in a biphasic medium. *Biomass Conversion and Biorefinery*, *0123456789*.

Xiu, S., Shahbazi, A., & Li, R. (2017). *Characterization , Modification and Application of Biochar for Energy Storage and Catalysis : A Review*. *3*(1), 86–101.

Xu, H., Xiong, S., Zhao, Y., Zhu, L., & Wang, S. (2021). Conversion of Xylose to Furfural Catalyzed by Carbon-Based Solid Acid Prepared from Pectin. *Energy and Fuels*,

35(12), 9961–9969.

Yadav, K., & Jagadevan, S. (2020). Influence of Process Parameters on Synthesis of Biochar by Pyrolysis of Biomass: An Alternative Source of Energy. *Recent Advances in Pyrolysis*, 1–14.

Yan, K., Wu, G., Lafleur, T., & Jarvis, C. (2014). Production, properties and catalytic hydrogenation of furfural to fuel additives and value-added chemicals. *Renewable and Sustainable Energy Reviews*, *38*, 663–676.

Yang, T., Li, W., Su, M., Liu, Y., & Liu, M. (2020). Production of furfural from xylose catalyzed by a novel calcium gluconate derived carbon solid acid in 1,4-dioxane. *New Journal of Chemistry*, *44*(19), 7968–7975.

Yang, T., Zhou, Y. H., Zhu, S. Z., Pan, H., & Huang, Y. B. (2017). Insight into Aluminum Sulfate-Catalyzed Xylan Conversion into Furfural in a Γ-Valerolactone/Water Biphasic Solvent under Microwave Conditions. *ChemSusChem*, *10*(20), 4066–4079.

Yang, Y., Hu, C. W., & Abu-Omar, M. M. (2012). Synthesis of furfural from xylose, xylan, and biomass using AlCl 3·6H2O in biphasic media via xylose isomerization to xylulose. *ChemSusChem*, *5*(2), 405–410.

Yemiş, O., & Mazza, G. (2011). Acid-catalyzed conversion of xylose, xylan and straw into furfural by microwave-assisted reaction. *Bioresource Technology*, *102*(15), 7371–7378.

Yu, I. K. M., Xiong, X., Tsang, D. C. W., Wang, L., Hunt, A. J., Song, H., Shang, J., Ok, Y. S., & Poon, C. S. (2019). Aluminium-biochar composites as sustainable heterogeneous catalysts for glucose isomerisation in a biorefinery. *Green Chemistry*, *21*(6), 1267–1281.

Yue, X., Chen, D., Luo, J., Xin, Q., & Huang, Z. (2020). Upgrading of reed pyrolysis oil by using its biochar-based catalytic esterification and the influence of reed sources. *Applied Energy*, *268*(January), 114970.

Zailan, Z., Ali, H., Chau, J. W., Jusoh, M., Tahir, M., & Zakaria, Y. (2020). *Development of Sulphonated Sago Pith Waste Catalyst for Esterification of Palm Fatty Acid Distillate to Methyl Ester*. *78*, 31–36.

Zhang, J., Lin, L., & Liu, S. (2012). Efficient production of furan derivatives from a sugar mixture by catalytic process. *Energy and Fuels*, *26*(7), 4560–4567.

Zhang, J., Zhuang, J., Lin, L., Liu, S., & Zhang, Z. (2012). Conversion of D-xylose into furfural with mesoporous molecular sieve MCM-41 as catalyst and butanol as the extraction phase. *Biomass and Bioenergy*, *39*, 73–77.

Zhang, L., Tian, L., Sun, R., Liu, C., Kou, Q., & Zuo, H. (2019). Transformation of corncob into furfural by a bifunctional solid acid catalyst. *Bioresource Technology*, *276*(December 2018), 60–64.

Zhang, T., Li, W., An, S., Huang, F., Li, X., Liu, J., Pei, G., & Liu, Q. (2018). Efficient transformation of corn stover to furfural using p-hydroxybenzenesulfonic acid-formaldehyde resin solid acid. *Bioresource Technology*, *264*(April), 261–267.

Zhang, T., Li, W., Xu, Z., Liu, Q., Ma, Q., Jameel, H., Chang, H. min, & Ma, L. (2016). Catalytic conversion of xylose and corn stalk into furfural over carbon solid acid catalyst in γ-valerolactone. *Bioresource Technology*, *209*, 108–114.

Zhang, X. L., Li, N., Qin, Z., & Zheng, X. C. (2020). Sulfonated porous biomass-derived carbon with superior recyclability for synthesizing ethyl levulinate biofuel. *Research on Chemical Intermediates*, *46*(12), 5325–5343.

Zhang, Y., Cui, Y., Chen, P., Liu, S., Zhou, N., Ding, K., Fan, L., Peng, P., Min, M., Cheng, Y., Wang, Y., Wan, Y., Liu, Y., Li, B., & Ruan, R. (2019). Gasification technologies and their energy potentials. In *Sustainable Resource Recovery and Zero Waste Approaches*. Elsevier B.V.

Zhao, L., Bacsik, Z., Hedin, N., Wei, W., Sun, Y., Antonietti, M., & Titirici, M. M. (2010). Carbon dioxide capture on amine-rich carbonaceous materials derived from glucose. *ChemSusChem*, *3*(7), 840–845.

Zhao, Y., Lu, K., Xu, H., Zhu, L., & Wang, S. (2021). A critical review of recent advances in the production of furfural and 5-hydroxymethylfurfural from lignocellulosic biomass through homogeneous catalytic hydrothermal conversion. *Renewable and Sustainable Energy Reviews*, *139*(January), 110706.

Zhou, Y., Niu, S., & Li, J. (2016). Activity of the carbon-based heterogeneous acid catalyst derived from bamboo in esterification of oleic acid with ethanol. *ENERGY CONVERSION AND MANAGEMENT*, *114*, 188–196.

Zhu, Y., Li, W., Lu, Y., Zhang, T., Jameel, H., Chang, H. M., & Ma, L. (2017). Production of furfural from xylose and corn stover catalyzed by a novel porous carbon solid acid in γ-valerolactone. *RSC Advances*, *7*(48), 29916–29924.

7. APPENDICES

Appendix A: Proximate Analysis of Flax Straw

1, Moisture content

The moisture content was determined in weight % according to Equation;

$$MC\% = \frac{w_1 - w_2}{w_1} \times 100\%$$

Mass of empty dry petridish (gm)	Mass of Petri dish plus sample (gm)	Mass of petridish plus sample after drying (gm)				
72.30	79.30	Trial 1	Trial 2	Trial 3	Average	
		74.57	73.95	72.85	73.79	

$$MC\% = \frac{79.30 - 73.79}{79.30} \times 100\% = 6.9 \approx 7\%$$

2, Ash content

$$AC\% = \frac{w_2}{w_1} \times 100\%$$

Number of samples	Mass of crucible + mass of sample (g)	Mass of crucible (g)	Mass of sample + mass of crucible after ignited to the muffle furnace (g)	Mass of the sample after ignited to the muffle furnace (g)	Percentage of ash contents (%)
Sample 1	42.55	40.55	40.62	0.07	3.5
sample 2	31.92	29.92	29.99	0.07	3.5
sample 3	30.28	28.28	28.34	0.06	3
	Average	**Ash**	**Content**		**3.3%**

3. Volatile matter

$$VM\% = \frac{w_1 - w_2}{w_1} \times 100\% - Moisture\ (\%)$$

Number of sample	Mass of crucible + mass of sample (g)	Mass of crucible (g)	Mass of sample + mass of crucible after ignited to the muffle furnace (g)	Mass of the sample after ignited to the muffle furnace (g)	Percentage volatile matter of the sample (%)
Sample 1	58.85	57.85	58.04	0.19	81
Sample 2	51.73	50.73	50.88	0.15	85
		Average	**Volatile**	**matter**	**83**

$$VM\% = 83 - 7 = \mathbf{76}\%$$

4, Fixed carbon content

Fixed carbon contents = 100- (VM+AC+MC) based on wet basis

= 100-(76+3.3+7)

=**13.7%**

Appendix B1: Solution Preparation Calculation for Synthesis of Catalyst

1, Mass of aluminum chloride calculation or percent elements of Al

To prepare 150ml of 20% $AlCl_3$ solution (w/v)

$$20\% = \frac{mass\ of\ the\ solute}{volume\ of\ the\ solution} * 100\%$$

$$20\% = \frac{mass\ of\ the\ solute}{150} \times 100\%$$

$$\boldsymbol{mass\ of\ the\ solute = 30g}$$

2, Solution preparation for acid density determination

To prepare 0.05M of NaCl solution in 20ml of solution and 0.05N of NaOH

Mass of the solute (NaCl) = molecular weight * molarity * volume

58.44*0.05*0.02 =**0.058g of NaCl**

For NaOH, $normality = Molarity\ \times \frac{1}{equivalent\ weight}$

$$mass\ of\ NaOH = V(l) \times N \times Eq.weight$$

$$\boldsymbol{mass\ of\ NaOH = 0.02 \times 0.05 \times 40 = 0.04g}$$

For total acid density determination, 0.05g of catalyst mixed with 20ml of 0.05M NaOH solution was added in an ultrasonic bath at room temperature for 1hr.

$$mass\ of\ NaOH = V(l) \times N \times Eq.weight = 0.02 * 0.0.05 * 40 = \mathbf{0.04g}$$

To prepare 0.05M of HCl in 20ml of solution

For 0.05M of HCl; assay% =37%, density=1.18g/cm^3, mol, weight=36.5g/ml

$$Volume\ of\ HCl = \frac{molarity \times M.weight \times Vol\ in\ liter \times 100}{density \times 37}$$

$$Volume\ of\ HCl = \frac{0.05 \times 36.5 \times 0.02 \times 100}{1.18 \times 37} = 0.084l$$

$$= 84\boldsymbol{ml\ of\ HCl\ in\ 20ml\ dissolved\ of\ solution}$$

Appendix B2: Determination of Acid Density of the Catalyst

Sample calculation of SO_3H acid density for sulfonated Al-biochar catalyst

The volume of 0.05 M NaOH (titrant) (data obtained from the titrate analysis): 1.2ml SO_3H acidity per gram of the catalyst.

$$SO_3H\left(\frac{\text{mmol}}{\text{l}}\right) = \frac{\text{Conc NaOH} \times \text{Volume of NaOH consumed in titration}}{\text{Mass of catalyst}}$$

$SO_3H = \frac{0.05\text{mol/l} \times 0.0012\text{l}}{0.05\text{g}} = \mathbf{1.2mmol/g}$ for first trial

$$SO_3H = \frac{\frac{0.05\text{mol}}{\text{l}} \times 0.001\text{l}}{0.05\text{g}} = \frac{\boldsymbol{1mmol}}{\boldsymbol{g}} \text{ for second trial}$$

$$SO_3H = \frac{\frac{0.05\text{mol}}{\text{l}} \times 0.0009}{0.05\text{g}} = \frac{\mathbf{0.9mmol}}{\mathbf{g}} \text{ for third trial}$$

Therefore, the average was calculated as; $SO_3H = \frac{1.2+1+0.9}{3} = \mathbf{1.033 \pm 0.1mmol/g}$

2, Sample calculation for the determination of total acid density

Number of moles of 20 mL 0.05 M NaOH (titrate)

$$= \frac{0.05\text{mol}}{\text{l}} \times 20\text{ml} \times \frac{1\text{l}}{1000\text{ml}} = \mathbf{0.001mol\ of\ NaOH}$$

Number of moles of 15.1 mL (from burette reading) 0.05 M HCl (titrant) (data obtained from the titrator analysis)

$$= \frac{0.05mol}{l} \times 15.1ml \times \frac{1l}{1000ml} = \mathbf{0.000755\ mol\ of\ HCl}$$

Total acid density$= \frac{V_{NaOH} \times [NaOH] - V_{HCl} \times [HCl]}{Mass\ of\ catalyst} = \frac{0.001 - 0.000755}{0.05} = \mathbf{4.9mmol/g}$

Second trial, $= \frac{0.001 - 0.000775}{0.05} = \mathbf{4.5mmol/g}$

Third trial, $= \frac{0.001 - 0.000755}{0.05} = \mathbf{4.9mmol/g}$

Therefore, the average total acid density $\frac{4.9+4.5+4.9}{3} = \mathbf{4.767 \pm 0.23}$

Table 1 Appendix B2: Effects of carbonization temperature and time on the total acid density and SO_3H of Al-biochar-based catalyst

Carbonization temperature (^oC)	Carbonization time (min)	Mass to H_2SO_4 ratio (w/v)	Sulfonation temperature and time	Total acid density (mmol/g)	SO_3H group (mmol/g)
350	30	1:20	145^{o}C for 18hr	3.033±0.1	0.473±0.02
	60	1:20	145^{o}C for 18hr	3.733±0.17	0.833±0.06
	90	1:20	145^{o}C for 18hr	3.492±0.15	0.667±0.04
400	30	1:20	145^{o}C for 18hr	3.233±0.12	0.566±0.03
	60	1:20	145^{o}C for 18hr	3.967±0.19	0.933±0.07
	90	1:20	145^{o}C for 18hr	3.650±0.18	0.800±0.05
450	30	1:20	145^{o}C for 18hr	4.233±0.22	0.967±0.09
	60	1:20	145^{o}C for 18hr	3.752±0.16	0.675±0.04
	90	1:20	145^{o}C for 18hr	3.250±0.13	0.600±0.03

Table 2 Appendix B2: Effects of sulfonation conditions on SO_3H group Al-bio char-based catalyst

Sulfonation Temperature and time	Mass to H_2SO_4 ratio (w/v)	Carbonization Temperature and Time	SO_3H group (mmol/g)
12hr -145 ^{0}C	1:20	450 ^{o}C for 30min	0.433±0.04
15hr -145 ^{0}C	1:20	450 ^{o}C for 30min	0.733±0.05
18hr -145 ^{0}C	1:20	450 ^{o}C for 30min	0.967±0.09
21hr -145 ^{0}C	1:20	450 ^{o}C for 30min	0.912±0.08
24hr -145^{o}C	1:20	450 ^{o}C for 30min	0.867±0.06
90 ^{o}C-18hr	1:20	450 ^{o}C for 30min	0.900±0.07
120 ^{o}C-18hr	1:20	450 ^{o}C for 30min	1.033±0.1
145 ^{o}C-18hr	1:20	450 ^{o}C for 30min	0.967±0.09
175 ^{o}C-18hr	1:20	450 ^{o}C for 30min	0.767±0.06
200 ^{o}C-18hr	1:20	450 ^{o}C for 30min	0.700±0.05

Appendix C: BET Analysis of Biochar, Al-Biochar and Sulfonated Al-Biochar

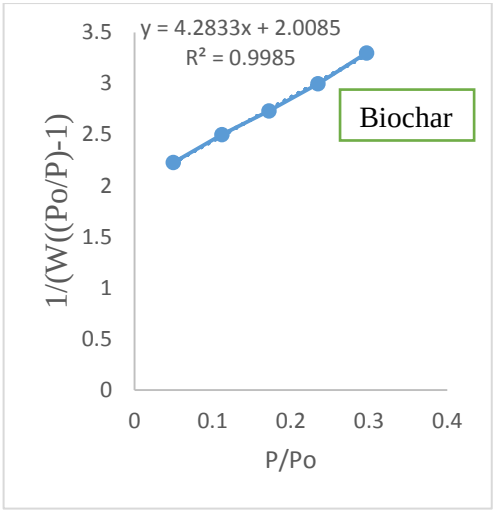

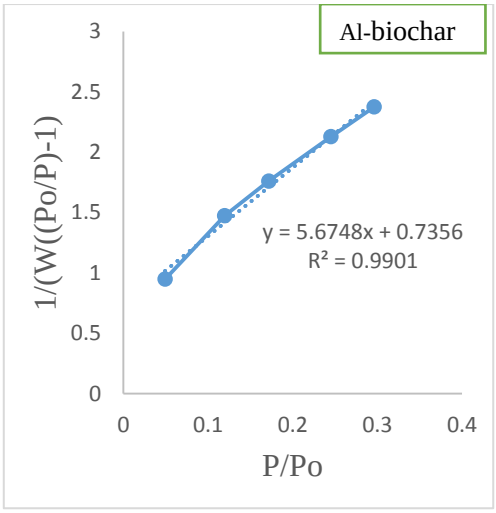

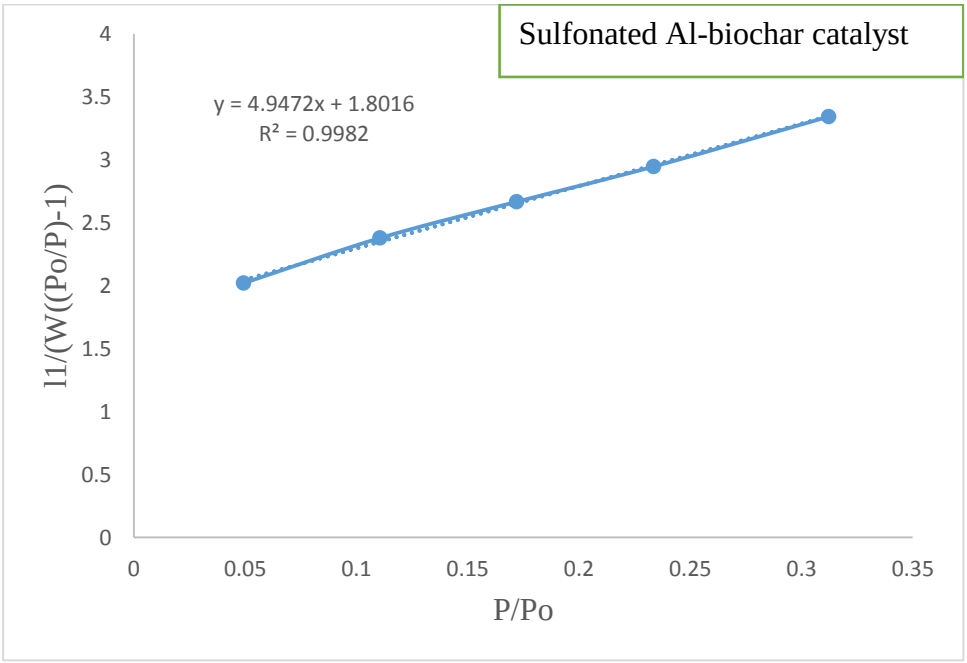

Appendix D: Effects of Reaction Condition on Furfural Formation

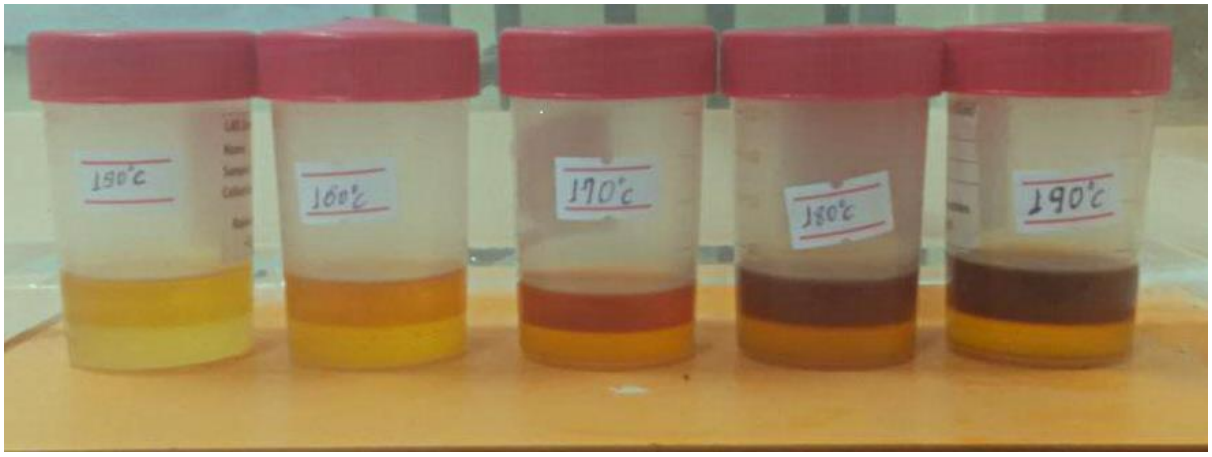

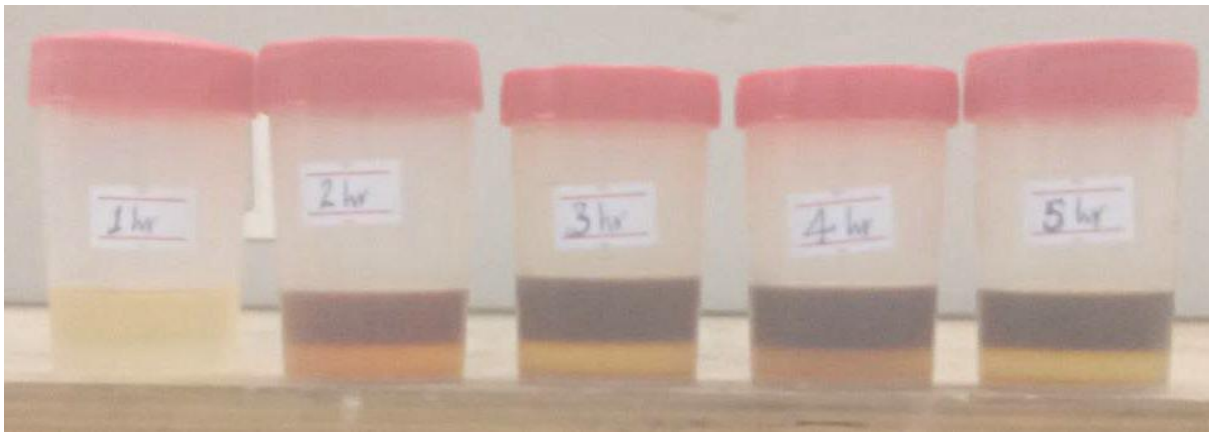

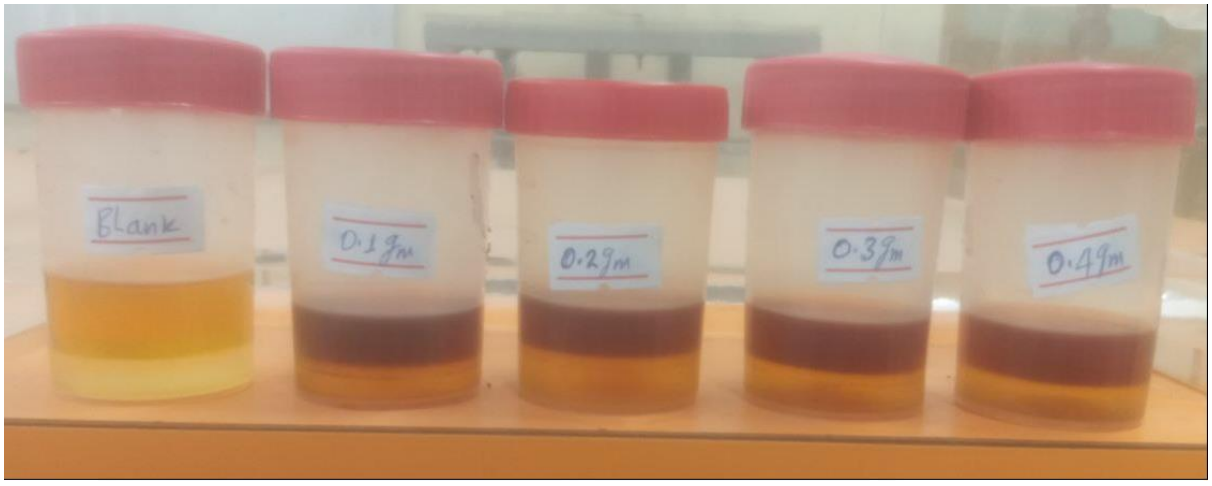

Appendix E: Determination of D-Xylose Conversion

The conversion or unreacted D-xylose can be determined as the following formulas

$$D - xylose\ conversion = \frac{C_{in} - C_{out}}{C_{in}} \times 100\%$$

Initial concentration of D-xylose C_{in}=0.025g/ml=25000mg/l

The **phenol-sulfuric acid** technique was used to calculate the final concentration of D-xylose with regard to absorbance at 477nm. The corresponding absorbance was measured 0.029 at 180 ^{o}C for 2 hours with 0.2g of catalyst loading. From the calibration curve of D-xylose standard Y = 0.0053x + 0.0009

$$Concentration\ of\ D - xylose\ in\ the\ sample = \frac{0.029 - 0.0009}{0.0053} = \mathbf{5.302}\boldsymbol{mg/l}$$

Then, total concentration of D-xylose in the sample can be calculated as; Concentration of D-xylose in the sample *dilution factor

Total concentration in the sample =5.302mg/l*25*50 = **6627.5mg/l**

$$D - xylose\ conversion = \frac{25000 - 6627.5}{25000} \times 100\% = \mathbf{73.5}\%$$

Table 1 Appendix E: Standard xylose concentration and their absorbance

Xylose concentration (mg/l)	Absorbance
0	0
10	0.06
20	0.104
30	0.154
40	0.214
50	0.269

Table 2 Appendix E: Furfural absorbance, unreacted xylose concentration and conversion of xylose at different reaction condition

Temperature (^oC)	Time (hr)	Catalyst loading (gm)	Absorbance of furfural	Concentration of xylose (mg/l)	Conversion of xylose (%)
150	2	0.2	0.490399	17476.42	30.09
160	2	0.2	2.57165	11816.04	52.73
170	2	0.2	3.91645	9221.69	63.11
180	2	0.2	3.99937	6391.50	74.43
190	2	0.2	3.82731	3325.47	86.69
180	1	0.2	0.173586	17712.26	29.15
180	2	0.2	4.06562	6627.36	73.49
180	3	0.2	3.84595	4976.41	80.09
180	4	0.2	3.24964	3089.62	87.64
180	5	0.2	2.47838	1674.53	93.30
180	2	0	1.0574	15353.77	38.58
180	2	0.1	3.57807	9693.39	61.23
180	2	0.2	3.83833	6155.66	75.38
180	2	0.3	3.91022	3561.32	85.75
180	2	0.4	3.87266	2617.92	89.53

Appendix F: HPLC Analysis of Synthesized Furfural for Determination of Furfural Yield and Selectivity

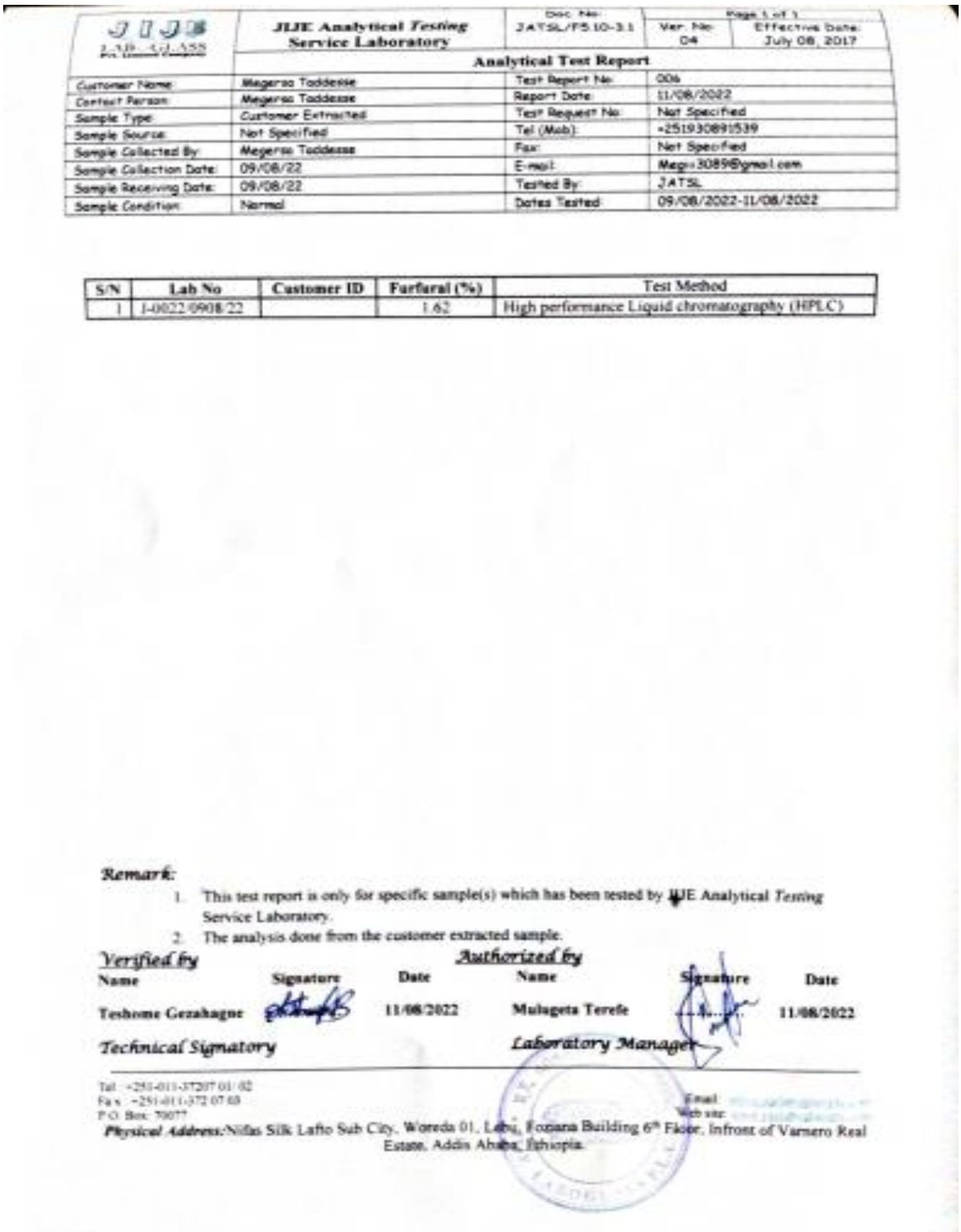

JJE LAB-AC-A555	JJE Analytical Testing Service Laboratory	Doc. No: JATSL/FS.10-3.1	Page 1 of 1 Ver. No: 04	Effective Date: July 08, 2017
	Analytical Test Report			
Customer Name:	Megersa Taddesse	Test Report No:	006	
Contact Person:	Megersa Taddesse	Report Date:	11/08/2022	
Sample Type:	Customer Extracted	Test Request No:	Not Specified	
Sample Source:	Not Specified	Tel (Mob):	+251930891539	
Sample Collected By:	Megersa Taddesse	Fax:	Not Specified	
Sample Collection Date:	09/08/22	E-mail:	Mego30891@gmail.com	
Sample Receiving Date:	09/08/22	Tested By:	JATSL	
Sample Condition:	Normal	Dates Tested:	09/08/2022-11/08/2022	

S/N	Lab No	Customer ID	Furfural (%)	Test Method
1	J-0022/0908/22		1.62	High performance Liquid chromatography (HPLC)

Remark:

1. This test report is only for specific sample(s) which has been tested by JJE Analytical Testing Service Laboratory.
2. The analysis done from the customer extracted sample.

Verified by			*Authorized by*		
Name	**Signature**	**Date**	**Name**	**Signature**	**Date**
Teshome Gezahagne		**11/08/2022**	**Mulageta Terefe**		**11/08/2022**
Technical Signatory			*Laboratory Manager*		

Tel: +251-011-372 07 01/02
Fax: +251-011-372 07 03
P.O. Box: 79077
Email:
Web site:
Physical Address: Nifas Silk Lafto Sub City, Woreda 01, Labu, Fozana Building 6th Floor, Infront of Varnero Real Estate, Addis Ababa, Ethiopia.

JIJE Analytical Testing Service Laboratory

We Serve Scientific Community

Data file:	C:\Chem32\1\Data\furfural\Furfural J-0022 11-08-2022 2022-08-11 15-03-43\026-0601.D		
Sample name:	J-0022 100X diluted		
Injection date:	8/11/2022 4:02:35 PM	Sample type:	Sample
Acq. method:	Furfuran SB column.M	Location:	26
Analysis method:	Furfural SB column.M	Injection:	1 of 1
Acq. operator:	SYSTEM	Injection volume:	20.000
Last changed:	8/11/2022 4:16:38 PM		

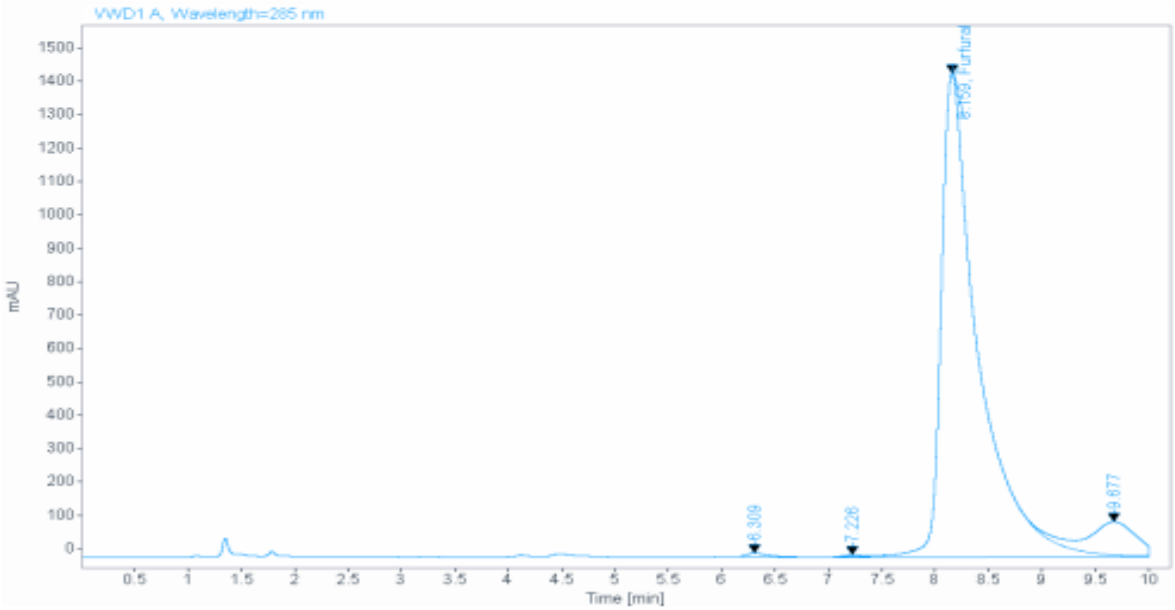

JIJE Analytical Testing Service Laboratory

We Serve Scientific Community

Sample statistics:

Compound: Furfural Signal: VWD1 A, Wavelength=285 nm

Line#	Location	RT [min]	Amount	Unit	Area	Height	Sample Name
6	26	8.159	161.63049	mg/l	34901.37500	1448.92395	J-0022 100X diluted
	Mean	8.159	161.63049		34901.37500	1448.92395	
	StdDev	0				0.00000	
	RSD	0.000	0.00000		0.00000	0.00000	

The concentration of synthesized furfural in the sample reading from the chromatography is 161.63049mg/l with the dilution factor 100x according to JIJE analytical testing service laboratory reports.

Therefore, total concentration furfural in the sample = 161.63049mg/l*100 = **16163.049mg/l**

The yield furfural produced could be calculated as follows;

$$Furfural\ yield = \frac{Concentration\ of\ furfural\ produced}{Concentration\ of\ xylose\ starting} \times 100\%$$

$$Furfural\ yield = \frac{16163.049mg/l}{25000mg/l} \times 100\% = \mathbf{64.7}\% \qquad \boldsymbol{OR}$$

$$FF\ yield = \frac{furfural\ percent\ *\ extracive\ volume}{mass\ of\ D-xylose} = \frac{1.6163049 * 20}{0.5} = \mathbf{64.7}\%$$

Again, the selectivity of furfural can be determined as the following formulas;

$$Furfural\ selectivity = \frac{moles\ of\ furfural\ produced}{moles\ reacted\ xylose} \times 100\%$$

$$Furfural\ selectivity = \frac{16163.049}{25000 - 6627.5} \times 100\% = \mathbf{88.0}\%\ \boldsymbol{OR}$$

$$FF\ sel = \frac{furfural\ yield}{Conversion\ of\ xylose} \times 100\% = \frac{64.7\%}{73.5\%} \times 100\% = \mathbf{88.0}\%$$

Appendix G: Standard Furfural HPLC Analysis

JIJE Analytical Testing Service Laboratory

We Serve Scientific Community

Data file:	C:\Chem32\1\Data\furfural\Furfural J-0022 11-08-2022 2022-08-11 15-03-43\021-0101.D		
Sample name:	50 ppm Furfural		
Injection date:	8/11/2022 3:05:10 PM	Sample type:	Calibration
Acq. method:	Furfuran SB column.M	Location:	21
Analysis method:	Furfural SB column.M	Injection:	1 of 1
Acq. operator:	SYSTEM	Injection volume:	20.000
Last changed:	8/11/2022 4:16:38 PM		

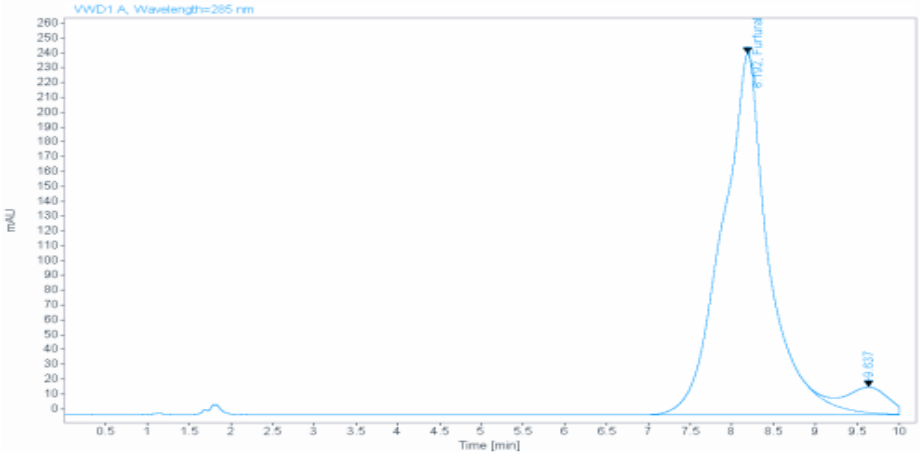

JIJE Analytical Testing Service Laboratory

We Serve Scientific Community

Data file:	C:\Chem32\1\Data\furfural\Furfural J-0022 11-08-2022 2022-08-11 15-03-43\022-0201.D		
Sample name:	100 ppm Furfural		
Injection date:	8/11/2022 3:16:40 PM	Sample type:	Calibration
Acq. method:	Furfuran SB column.M	Location:	22
Analysis method:	Furfural SB column.M	Injection:	1 of 1
Acq. operator:	SYSTEM	Injection volume:	20.000
Last changed:	8/11/2022 4:16:38 PM		

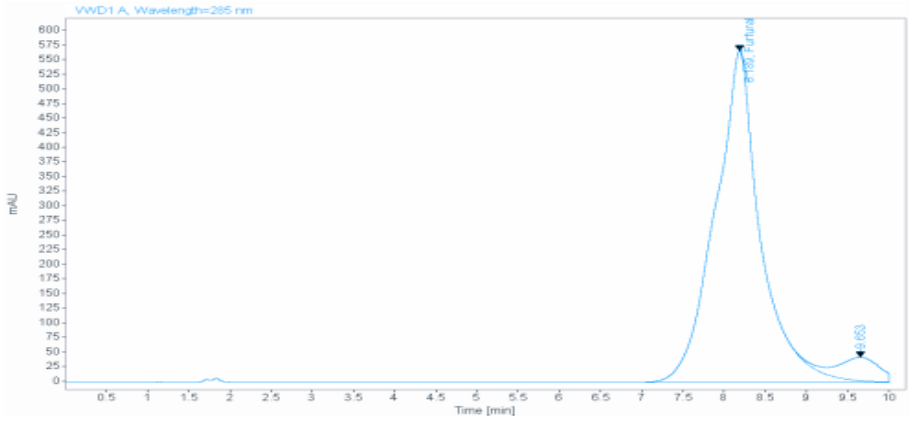

JIJE Analytical Testing Service Laboratory

Data file:	C:\Chem32\1\Data\furfural\Furfural J-0022 11-08-2022 2022-08-11 15-03-43\023-0301.D		
Sample name:	150 ppm Furfural		
Injection date:	8/11/2022 3:28:08 PM	**Sample type:**	Calibration
Acq. method:	Furfuran SB column.M	**Location:**	23
Analysis method:	Furfural SB column.M	**Injection:**	1 of 1
Acq. operator:	SYSTEM	**Injection volume:**	20.000
Last changed:	8/11/2022 4:16:38 PM		

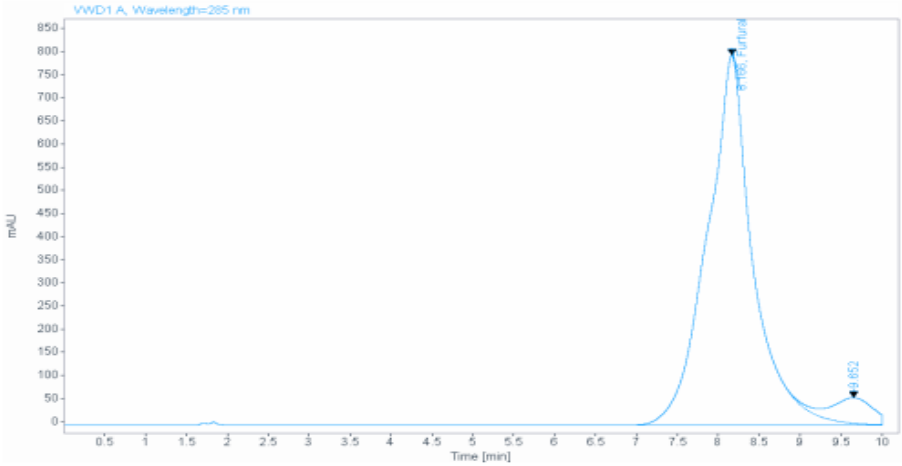

JIJE Analytical Testing Service Laboratory

Data file:	C:\Chem32\1\Data\furfural\Furfural J-0022 11-08-2022 2022-08-11 15-03-43\024-0401.D		
Sample name:	200 ppm Furfural		
Injection date:	8/11/2022 3:39:37 PM	**Sample type:**	Calibration
Acq. method:	Furfuran SB column.M	**Location:**	24
Analysis method:	Furfural SB column.M	**Injection:**	1 of 1
Acq. operator:	SYSTEM	**Injection volume:**	20.000
Last changed:	8/11/2022 4:16:38 PM		

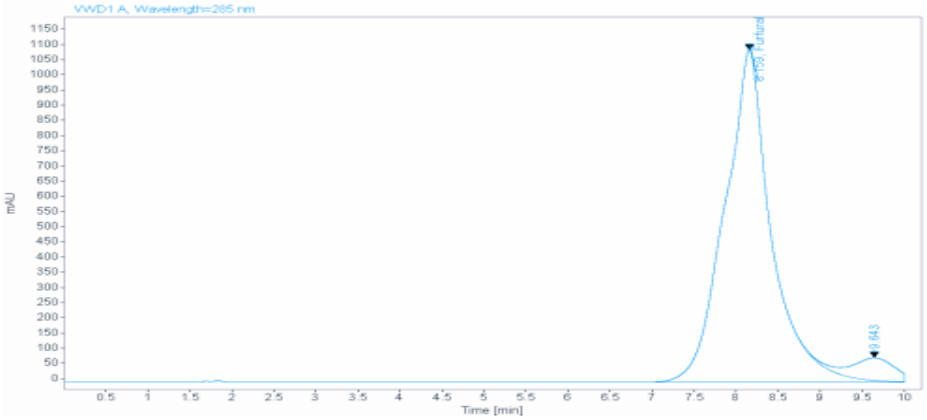

JIJE Analytical Testing Service Laboratory

Data file:	C:\Chem32\1\Data\furfural\Furfural J-0022 11-08-2022 2022-08-11 15-03-43\025-0501.D
Sample name:	300 ppm Furfural
Injection date:	8/11/2022 3:51:08 PM
Sample type:	Calibration
Acq. method:	Furfuran SB column.M
Location:	25
Analysis method:	Furfural SB column.M
Injection:	1 of 1
Acq. operator:	SYSTEM
Injection volume:	20.000
Last changed:	8/11/2022 4:16:38 PM

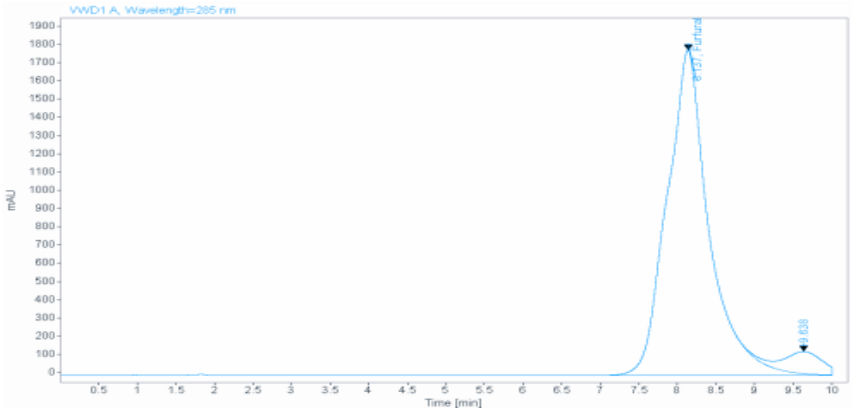

JIJE Analytical Testing Service Laboratory

Calibration Update:	**8/11/2022 4:17:34 PM**
Compound:	Furfural
Signal:	VWD1A
Exp. RT:	8.144
Corr. Coeff.:	0.998688
Residual:	1310.48576
RF RSD%:	
Formula:	y = ax + b
a:	230.17103
b:	-2301.28141
c:	0.00000
d:	0.00000